UCRL-10598

University of California

Ernest O. Lawrence Radiation Laboratory

TWO-WEEK LOAN COPY

This is a Library Circulating Copy which may be borrowed for two weeks. For a personal retention copy, call Tech. Info. Division, Ext. 5545

PHYSICAL ASPECTS OF CREEP

Berkeley, California

DISCLAIMER

This document was prepared as an account of work sponsored by the United States Government. While this document is believed to contain correct information, neither the United States Government nor any agency thereof, nor the Regents of the University of California, nor any of their employees, makes any warranty, express or implied, or assumes any legal responsibility for the accuracy, completeness, or usefulness of any information, apparatus, product, or process disclosed, or represents that its use would not infringe privately owned rights. Reference herein to any specific commercial product, process, or service by its trade name, trademark, manufacturer, or otherwise, does not necessarily constitute or imply its endorsement, recommendation, or favoring by the United States Government or any agency thereof, or the Regents of the University of California. The views and opinions of authors expressed herein do not necessarily state or reflect those of the United States Government or any agency thereof or the Regents of the University of California.

UCRL-10598

"Physical Aspects of Creep"

by

John E. Dorn[1] and Jim D. Mote[2]

Prepared for Presentation at the

International Conference on Elevated Temperature Structural Mechanics

at

Columbia University, New York

January 23-25, 1963

1 Miller Professor('62-'63) of Materials Science, Department of Mineral Technology, and Research Metallurgist of the Lawrence Radiation Laboratory, University of California, Berkeley, California.
2 Research Metallurgist of the Lawrence Radiation Laboratory, University of California, Berkeley, California.

1. Introduction

Over the past 100 years, engineers, metallurgists and ceramists have expressed ever increasing technical interest in the high-temperature plastic behavior of materials. Most of this period was characterized by extensive creep testing of numerous alloys and some ceramic materials leading to empirical descriptions of the dependency of the creep rate on stress and temperature, as well as qualitative concepts concerning the various metallurgical and structural factors that provide creep resistance. In spite of the substantial effort expended on this problem, no simple unique rationale developed over the first 90% of this period, either to permit predictions of creep behavior, or to provide the basis for the scientific design of creep resistant alloys.

Slightly more than ten years ago, however, based principally on the marriage of dislocation theory with the theory for kinetics of reactions, a new atomistic approach to unraveling the complicated nature of creep was initiated. Although much yet remains to be done before a satisfactorily complete picture of creep matures, and despite the continued need for semi-empiricism in the development of creep resistant materials, it is, nevertheless, now rather clearly established that the continued persuit of this new method of attack on the problem will eventually lead to the desired knowledge. It is the major purpose of this report to indicate those areas where some progress has been made in the theory of creep and to identify those issues that need additional clarification.

Since creep is the result of thermally activated flow mechanisms, the shear-strain rate, $\dot{\gamma}_i$, arising exclusively as a result of the operation

of the ith mechanism, can be formally established to be

$$\dot{\gamma}_i = f_i^+\{\tau, T, st_i\}\, e^{-\frac{h_i^+\{\tau, T, st_i\}}{kT}} - f_i^-\{\tau, T, st_i\}\, e^{-\frac{h_i^-\{\tau, T, st_i\}}{kT}} \qquad (1.1)$$

Whereas τ, T, and k have the usual meanings of the applied shear stress, the absolute temperature, and Boltzmann's constant, the remaining terms deserve at least a brief description. The quantity h_i^+ is the enthalpy of activation for the reaction in the forward direction. With rare exceptions, the pressure under consideration is so low that the enthalpy of activation very nearly equals the activation energy. It does depend, however, on the applied shear stress, which assists the forward reaction (+) and hinders the reverse reaction (-), thus giving magnitude and directionality to the strain rate. Since the dependence of the enthalpy of activation on the stress arises as a result of the force acting on the dislocations and thus assisting the reaction, it also depends on the substructure, st, that is present. Although in certain cases, e.g., those mechanisms that are diffusion controlled, the enthalpy of activation is practically insensitive to the temperature, in other cases it might depend on the temperature in harmony with the effect of temperature on the shear modulus of elasticity. The frequency term, f_i^+, into which we have incorporated the activation entropy, can also depend on τ, T, and st. The influence of temperature on this term, however, is always small in contrast to its effect in the exponential Boltzmann term. As in all kinetics of reaction problems, the net forward rate is determined by the total contribution to the forward rate munus the total contribution to the reversed rate, which gives rise to the two terms of Eq. 1.1 that contribute to the net creep rate due to the ith process.

When processes are sequential, such that j follows k which follows ℓ, etc., the creep rate for the sequence is dictated by the slowest

process, which we designate here as the ith process. But when the total creep rate arises from a series of parallel, and independently operative mechanisms, the total creep rate, $\dot{\gamma} = \sum \dot{\gamma}_i$, is given by the sum of the contributions over all such independent processes. When more than one process determines the creep rate, the difficulties of identifying these mechanisms become almost insurmountable. Consequently, most of the existing information about creep has been deduced for those conditions of experimentation at which one mechanism predominates. Only those mechanisms for which $h_i < 50\,kT$ can be stimulated by thermal fluctuations. Consequently only the easier (lower enthalpy) mechanism can take place at low temperatures. As the temperature is increased, such easier mechanisms occur so rapidly that they permit almost instantaneous straining. Continued creep at these intermediate temperatures thus occurs as a result of the operation of more difficult processes having higher values of h_i^+. At the highest temperatures only the most difficult processes determine the creep rate, and the easier processes account for the almost instantaneous initial strain. Dislocation theory, however, is not yet sufficiently sophisticated to be able to predict unambiguously which of the various individual rate controlling mechanisms might be the operative one. Nevertheless it is occasionally possible to identify, from experimental evidence in specific examples, several temperature regions over each of which different dislocation mechanisms of creep predominate.

It is the objective of creep theory to determine the functional dependency of f_i and h_i on the pertinent mechanical and structural variables for each of the series of permissible thermally activatable dislocation reactions. Our analyses here will be limited to discussion of such

high-temperature creep phenomena that are controlled by diffusion mechanisms. Such diffusion controlled processes assume significance at temperatures above about one-half of the melting temperature. In this range of temperatures the creep rate is almost always determined by one or more of several diffusion controlled mechanisms. The only known exceptions to this generalization concern the high-temperature creep of single crystals of Al,[1] Mg,[2] and Zn.[3] No light has yet been shed on why these materials gave exceptions to the general rule. Perhaps in the single crystal tests of Al and Mg the types of barriers that are essential for blocking dislocations, and thereby necessitating the operation of the climb processes to provide additional creep, were not formed, whereas they are formed in polycrystals which are subjected to polyslip. The possible validity of this explanation is supported by the fact that the high-temperature creep of polycrystalline Al is diffusion controlled. Prismatic slip in Zn may be controlled by the Peierls mechanism.

The various diffusion controlled mechanisms for high-temperature creep include:

1. Stress-Directed Diffusion of Vacancies in Polycrystals
2. Thermally Activated Motion of Jogged Screw Dislocations
3. Climb of Edge Dislocations
4. Solute Atom Diffusional Processes and Viscous Drag
5. Structural Instability of Dispersed Phases

The importance of high-temperature creep is well documented in a number of outstanding reviews, symposia, and monographs on this subject.[4-9] It would indeed be impossible, in terms of the limitations of time and space, to review everything that has been done and said about creep here. Rather we plan to concentrate our attention on the mechanisms

for creep; we will briefly review some of the significant evidence and illustrate known mechanisms with some of the more recent data; we will also point out where creep theory is weak and, in some instances, how it might be improved.

2. Nabarro Creep

Creep by the stress-directed diffusion of vacancies, formulated originally by Nabarro,[11] is one of the best understood, theoretically, of the various mechanisms for high-temperature creep. Although Herring[12] subsequently presented a more sophisticated and detailed analysis of this process, we shall review the original Nabarro approach here, because it provides a more vivid physical picture of the mechanism.

This creep mechanism applies only to polycrystalline aggregates at very high temperatures and differs from the other high temperature creep processes that crystalline materials might undertake insofar as it does not depend on the motion of dislocations. Consequently it can occur in polycrystals when the grains contain no dislocations or where all dislocation motion is blocked either by high Peierls stresses or by some other very effective locking mechanism. If a polycrystalline aggregate cannot creep by any other mechanism, it will, under appropriate conditions of stress and temperature, creep by means of stress-directed diffusion of vacancies.

In reviewing Nabarro creep, we will first consider a polycrystalline aggregate of one phase and one component. The grain boundaries of the aggregate are regions of discontinuity in the structure and are therefore excellent regions which serve as sources and sinks for vacancies. When a tensile stress, p, is applied normal to a boundary, it can assist in the formation of a vacancy since it will do work $p\Omega_v$ per vacancy produced, where Ω_v, the volume of a vacancy, is about equal to the atomic volume. In the absence of a stress, the probability of finding a vacancy at a given site is

$$\frac{n_v}{n_s} = e^{-g_f/kT} \tag{2.1}$$

where n_v is the number of vacancies among n_s lattice sites and g_f is the free energy of formation of a vacancy. Consequently, assuming equilibrium can be established, the probability of finding a vacancy in the lattice just below a grain boundary subjected to a tensile stress, p , is

$$\frac{n_v'}{n_s} = e^{-g_f/kT} e^{p\Omega_v/kT} \tag{2.2}$$

a quantity which is somewhat greater than the equilibrium value in the absence of a stress.

Consider now a cubic grain of demensions d, as shown in Fig. 2.1, so stressed to give a shear stress, p, at 45° to the specimen axis. Whereas the probability of finding a vacancy along AB and CD is proportional to $e^{\frac{p\Omega_f}{kT}}$, that of finding a vacancy along AD and BD is proportional to $e^{-\frac{p\Omega_f}{kT}}$. Due to the concentration gradient, vacancies are presumed to flow as shown by the arrows in the figure. This flow of vacancies will be matched by an equal and opposite flow of atoms resulting in a longitudinal extension and lateral contraction of the grain with time under stress.

It is not immediately apparent however, that the vacancies should enter the volume of the grain and undertake volume diffusion in the grain as was postulated by both Nabarro and Herring. This question is emphasized by the fact that both the free energy of formation and the free energy of activation of motion of a vacancy in the grain boundary is appreciably less than that in the grain itself. Obviously the total creep rate will depend on the sums of the contributions from the volume and boundary diffusion processes. For the present, however, we will assume that the volume diffusion mechanism predominates and we will describe in some detail later the thus far neglected mechanism involving grain boundary diffusion.

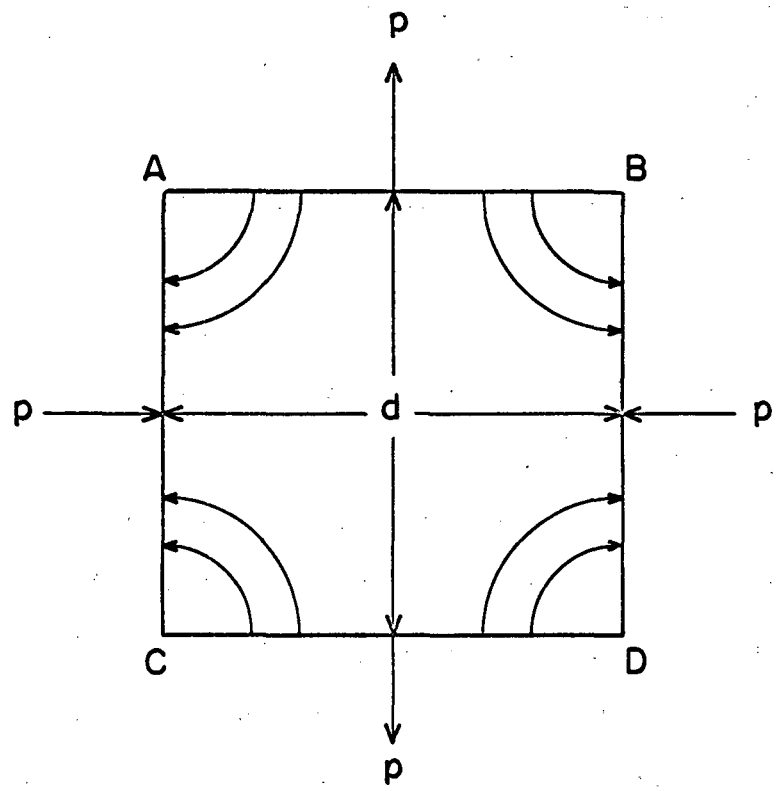

MU-29095

Fig. 2.1. Vacancy flow in a grain.

Three steps are involved in the original stress-directed diffusion model for creep, namely, the formation of a vacancy in the grain volume near the grain boundary under a positive stress, its migration to the boundary that is under a negative stress and its annihilation at that boundary. Both Nabarro and Herring assumed that the generation and annihilation steps were so rapid in contrast to the diffusional step that the rate of creep was dictated by the diffusional flux. In view of the disorder in the grain boundary, this assumption appears to be quite good and it will be accepted here, particularly because it enjoys some experimental verification.

Under these assumptions, the difference in concentration of vacancies between the grain sides AB and AC becomes about

$$c^+ - c^- = \frac{\alpha}{\Omega} e^{-g_f/kT} \left\{ e^{p\Omega_v/kT} - e^{-p\Omega_v/kT} \right\} \tag{2.3}$$

where Ω is the atomic volume and α is to be taken as slightly less than unity. The value α thus corrects somewhat for the fact that under diffusional conditions the concentration of the vacancies at the grain boundaries differs slightly from the equilibrium value. Eq. 2.3, however, can only represent an approximation to the facts since vacancies will have a shorter diffusion path near the corners of the grain than in the centers of the edges. Thus, under steady state conditions, the stress is somewhat relaxed near the corners and increases as the center of the boundary is approached. Consequently, p varies over the surface of the grain and has its maximun value at the center of the boundary. At d/4 from the corner of a grain, we assume that $p = \beta\tau$ where τ is the macroscopic shear stress and β has a value of near unity. For this point the diffusion path is apporximately $\pi/2\,(d/4)$ and therefore the concentration gradient for this path is about

$$\frac{c^+ - c^-}{\pi d/8} = \frac{16\alpha e^{-g_f/kT}}{\Omega \pi d}\left\{\frac{e^{\frac{\beta\tau\Omega_v}{kT}} - e^{-\frac{\beta\tau\Omega_v}{kT}}}{2}\right\}$$

or, since $\frac{\beta\tau\Omega}{kT} < 1$ for the usual values of the applied stress,

$$\frac{c^+ - c^-}{\pi d/8} = \frac{16\alpha\beta\Omega_v e^{-g_f/kT}\tau}{\Omega \pi d kT} \tag{2.4}$$

If h is taken as the height of an atom, the area of an atom is Ω/h. The flux of atoms across an atomic area at d/4 from the corner along AC and at d/4 from the corner along AB is

$$J = \frac{\Omega}{h} D_v \frac{c^+ - c^-}{\pi d/8} \tag{2.5}$$

where D_v is the diffusivity of a vacancy. Each such atomic transfer results in increasing AC by h and decreasing AB by h. The shear strain is therefore $\gamma = 2h/d$ per atom transferred. Consequently the creep rate approximates

$$\dot{\gamma} = \frac{32\alpha\beta\Omega_v}{\pi d^2 kT} D_v e^{-g_f/kT}\tau \simeq \frac{32\alpha\beta\Omega_v D\tau}{\pi d^2 kT} \tag{2.6}$$

where D , the self diffusivity, is equal to $D_v e^{-g_f/kT}$. The more sophisticated analysis of Herring gives approximately the same answer. Herring also discussed the effect of various grain shapes on the creep rate.

The significant characteristics of creep by means of the stress-directed diffusion of vacancies are as follows:

1. Absence of a primary stage or any pronounced transients
2. An activation energy that equals that for volume self-diffusion
3. A creep rate that increases linearly with the stress
4. A creep rate that varies inversely with the square of the grain diameter

5. A creep rate that can be approximated by Eq. 2.6 allowing for small variations of ($\alpha\beta$) from unity because of variations in grain size and irregularities in grain shape.

The Nabarro approach assumes that a vacancy has a high probability of moving out of the boundary so that diffusion occurs primarily through the volume of the grain. We will now explore this assumption. If diffusion takes place along the boundary, say over an average distance $d/2$, the time, t, for this migration will be given by approximately

$$\frac{\left(\frac{d}{2}\right)^2}{4 D_{vb} t} = 1 \qquad (2.7)$$

where D_{vb} is the vacancy diffusivity in the boundary. We wish now to determine what the probability might be for a vacancy to remain in the boundary for a time as long as t. The probability that a boundary vacancy will leave the boundary in any one vibration is

$$p^+ = 1/6\, e^{-\frac{g_f - g_{fb}}{kT}}\, e^{-g_m/kT} \qquad (2.8)$$

The one-sixth term arises from the fact that the vacancy can leave the boundary only in the $+z$ direction, the x and y directions being selected to be the boundary. In order to escape from the boundary, the vacancy must acquire the additional energy $g_f - g_{fb}$ where g_f is the free energy of formation of a vacancy in the grain and g_{fb}, which is smaller than g_f, is the free energy of formation of a vacancy in the grain boundary. Furthermore, to move the vacancy it must also acquire the free energy for activation of motion of a vacancy across the boundary, namely g_m. Vacancies can also enter the boundary from the grain. For the purpose of the present calculation, we assume that there are ample sources and sinks in the form

of jogs on the dislocations to maintain the equilibrium number of vacancies in the grain. Consequently the probability that a vacancy will enter the boundary is

$$p^{-} = \frac{1}{6} e^{-\frac{g_f}{kT}} e^{-\frac{g_m}{kT}} \tag{2.9}$$

and the net probability that a vacancy will leave the boundary is then given by

$$p = \frac{1}{6} e^{-\frac{g_f + g_m}{kT}} \left\{ e^{\frac{g_{fb}}{kT}} - 1 \right\} \tag{2.10}$$

The probability that a vacancy will not move out of the boundary in one vibration is (1 - p), and therefore the probability it will remain in the boundary for n shakes is

$$P = (1-p)^n = (1-p)^{\nu_b t} \tag{2.11}$$

where ν_b is the frequency of vibration of an atom in the boundary. Therefore the probability that grain boundary diffusion will predominate is about

$$P \simeq \left[1 - \frac{1}{6} e^{-\left(\frac{g_f - g_{fb} + g_m}{kT} \right)} \right]^{\frac{\nu_b d^2}{16 D_v b}} \tag{2.12}$$

To estimate this probability we let

$$D_{vb} = \frac{b^2 \nu_b}{6} e^{-g_{mb}/kT} \tag{2.13}$$

and write Eq. 2.12 as

$$P = \left[1 - \frac{1}{6} e^{\frac{-(g_f - g_{fb})}{kT}} e^{-\frac{g_m}{kT}} \right]^{\frac{8d^2}{3b^2} e^{+\frac{g_{mb}}{kT}}} \tag{2.14}$$

We note that the larger d is and the larger g_{mb} is, the less probable is grain boundary diffusion. But the larger $g_f + g_m - g_{fb}$ is, the more probable grain boundary diffusion becomes. In order to illustrate this problem, we take the following sets of values

I	II	III
$d = 1000b$	$d = 1000b$	$d = 100b$
$\frac{g_{mb}}{kT} = 20$	$\frac{g_{mb}}{kT} = 40$	$\frac{g_{mb}}{kT} = 20$

and arrive at the values of P given in Fig. 2.2. These data reveal that the principal variable that discriminates between volume and grain boundary creep is $\frac{g_f + g_m - g_{fb}}{kT}$. For the lower melting temperature metals, where this is less than about 30, volume diffusion will predominate. But where $\frac{g_f + g_m - g_{fb}}{kT}$ is more than about 30, which might apply to the refractory metals and some ceramic materials, the process should occur predominately by grain boundary diffusion.

The derivation of the equation for stress-directed diffusion of vacancies exclusively by means of grain boundary diffusion follows the same principles already established by Nabarro for volume diffusion. The result is easily shown to be approximately

$$\dot{\gamma} = \frac{8\alpha\beta\Omega_v D_{vb}\tau}{d^2 kT} \tag{2.15}$$

The only significant difference between the creep rate by grain boundary diffusion, Eq. 2.15, as contrasted to that for volume diffusion, Eq. 2.6, concerns the diffusivity: Therefore the activation energy for the grain boundary diffusion mechanism is somewhat less than that for the volume diffusion mechanism.

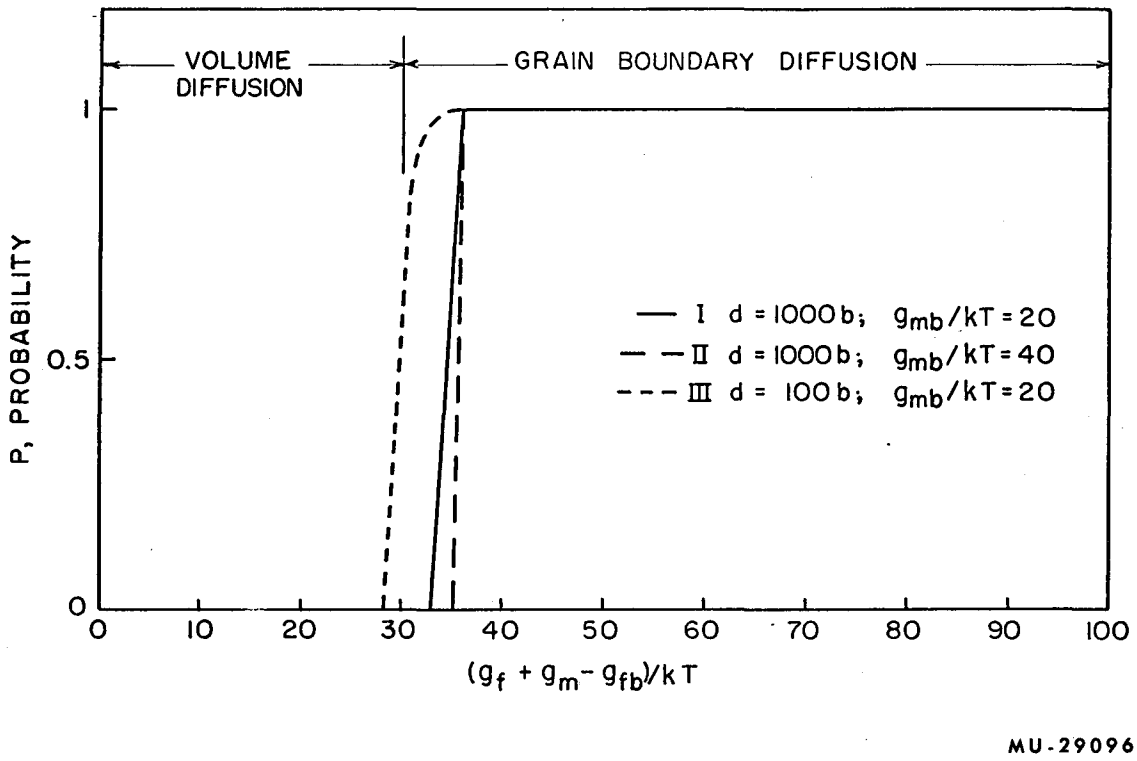

Fig. 2.2. Probability that a vacancy will remain in the grain boundary during diffusion.

Whereas Eq. 2.6 and 2.15 represent the two extremes that might be encountered, in many cases both mechanisms might contribute simultaneously. The creep rate in such cases is not given by a linear average of the two alternate mechanisms. The theory for this general case must yet be developed.

At high temperatures and low values of the stress, polycrystalline Cu,[13] Ag[14] and Au[15] have been shown to creep at rates that increase linearly with the applied stress. The following Table permits a comparison of the activation energies obtained from the creep tests with those for self-diffusion.

Table 2.1

Activation Energies (cal/mole)

Metal	For Creep	For Volume Self-Diffusion
Cu	56,800	46,500
Ag	(not determined)	46,000
Au	51,000	53,000

The agreement between the activation energies for creep and volume self-diffusion in Au are excellent. It is not evident, however, why the activation energy for creep of Cu is higher than that for self-diffusion. In either event, however, volume diffusion and not grain boundary diffusion appears to be the preferred mechanism.

For providing a basis of comparing theory with experiment, we write Eq. 2.6 as

$$\dot{\gamma} = A D \frac{\tau}{T} \tag{2.16}$$

Using the data recorded in Table 2.2, we arrive at the recorded values of A.

Table 2.2

Nabarro Creep

Metal	T ^{o}K	D cm^2/sec	d cm	A calc	A observed
Cu	1324	40.4×10^{-10}	19×10^{-3}	0.0034	0.0052
Au	1315	2.3×10^{-10}	6.6×10^{-3}	0.04	0.4

These data reveal that the Nabarro equation gives the correct order of magnitude for the creep rate.

It is necessary to emphasize, however, that other mechanisms of creep can also give a linear dependence of creep rate of stress and an activation energy for volume self-diffusion. Harper and Dorn[16] have clearly demonstrated that although these conditions are fulfilled for the high temperature low stress creep rate of polycrystalline aluminum, the Nabarro mechanism cannot apply. Markers on the specimen reveal that creep was not due to increase of atoms in the horizontal grain boundaries but that the interior of the grains strained. Single crystals gave about the same creep rate of polycrystals. And the creep rate was about 1300 times greater than that suggested by the Nabarro equation. It will be shown later in this report that the creep observed by Harper and Dorn can be attributed to the motion of jogged screw dislocations.

Considerable interest has developed recently in ascertaining the basic mechanisms for high temperature creep of ceramic materials. We will review here those data that appear to be pertinent to the Nabarro mechanism. A number of ceramic materials give creep rates at high

temperatures that increase linearly with the applied stress. The activation energies for creep of these materials are compared with those for sintering and volume diffusion in Table 2.3.

Table 2.3

Activation Energies For Ceramic Materials

Ref	Material	Temperature Range °K	Grain Size Microns	Activation Energies in Cal/Mole			
				Creep	Sintering	Vol. Diffusion	
						Anion	Cation
17	Al_2O_3		Single Xl			152,000	
18	Al_2O_3	1773-2073	7-34	130,000			
19	Al_2O_3				150,000		
20	Al_2O_3	1873-2073	3-13	130,000			
20	Al_2O_3	1873-2073	50-100	200,000			
21	Al_2O_3	1773	coarse grain	200,000			
21	BeO	1923-2018	25	120,000			
22	BeO	1873-2273	80-100				116,000 ±10,000
23	BeO	1644-1811	7.4-10.5	95,800			
24	UO_2	1073-1273	--	95,000			
24	$UO_{2.06}$	"	--	72,000			
24	$UO_{2.16}$	"	--	65,000			
25	UO_2					29,700 ±2300	
26	UO_2(?)						68,000

Although these data exhibit considerable scatter and must be deemed somewhat preliminary, several interesting correlations nevertheless emerge. The best data for creep of Al_2O_3 give activation energies for creep that are slightly below those for sintering and anion volume diffusion. It is therefore possible that the high temperature creep of Al_2O_3 might be controlled principally by means of volume anion diffusion although some grain boundary diffusion may also take place. It is expected that vacancy diffusion in Al_2O_3 is principally controlled by anion diffusion since the activation energy for cation diffusion is expected to be much lower than that for anion diffusion. The agreement between the activation energy for creep of BeO and the cation volume diffusion seems to be somewhat fortuitous since anion diffusion is expected to have a higher activation energy and therefore is the slower diffusing species that would control the rate of vacance diffusion. It is possible here that the high temperature creep of BeO occurs primarily as a result of grain boundary diffusion in which event the observed activation energy of 95,800 cal./mole for creep might refer to the activation energy for grain boundary diffusion of the anion. The activation energies for creep in defect lattices of UO_2 are sensitive to composition as would be expected.

The data of Folweiler[18] on the high temperature creep of polycrystalline Al_2O_3, shown in Figs. 2.3 and 2.4, reveal that both the effects of stress and grain size on the creep rate agree with the expectations of the Nabarro mechanism. Similar results have been given by Warshaw and Norton.[20]

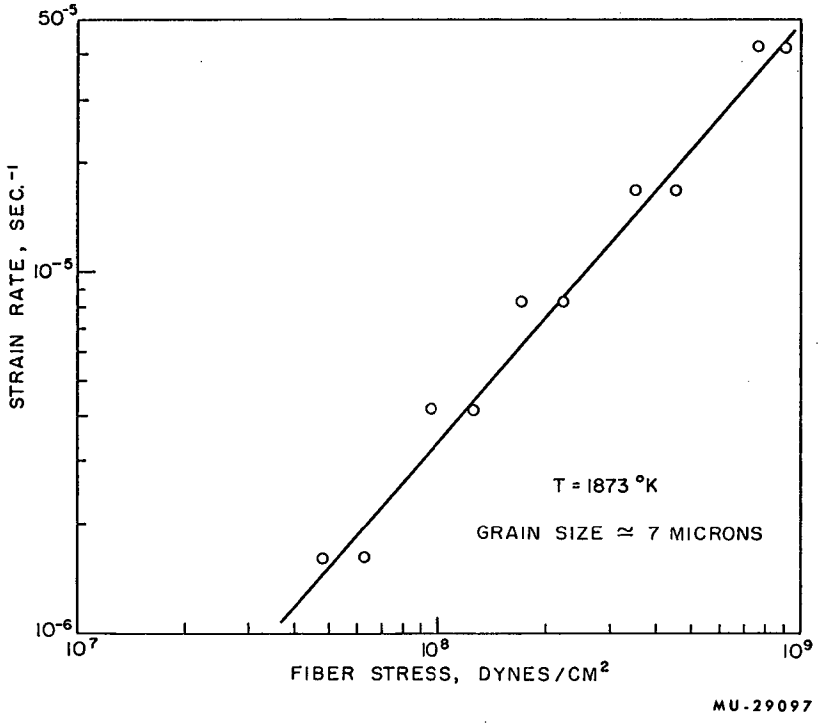

Fig. 2.3. Effect of stress on the strain rate of Al_2O_3. (After Folweiler)

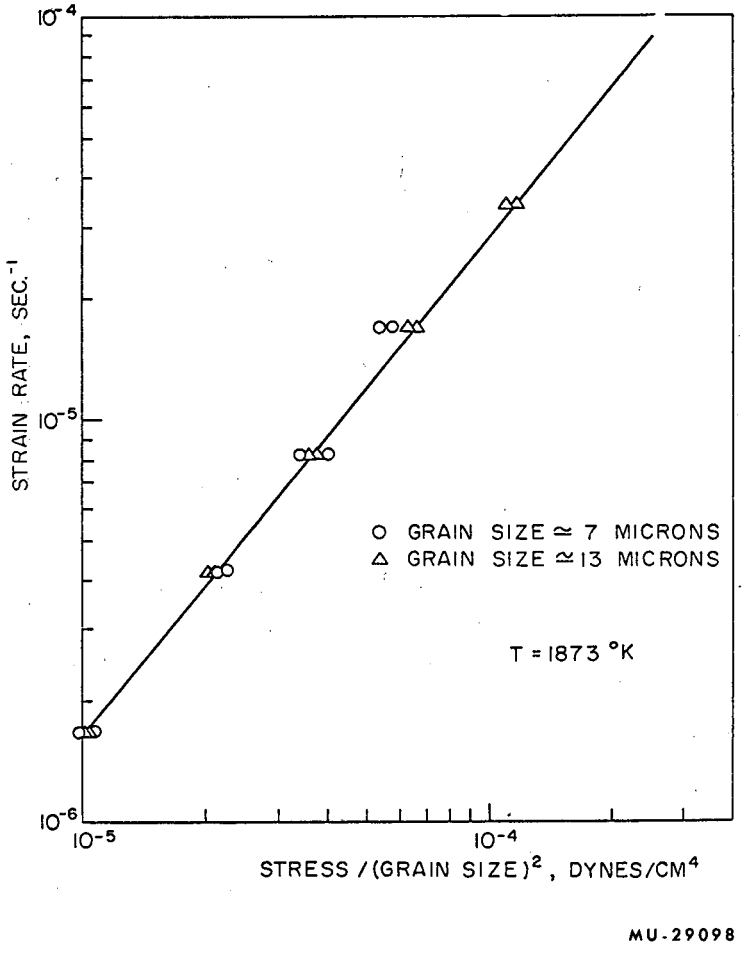

Fig. 2.4. Effect of grain size on the strain rate. (After Folweiler)

Assuming

$$D_{Al_2O_3} = 1.5 \times e^{-\frac{130,000}{RT}}$$

$$d = 7 \times 10^{-4} \text{ cm}$$

$$= 14 \times 10^{-24} \text{cm}^3$$

we calculate, for volume diffusion, that A of Eq. 2.6 is $0.825 \times 10^{-12} \frac{\text{cm}^2}{\text{dyne sec.}}$. The experimentally determined value is $2.4 \times 10^{-12} \frac{\text{cm}^2}{\text{dyne sec.}}$ which constitutes good verification of the Nabarro mechanism.

The most complete data in support of the Nabarro mechanism of creep was reported recently by Vandervoort and Barmore.[23] Their data for high temperature creep of BeO covered ranges of temperature, stress and grain size. If we assume that for grain boundary diffusion in BeO that

$$D = 1.5\, e^{-\frac{92,000}{RT}}$$

we can plot their data as shown in Fig. 2.5, as

$$\frac{\dot{\gamma}\, kT}{D} = K\, \tau / d^2 \qquad (2.17)$$

The experimental slope of this curve is $K_{exp} = 9.0 \times 10^{-23} \text{cm}^3$, whereas the theoretical value deduced from Eq. 2.15 is $2 \times 10^{-23} \text{cm}^3$. Thus, good confirmation of the theory has been achieved with experiment.

Additional critical experiments, however, are needed to provide information on the activation energies for creep and for diffusion of the anions and cations in the volume and along the grain boundary. Such experiments should explore the effects of all of the significant variables. Further theoretical work is needed to establish the creep equation under conditions where grain boundary and volume diffusion can occur simultaneously.

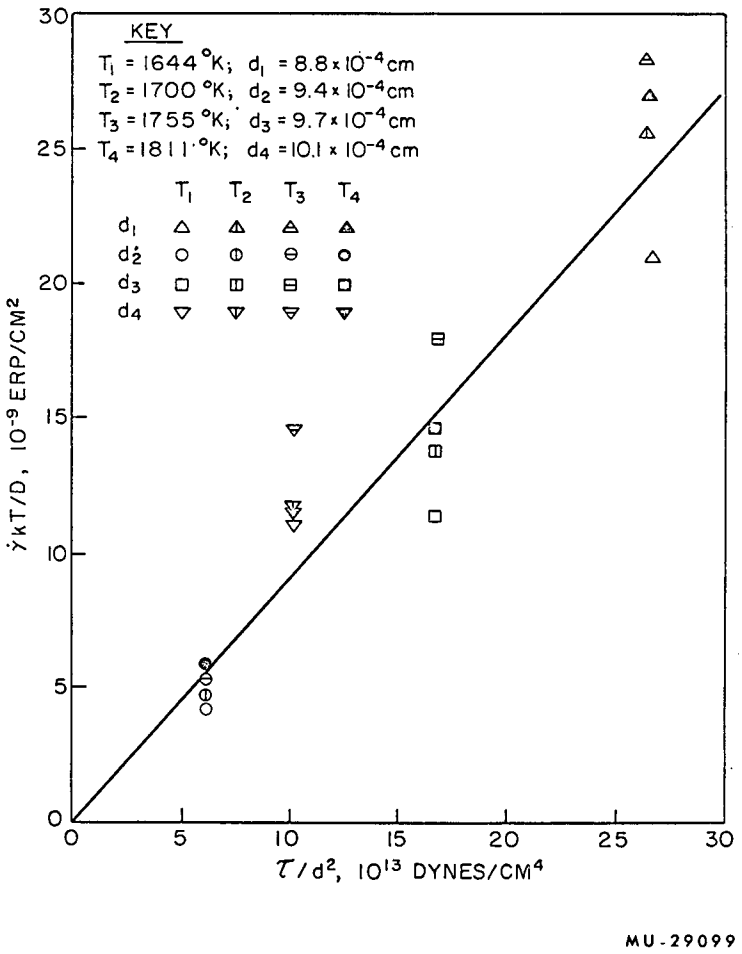

Fig. 2.5. $\dot{\gamma}\, k\, T/D$ vs τ/d^2 (data of Vandervoort and Barmore).

3. High Temperature Creep of Pure Metals

Predictions based on theoretical considerations of the climb of edge dislocations agree more closely with the known experimental facts on the high-temperature steady-state creep of pure polycrystalline metals, some dilute alpha solid solutions, and some rather stable dispersion strengthened alloys, than predictions based on any other single mechanism. Unfortunately, however, none of the several different versions of the climb theory formulated so far, provide predictions that agree precisely with all of the known facts. Therefore a critical reanalysis will be made of this theory, leading to a better appreciation of primary creep and consequently, to a more realistic version of steady state creep that is in better harmony with current knowledge. Preliminary to such theoretical discussion however, we will restate here some of the major experimental observations for which any good theory of high-temperature creep must account:

1. During constant elevated-temperature creep at high stress levels, creep curves of polycrystalline pure metals exhibit, as shown by the example in Fig. 3.1,[27] an initial plastic strain on loading, a primary stage of decreasing creep rates, a secondary stage of constant creep rate, and a tertiary stage of accelerating creep rates leading to rupture. We shall not be concerned here with this terminal stage of creep in spite of its importance, because it involves the auxiliary factor of microfracturing, and we wish to confine our attention to the simple case of creep per se.

2. The initial straining is due to the motion of dislocations. Because of the high temperatures, such low activation energy mechanisms as the Peierls process, intersection of dislocations and cross-slip, especially in high stacking fault metals, occur almost without delay. But as the dislocations move they interact with each other and produce barriers to further motion.

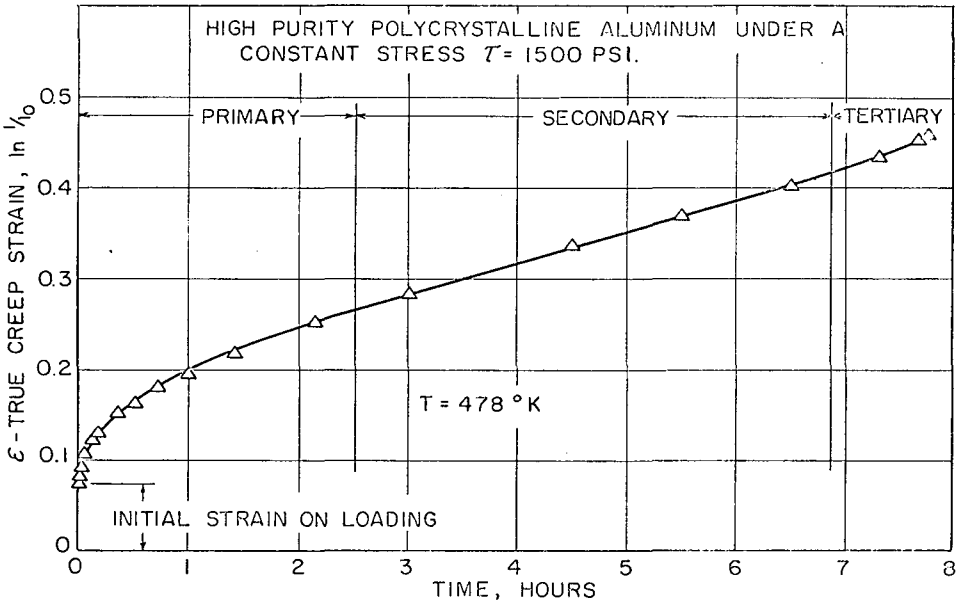

MU-29100

Fig. 3.1. Typical creep curve at elevated temperature.

3. Once a pattern of barriers is established, further motion of dislocation can only occur as a result of thermal activation over these barriers. Only those processes that have activation energies of less than about 50 kT can be operative.

4. During primary creep, dislocations are being thermally activated principally over the lower energy barriers. But since the creep rate is continuously decreasing over this range, more barriers are being introduced as a result of such creep. Since more dislocations are being held up at barriers, this means that the reduction in the creep rate over the primary stage is due to the fact that the density of moving dislocations is decreasing.

5. If the barriers are removable by recovery, a balance is eventually achieved between the rate of recovery of the barriers and the rate at which they are reintroduced as a result of creep straining. This happens at the secondary stage of creep.

6. The strain over the primary stage of creep increases with increasing stress as shown in Fig. 3.2.[28] This arises because the higher strain rate due to the higher stress causes a more rapid introduction of barriers. Therefore higher strains must be reached, in higher stress tests, before a balance can be achieved between the rate of recovery and the rate of reintroduction of barriers is reached.

7. During high-temperature creep of high stacking fault energy metals, subgrains are produced as a result of the formation of both twist and tilt boundaries. Low energy twist boundaries are produced by patterns of screw dislocations. The formation of the tilt boundaries is due to polygonization arising from the introduction of edge dislocations into the tilt wall and the subsequent climb of such edge dislocations.

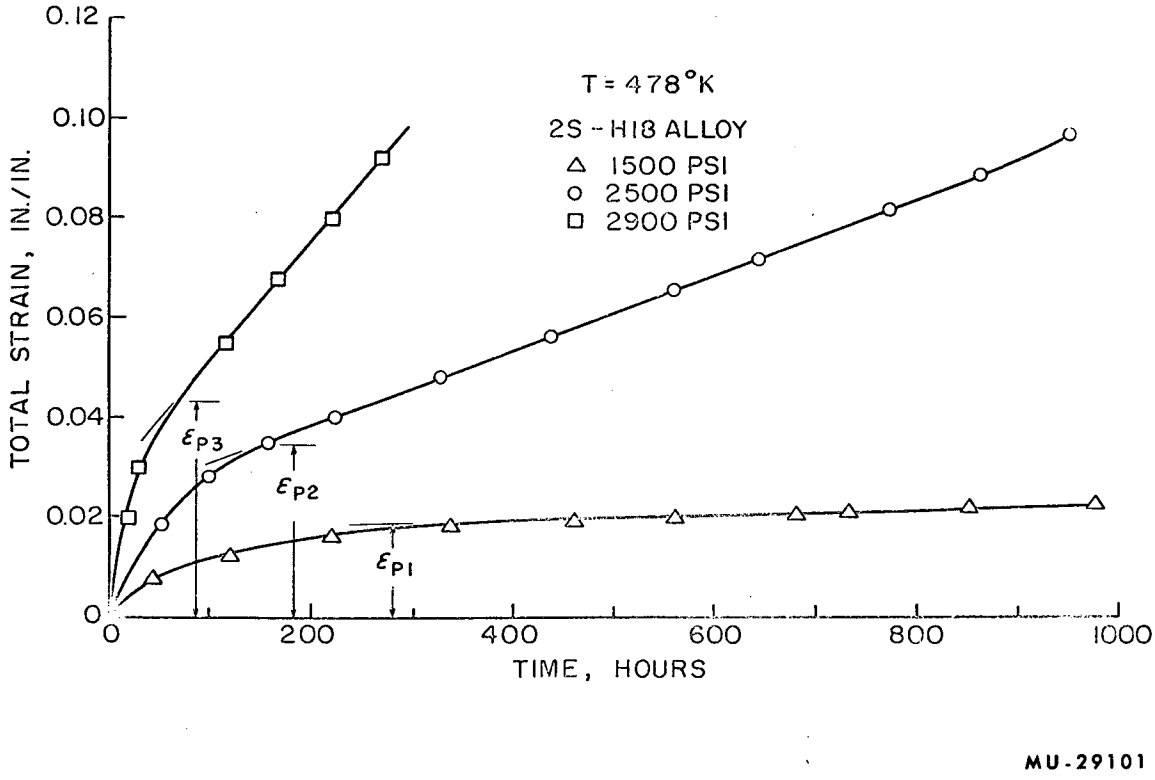

Fig. 3.2. Plot illustrating increasing strain over primary stage of creep with increasing stress. (After Sherby and Dorn)

8. McLean[29] has shown, in a case where grain boundary shearing was small, that about one-half of the moving dislocations that account for the creep rate enter the subgrain boundaries. Evidently the remainder disappear as a result of mutual annihilation.

9. The angle between adjacent subgrains continues to increase uniformly throughout both the primary and secondary stages of creep. Consequently the disorientation of the subgrains does not affect the secondary creep rate. The subgrain boundaries therefore appear to act merely as good sinks for excess dislocations. This concept is in harmony with the knowledge that low angle boundaries exhibit only very local stress fields.

10. The subgrain sizes during the primary and secondary stages of creep are independent of the temperature of test and the strain. They decrease, however, with increasing stresses, as shown in Fig. 3.3.[30]

11. These observations suggest that the subgrain sizes are due to the nonhomogeneous straining in any one grain as a result of the dissimilarly oriented neighboring grains. More severe bending and twisting and finer subgrain sizes are therefore expected for the higher stress tests.

12. Assuming that the degree of disorientation of the subgrains does not affect the creep rate, and that the subgrains merely act as suitable sinks for excess dislocations, the barriers that build up during the initial straining and primary creep must be found within the subgrains.

13. Transmission electron micrography clearly reveals that most of the dislocations in crept metals that have high stacking fault energies lie in the subgrain boundaries. Garafalo, Zwell, Keh and Weissman[34] have shown that throughout primary creep of Fe, the subgrain size remains substantially constant but that the disorientation of the subgrains increases and the density of the dislocations within the subgrains decreases throughout primary creep.

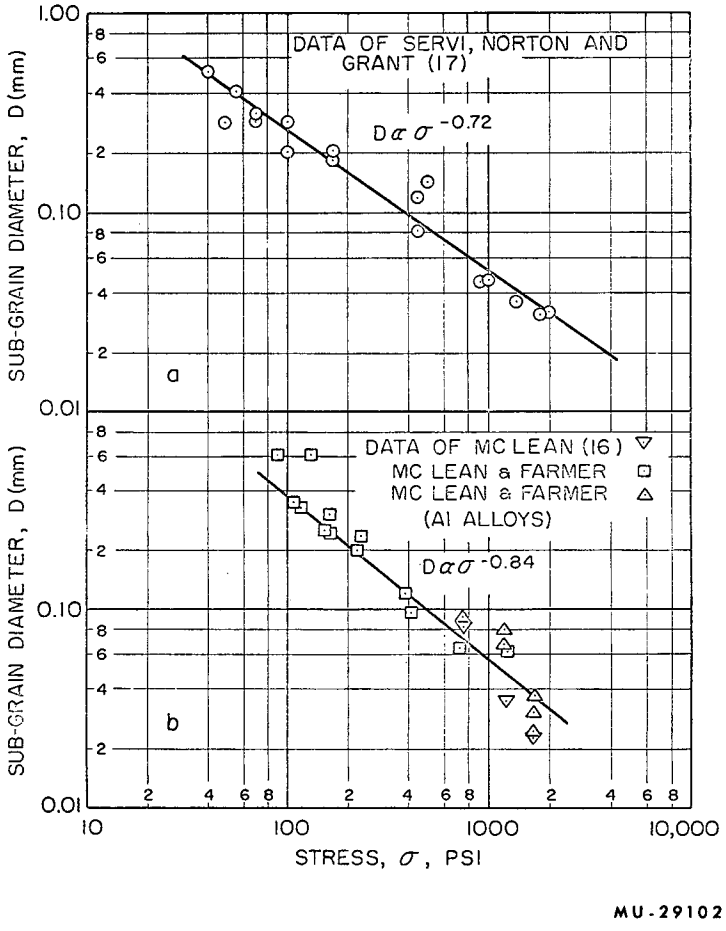

Fig. 3.3. The variation of sub-grain diameter with creep stress. (After Shepard and Dorn)

14. No piled-up arrays of dislocations have been seen in crept specimens of high stacking fault metals. The dislocation arrangements within the subgrains of crept metals are characterized by (a) isolated dislocations, (b) dipoles and (c) entanglements. Electron transmission micrographs, shown in Figs. 3.4 to 3.8, that illustrate typical arrangements of dislocations in crept metals, were kindly furnished by Dr. Gareth Thomas.

15. More barriers are produced following creep at a higher stress to the same strain. This fact is illustrated in Fig. 3.9.[35] When following creep to point A under a high stress at 4000 psi, the stress is changed to 2000 psi, the resulting creep rate immediately following the change in stress is lower than that obtained at the same strain when crept exclusively at the lower stress level.

16. All of the barriers, however, are recoverable. Regardless of differences in the original creep stress history, as shown in Fig. 3.9,[35] the same final secondary creep rate is reached as is obtained by testing exclusively at the final stress level. Incidently, the subgrain size is also recoverable and it is dictated only by the final stress level.

17. The creep curves for a given stress agree well with the empirical relationship

$$\gamma = f(t e^{-q/kT}) \qquad (\tau = \text{const.})$$

An example of this is given in Fig. 3.10.[27] The value of the apparent activation energy, q, so obtained, at least within somewhat limited ranges of the creep rate for high stacking fault metals, appears to be independent of the stress and strain.

18. The creep rate therefore can be approximated by

$$\dot{\gamma} = f'\{t e^{-q/kT}\} e^{-q/kT} \qquad (\tau = \text{const})$$

and consequently the substructural changes during primary creep are a

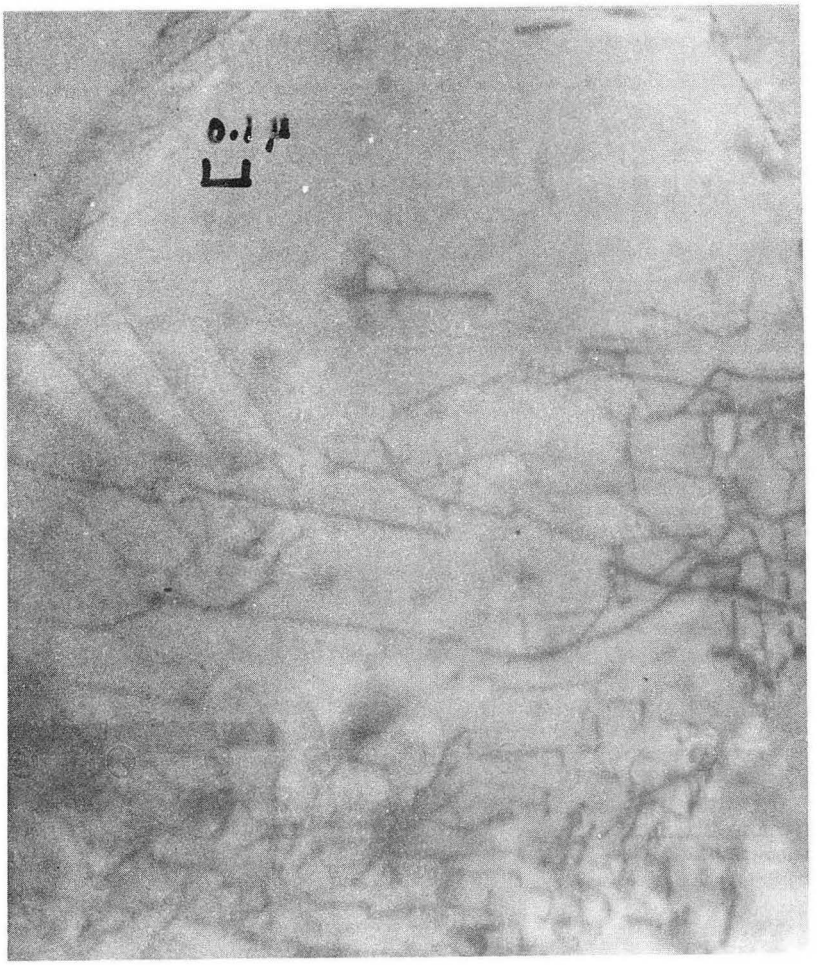

ZN-3496

Fig. 3.4. Regions showing entanglements and dipoles.
(Al-1% Mg crept under 2200 psi to ε = 0.078 at 330 °C)

ZN-3494

Fig. 3.5. Twist boundary and isolated dislocations. (Mo strained 0.05 and recovered at 1200°C for 3 hours.)

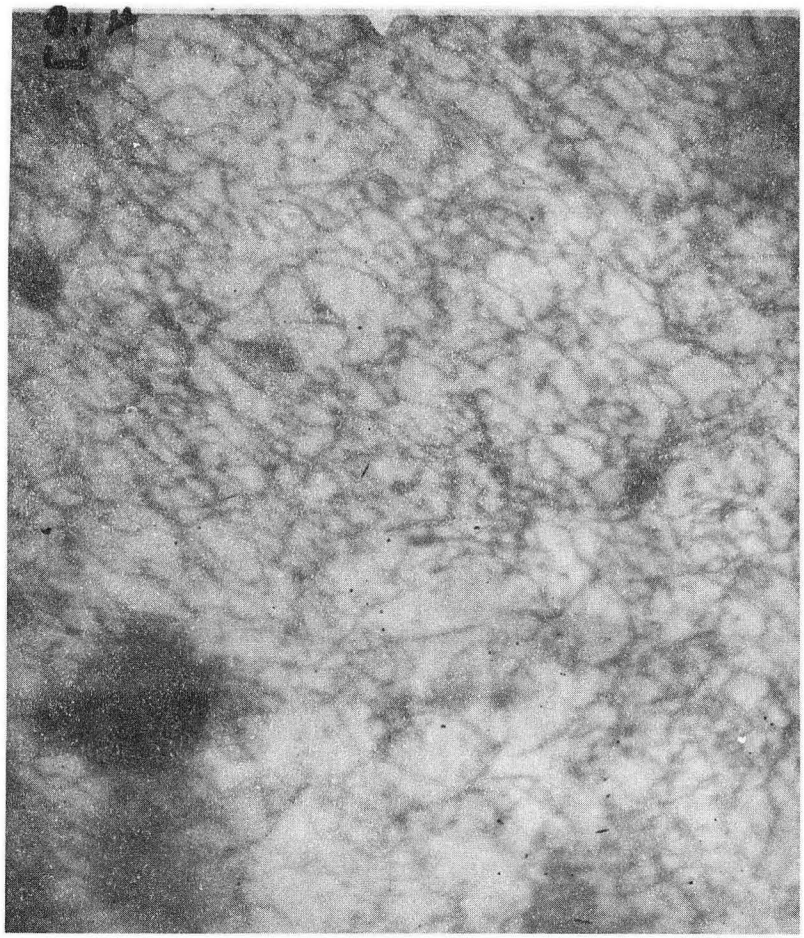

ZN-3493

Fig. 3.6. Region of severe entanglement leading to large density of loops and edge dipoles.
(Al-1% Mg crept to ε = 0.037 at 300°C under 3745 psi.)

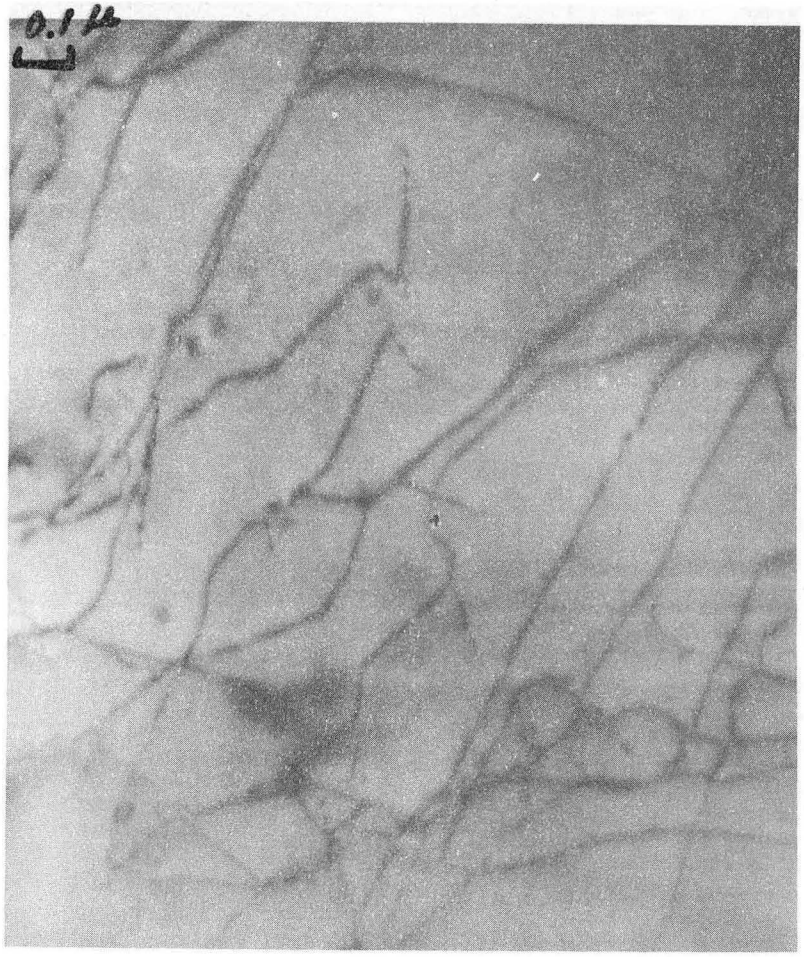

ZN-3495

Fig. 3.7. Region showing more or less free dislocations. (Al-1% crept to ε = 0.026 at 303°C under 2200 psi.)

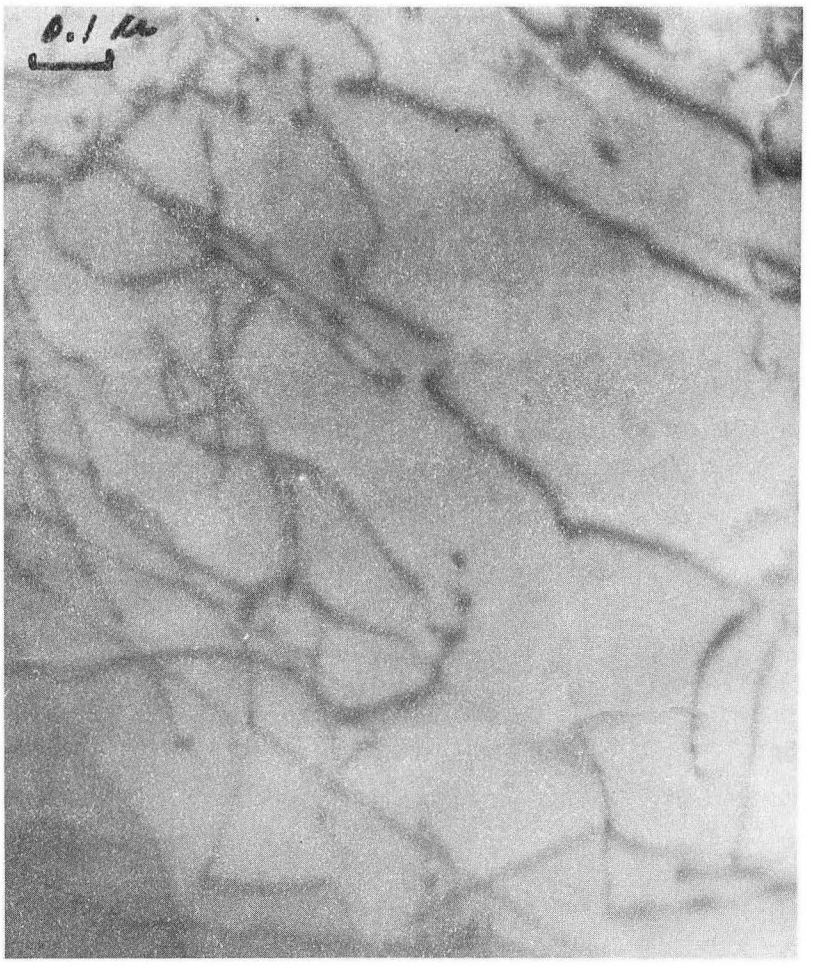

ZN-3497

Fig. 3.8. More or less free dislocations and some dipoles. (Al-1% Mg crept to ε = 0.026 at 303°C under 2200 psi.)

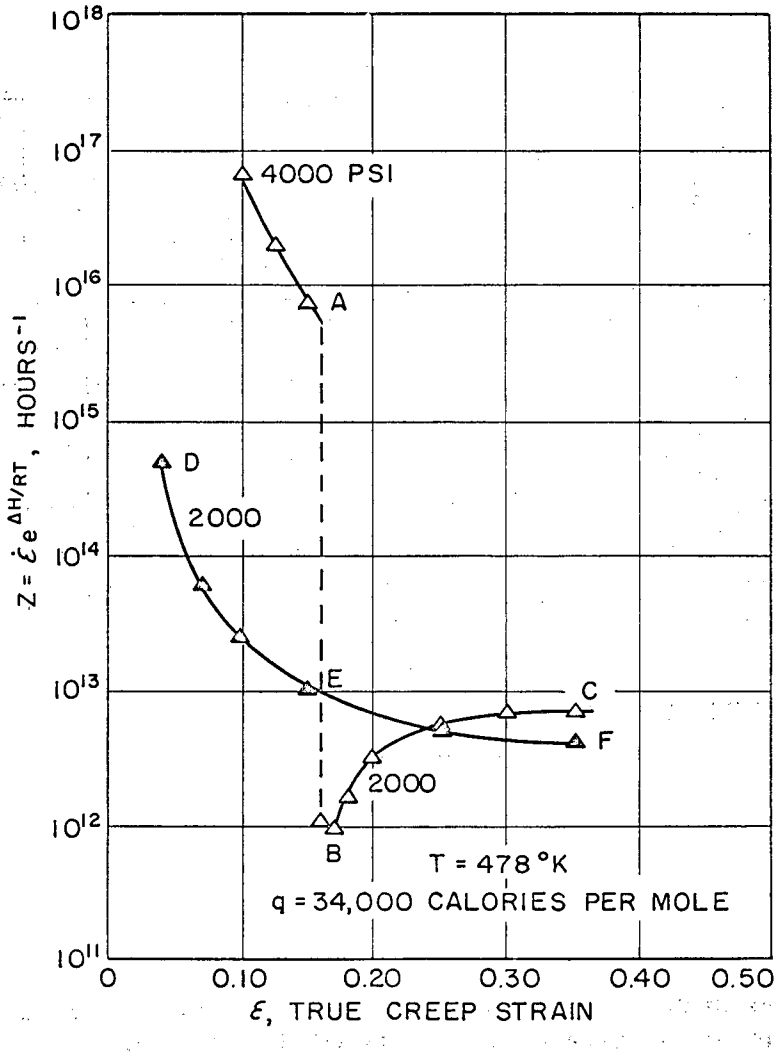

MU-29103

Fig. 3.9. Effect of change in stress on creep rate of aluminum. (After Sherby, Trozera and Dorn.)

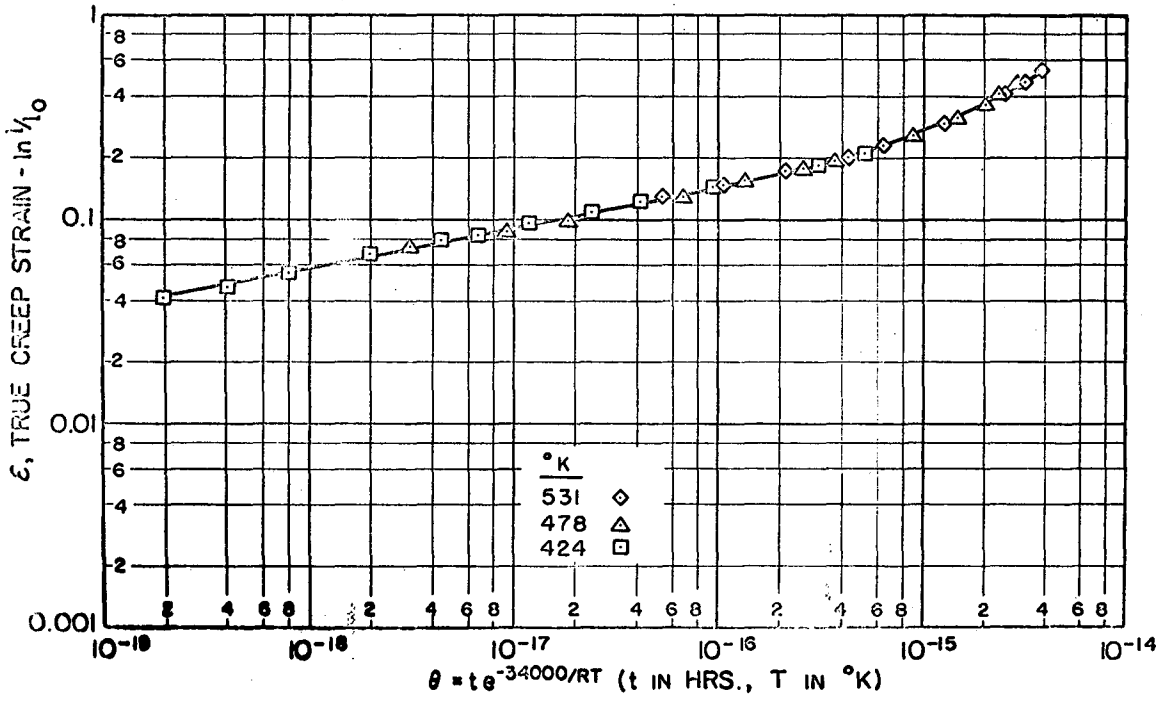

MU-29104

Fig. 3.10. Creep strain as a function of the temperature compensated time for a constant true stress of 3000 psi.

function of $te^{-q/kT}$ and have about the same apparent activation energy as creep itself.

19. When we define the apparent activation energy for creep by, q', where

$$q' = \frac{\partial \ln \dot{\gamma}}{\partial(-1/kT)} = \frac{\Delta \ln \dot{\gamma}}{\Delta - \left(\frac{1}{kT}\right)}$$

we again find that q' is a constant that is insensitive to the stress level and the strain.

20. The values of q and q' obtained by the techniques described above agree very well with each other.

21. Additional confirmation of the significance of diffusion to the creep rate was illustrated by the interesting correlation shown by Sherby.[36] The self-diffusivity of Fe in austenite is known to increase with carbon content. As shown in Fig. 3.11,[36] an analogous increase in the secondary creep rate also is obtained.

22. Furthermore, as shown in Fig. 3.12,[40] the values of q and q', for many pure metals, agree quite well with the activation energies for self-diffusion.

23. For low and moderate stresses, as shown in Fig. 3.13,[27, 41] the secondary creep rate is related to the stress by

$$\dot{\gamma}_s = A\tau^n \qquad T = const$$

where $2.5 \lesssim n \lesssim 5.5$, dependent on the metal under test.

24. Introducing an empirical activation energy suggests that

$$\dot{\gamma}_s = A' e^{-q/kT} \tau^n$$

The nominal validity of this equation for a number of metals was recently reviewed by McLean and Hale, as shown in Fig. 3.14.[42] The agreement is good at the lower stress levels but the creep rate appears to increase

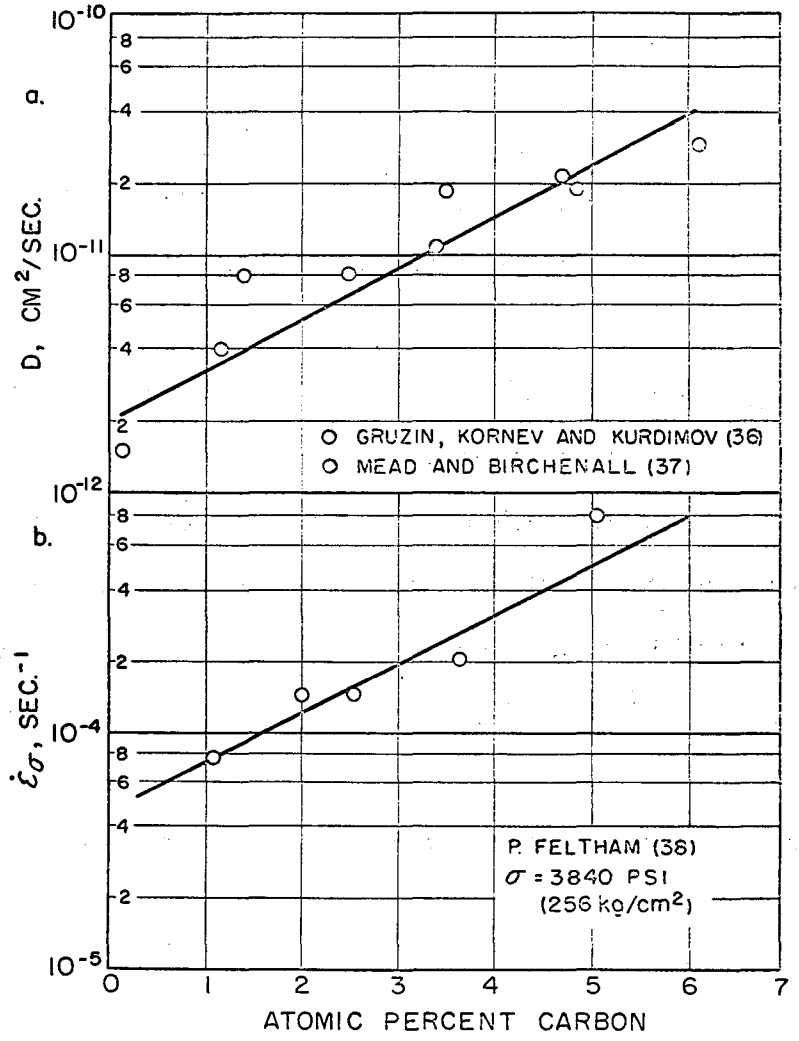

Fig. 3.11. Effect of carbon on the diffusion rate and creep rate of gamma iron at 1000°C. (After Sherby.)

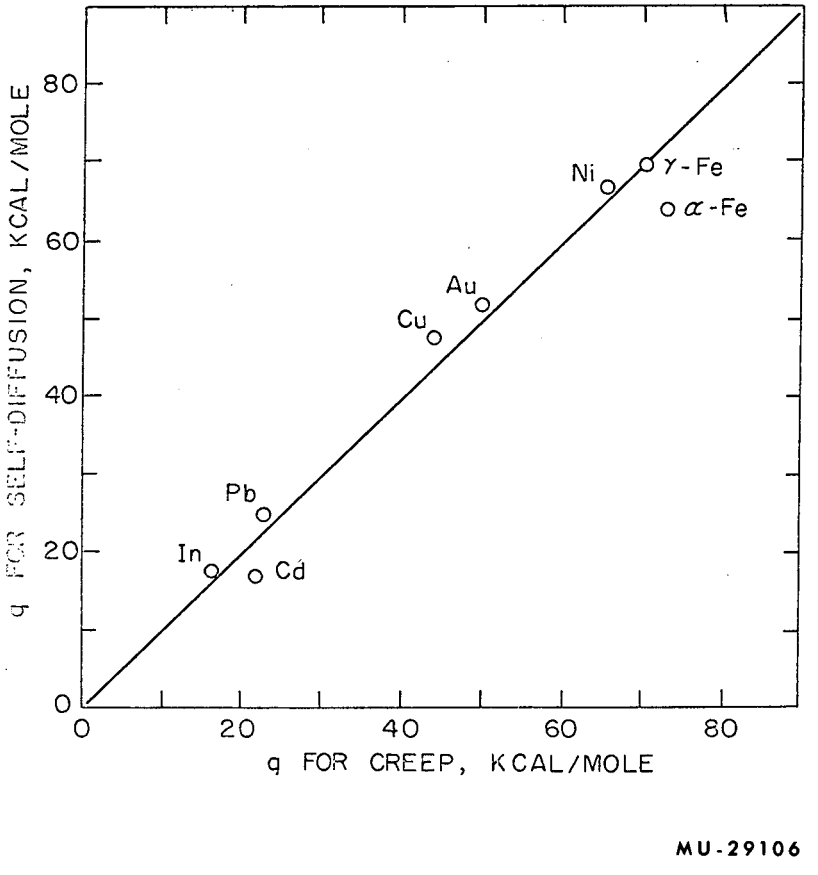

Fig. 3.12. Activation energies for high temperature creep and self-diffusion.

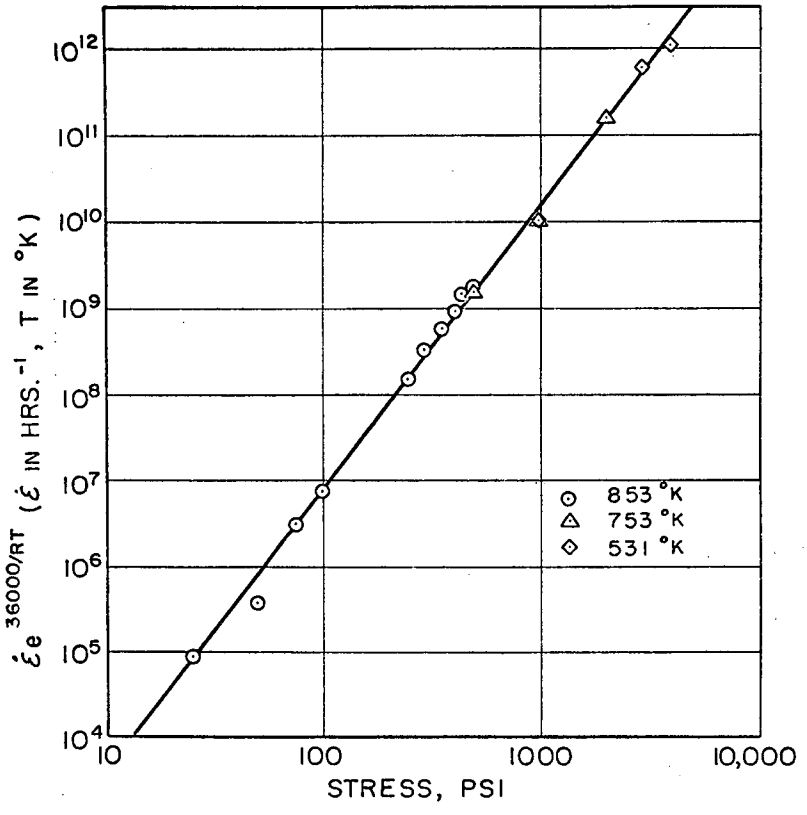

Fig. 3.13. Effect of small stresses on the creep rate of aluminum containing 3.1 atomic percent magnesium. (After Laks.)

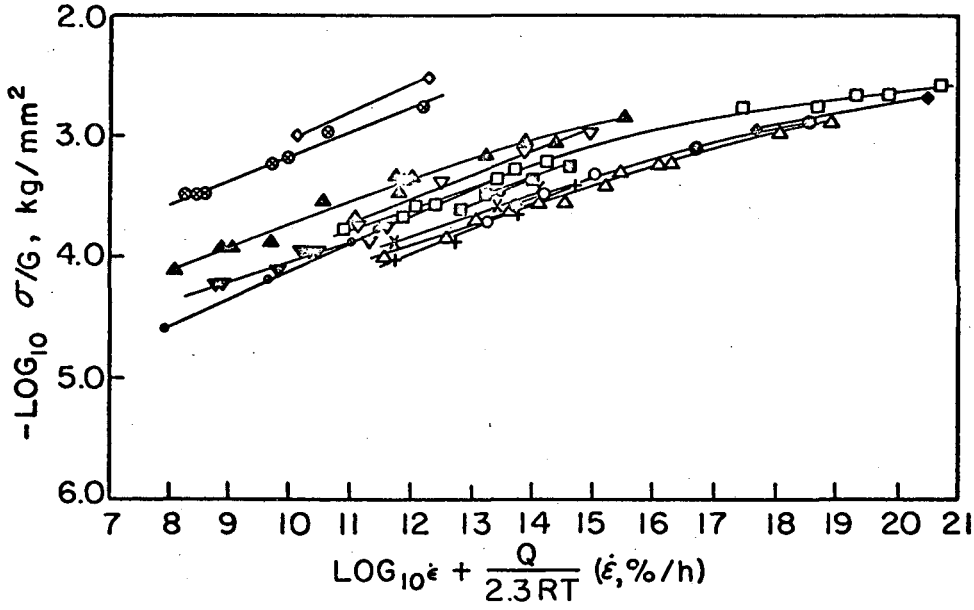

Symbol	○	● +	▽	◇	⊗	△
Metal and temp. °C	Al, 200°	Al, 204° Al, 371°	70-30 brass 400°	Cd, 25-149°	Cu, 400°, 500° 630°, 700°	αFe, 550°, 700°
Ref.	43	44	45	46	47	42

Symbol	▣	□ •	◆	X	▲	▼
Metal and temp. °C	γFe, 950°, 1000°	Ni, 400°, Ni, 1100°	Pb, 25°	Sn, 130°-230°	αTl, 62-215°	βTl, 234-280°
Ref.	48	49	50	46	51	

MUB-1580

Fig. 3.14. Correlation of creep data according to equation of paragraph 24. (After McLean and Hale.)

slightly more rapidly than with a fixed power of the stress at the higher stress levels.

25. Decrease in stress tests, for creep at the higher stress levels, as shown in Fig. 3.15,[27,52] reveal that

$$\dot{\gamma} \propto e^{\beta\tau} \qquad T = \text{const}$$

where β appears to be insensitive to the temperature and substructure.

26. When, in the course of a high temperature creep test, the stress is removed, the elastic strain recovers immediately, following which some time-dependent negative creep takes place as shown by Bayce, Ludemann, Shepard, and Dorn.[53] We necessarily conclude that some dislocations are restrained in moving forward by barriers that provide back stresses.

27. Butcher[54] has shown that the creep rate for a constant shear stress test decreases when the hydrostatic pressure, p, is increased according to

$$\frac{\partial \ln \dot{\gamma}}{\partial p} = -\frac{K\Omega_o}{kT}$$

where Ω_o is the atomic volume. In the cross slip region $K \simeq 1.4$, but at higher temperatures where the activation energy approximates that for self-diffusion $K \simeq 0.80$. This is in good agreement with the value expected when the activation enthalpy for creep is equal to that for self-diffusion and $h_c = h_d = U_d + p\Omega_d$.

The above mentioned experimental observations constitute the major factors for which any reasonable theory of high-temperature creep must account. Although other issues of lesser importance might be added to this summary, they do not appear to be as critical for the formulation of a theory as those recorded above.

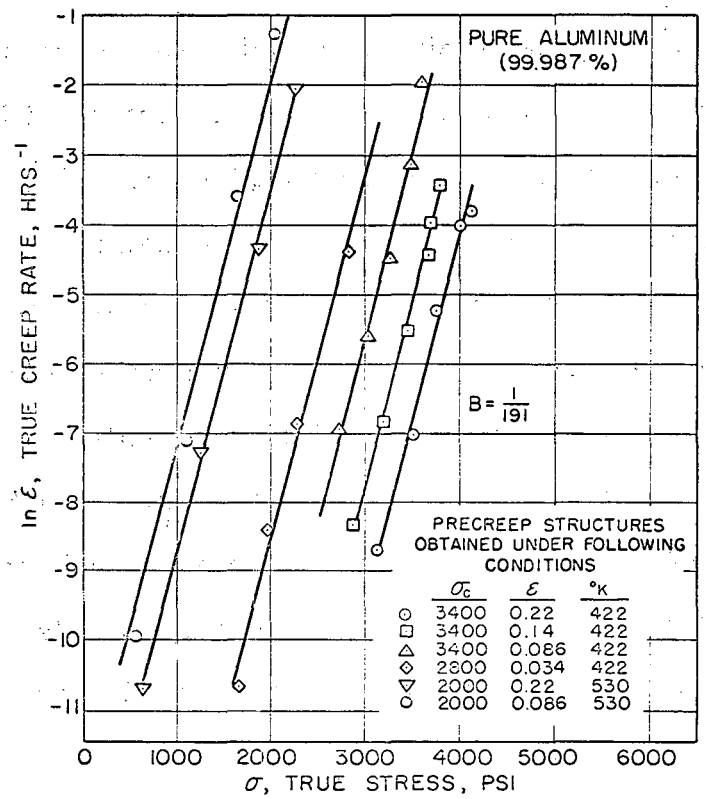

MU-29108

Fig. 3.15. Effect of stress on the creep rate for a constant structure. (After Sherby, Frenkel, Nadeau and Dorn.)

4. Qualitative Description of A Theory for Creep of Pure Polycrystalline Metals at High Temperatures

We will now formulate the theory for creep of pure polycrystalline metals at high temperatures based on the motion of jogged screw dislocations and the climb of edge dislocations. In doing so we will borrow extensively from previous theoretical deductions. But we will so adjust the assumptions to agree more accurately with the known facts, which were described in Sec. 3 of this report, than was done in previous formulations of this problem. Although the end result will provide a better appreciation of creep than was available heretofore, particularly the primary stage, a complete solution of the problem in all of its generalities cannot yet be given. This arises because several significant issues are not yet understood in sufficient detail to provide the desired analytical formulation, and also because high Peierls energy materials and very low stacking fault energy metals, might creep by different mechanisms than those formulated here.

We will confine our attention to pure polycrystalline high stacking fault energy metals that are creeping at temperatures above one-half of their melting temperature. Under these conditions we will assume that the activation energies for the Peierls mechanism, intersection and cross-slip are so much less than 50 kT, that these processes take place almost instantaneously.

As creep takes place dislocations move to the subgrain boundaries. But since the creep rate is not affected by the disorientation of adjacent subgrains, the subgrain boundaries merely serve as sinks for the dislocations. As shown by Li,[55] stress fields due to subboundaries are short

range and, therefore, they do not introduce any appreciable long-range back stresses on the moving dislocations. Subgrains are formed in high stacking fault energy metals by the non-homogeneous stressing at the grain boundary due to the different orientations of the adjacent grains. The local bending moments and torques to which each grain is subjected also increase with the applied stress. Consequently, finer subgrain sizes are produced by the higher stresses. On this basis we assume that the significant creep-rate controlling mechanism is determined by the motion of dislocations within each subgrain and we here dissociate our analysis from the subgrain-size considerations that played a role in some of the previous theories of high temperature creep.

Although most of the dislocations in creep specimen reside in the subgrain boundary, transmission electron microscopy reveals that there are also dislocations in the subgrain volume. Some of these dislocations are responsible for continued creeping; but the question arises as to how free dislocations are formed. They might arise as a result of escape from the subgrain boundaries and grain boundaries, or they maybe produced at grain boundaries from permanent Frank-Read sources in the subgrain, from generation of dislocations at points of high stress concentration in the volume or on the boundary of the subgrains, by multiplication due to cross-slip, or by climb over barriers and from entanglements. Since the subgrain boundaries are presumed to be sinks, it is unlikely that they permit escape of dislocations when the stress is held constant. There is no evidence of multiplication of dislocations in high-temperature creep by either primary Frank-Read sources or at points of stress concentration. Cross-slip and climb, however, can provide the necessary generation of free dislocations. As a result of cross-slip and climb, each subgrain

continues to contain in its volume a number of moving dislocations. Subgrain volume dislocations are never completely exhausted as a result of migration to the subgrain boundaries because of facile cross-slip and because of climb from entanglements. Therefore there is no need to postulate the existence of special Frank-Read sources, as was done in some of the previous theories on high temperature creep, which neglected the role of screw dislocations, facile cross-slip, and climb from entanglements in their formulation.

Dislocations produced by cross-slip migrate under the applied stress. As the cross-slipped segment bows out, edge components are formed. Such edge components, although jogged, can move very rapidly until they are arrested at some barrier, because the jogs on edge dislocations can move conservatively. But the forward motion of the jogs on screw segments of dislocations, restrain the motion of these segments because they move nonconservatively and therefore require the formation, diffusion and annihilation of either vacancies or interstitials. Since the energy of formation of an interstitial is extremely high, however, the motion of jogged screw dislocations must be almost exclusively attributed to the vacancy mechanism.

Screw dislocations can undertake several different processes, dependent on the local geometry: (1) Screw dislocations of opposite signs on the same slip plane will annihilate each other; (2) screw dislocations of the opposite sign on nearby slip planes can cross-slip and annihilate each other; (3) some can leave the subgrain and enter twist boundaries; (4) and others will cross-slip to provide additional dislocations.

As shown by Friedel,[56] the length, l_j, between unit high jogs on a straight screw dislocation will be given by

$$b/\ell_j = e^{-g_j/kT} \tag{4.1}$$

under equilibrium conditions where b is the Burgers vector, and g_j is the free energy of formation of a jog. When, however, a screw dislocation is moving, additional jogs having heights of p atomic planes, where p can be more than unity, are formed. Therefore moving screw dislocations can have many more jogs than the static equilibrium number dependent on the frequency of double cross-slip. There are several consequences of cross-slip: (1) When the superjog length on the cross-slip plane is longer than $2\Gamma / b(\tau - \tau^*)$, the jog itself will act like a Frank-Read source and so can provide a supply of dislocations on the cross-slip plane. Here Γ is the line energy per unit length, τ is the applied stress and τ^* is the back stress due to other dislocations. Other possibilities are shown in Fig. 4.1, (2) when L' is longer than $\frac{2\Gamma}{(\tau - \tau^*)}$ and the jog HI is sufficiently high so that the positive and negative screw edge segments of the dislocations can pass each other, the section IJ permits continued multiplication of dislocations like a Frank-Read source; (3) when L' is longer than $2\Gamma / b(\tau - \tau^*)$, but FG is sufficiently short so that $FG < \frac{Gb}{8\pi(1-\mu)(\tau - \tau^*)}$ (G = the shear modulus of elasticity and μ is Poissons ratio), a dipole FF' and GG' of positive and negative edge dislocations is formed; (4) But when L is shorter than $2\Gamma/b(\tau - \tau^*)$, the situation over ABCD prevails. Here the continued motion of the dislocation results in either the formation or adsorption of vacancies at the jog, dependent upon whether the jog at BC is a vacancy forming or an interstitial forming jog respectively.

Dipoles also form when positive and negative edge segments of dislocations on two nearby slip planes cannot pass each other. Because

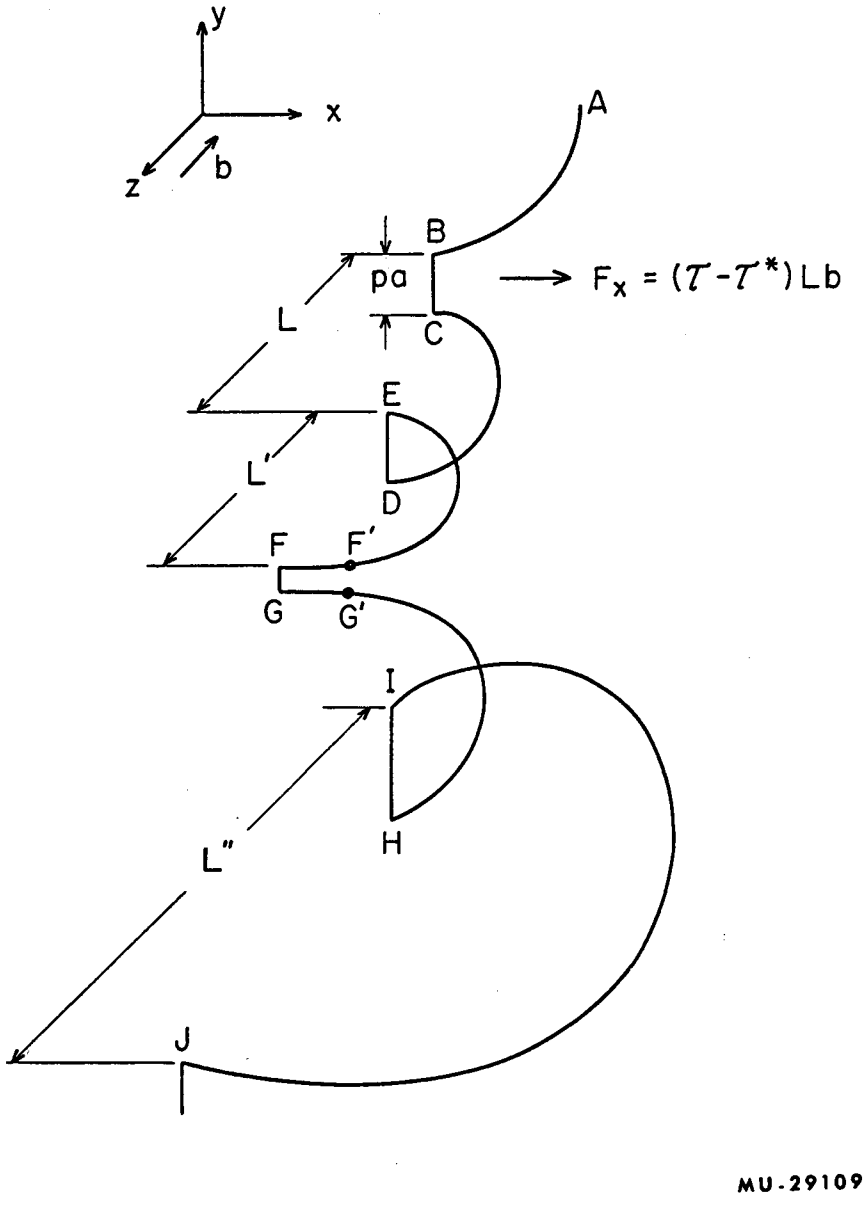

Fig. 4.1. Classes of jogs.

piled-up arrays of dislocations are not seen in transmission electron micrographs of crept metals, long-range back stresses cannot arise from this source. But there are other sources of back stress fields that provide barriers that cannot be surmounted by thermal fluctuations. We have already mentioned the formation of positive and negative edge dislocation dipoles, which constitutes one example of stress field interactions. Such dipoles, although they have no long-range stress fields, can nevertheless interact with other dislocations in their immediate vicinity. Other stress field barriers that cannot be surmounted by thermal fluctuations can arise from screw dislocations under certain conditions. When screw dislocations are severely jogged, they move slowly and introduce back stresses on other nearby screw dislocations. Entanglements are undoubtedly excellent sources of interacting stress fields. The recovery of some of the plastic strain where the stress is removed following high temperature creep attests to the presence of such back stresses.

The preceding deductions then suggest the following summary of our model for high-temperature creep: (1) Dislocations in high stacking fault energy crystals cross-slip with ease at high temperatures; (2) Edge components move rapidly but become arrested near dislocations of the opposite sign on nearby slip planes forming dipoles; (3) Other dipoles are formed by cross-slip of the screw segments of dislocations; (4) Entanglements are produced in the subgrain volumes perhaps due to interactions between dipoles and glissile dislocations and as a result of facile cross-slip; (5) Continued creep however depends on the motion of jogged screw dislocations; (6) As we shall see, both vacancy forming and interstitial forming jogs can move with about the same velocity at high temperatures; (7) But the presence of the dipoles and entanglements limits the length of

the glissile screw segments of dislocations; (8) And back stresses restrain their motion; (9) If the dipoles did not recover, the subgrains would become cluttered up with dipoles and the creep rate would become vanishingly small; (10) The positive and negative dislocations of the dipoles annihilate each other by the climb mechanism; (11) The creep rate, however, as seen by this model depends on the motion of jogged screw dislocations; (12) The substructure in the volume of the subgrain provides more substantial barriers and the length of the glissile screw dislocations decreases over the primary stage of creep, thus accounting for the decreasing creep rate; (13) But the secondary creep rate is reached when the rate of annihilation of the dipoles and entanglements by climb equals their rate of formation; (14) The subgrain boundaries play only a rather passive role in this process so long as the stress is constant.

5. Quantitative Formulation of a Theory for Creep of Pure Polycrystalline Metals at High Temperatures

The quantitative theory for high temperature creep that will be presented here, is formulated in terms of the concepts discussed qualitatively in Sec. 4. Although some of the details of each issue that is involved have been stated previously in the literature, they will be briefly reviewed here again for the sake of completeness. The only new issue concerns the viewpoint that will be taken and how the individual items will be specialized and introduced into this reformulation to provide a more complete and more realistic theory of high temperature creep than those that were presented previously. We shall particularly emphasize the primary stage of creep since this has been largely neglected in the past.

High-temperature creep will be considered to be controlled by the thermally activated motion of jogged screw dislocations. This subject has already been discussed by Mott,[57] Seeger[58] and Friedel.[59] The approach we will use here is based essentially on the discussion by Hirsch and Warrington.[60] The strain rate due to the motion of jogged screw dislocations is simply

$$\dot{\gamma} = {}^{s}\rho \, b \, {}^{s}v$$

where the superscripts refer only to the screw components, ${}^{s}\rho$ being the total length per unit volume and ${}^{s}v$ is the mean velocity of the active screw dislocations. We emphasize the point that ${}^{s}\rho$ is the total length of the moving screw dislocations. It does not include screw dislocations held up at barriers or incorporated in the entanglements. The reason for this definition of ${}^{s}\rho$ will become clear later.

The mean velocity of a screw dislocation depends on the details of the mechanism that takes place at the jog. As shown in Fig. 5.1, the

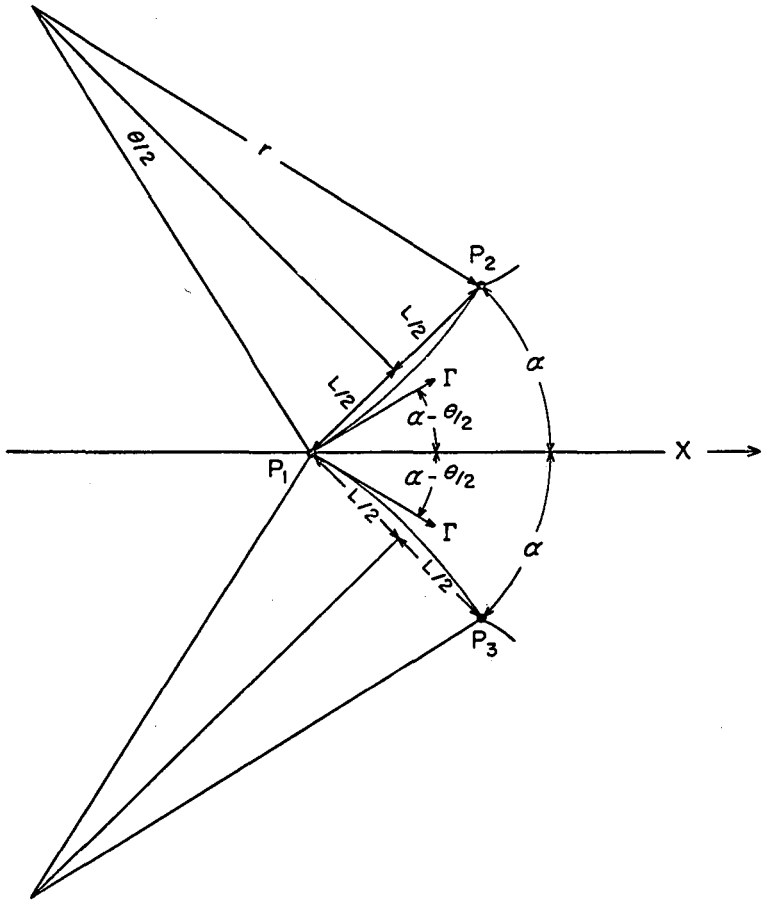

MU-29110

Fig. 5. 1. Force on a jog due to a stress.

motion of the dislocation is restrained at the jogs P_2, P_1, and P_3, etc. But as a result of the local stress $\tau - \tau^*$, the screw dislocation will bow out and acquire a radius of curvature given by

$$r = \frac{\Gamma}{b(\tau - \tau^*)} \tag{5.1}$$

Thus a force

$$F_x = 2\Gamma \cos(\alpha - \theta/2) = 2\Gamma(\cos\alpha \cos\theta/2 + \sin\alpha \sin\tfrac{\theta}{2}) \tag{5.2}$$

acts to move the jog forward. But since

$$\sin\theta/2 = \frac{L}{2r} = \frac{(\tau - \tau^*)\ell_j b}{2\Gamma} \tag{5.3}$$

and

$$\cos\theta/2 = \left\{r^2 - \left(\ell_j/2\right)^2\right\}^{1/2}/r = \left\{1 - \left[\frac{(\tau - \tau^*)\ell_j b^2}{2\Gamma}\right]^2\right\}^{\frac{1}{2}} \tag{5.4}$$

the angle $\theta/2$ depends only on ℓ_j and $(\tau - \tau^*)$. If the most difficult process occurs at P_1, the point P_1 will lag behind P_2 and P_3 causing α to decrease and therefore the force on P_1 to increase. Thus local adjustments of this type give a rather uniform forward motion of all of the jogs. As a statistical average, therefore, the mean force per atom plane height is

$$\frac{F_x}{p} = (\tau - \tau^*)\frac{\ell_j b}{p} \tag{5.5}$$

But since long-range back stresses vary periodically over the volume of a lattice such that $\int \tau^* dv = 0$, the mean force acting on a unit height of a

jog on a moving dislocation is simply about

$$\frac{F_x}{p} = \frac{\tau L b}{p} \tag{5.6}$$

As described by Friedel,[56] thermal fluctuations assist the mean force acting on each atomic plane height of the jog to either produce or absorb vacancies respectively, dependent on whether the jog is a vacancy forming or an interstitial forming jog. For example, the net frequency of the absorption of a vacancy at an interstitial forming jog is given by

$$\nu_i = \nu\left(\frac{n^-}{n_s}\right)(z-1)\, e^{-g_m/kT}\, e^{\frac{\tau l_j b^2}{pkT}} - \nu(z-1)\, e^{-g_f/kT}\, e^{-g_m/kT} \tag{5.7}$$

where

ν = the Debye frequency

$\frac{n^-}{n_s}$ = the probability of a vacancy being adjacent to the jog

n_s = the number of lattice sites per unit volume

n^- = the number of vacancies per unit volume of the jog

z = the coordination number

$e^{-\frac{g_m}{kT}}$ = the probability of a thermal fluctuation needed to move the vacancy to the jog

g_m = the free energy of activation for the motion of a vacancy

$\frac{\tau l_j b^2}{p}$ = the average work done by the applied stress per vacancy absorbed.

g_f = the free energy for the formation of a vacancy.

Whereas the first term following the equality gives the frequency of absorption of a vacancy, the second term refers to the frequency with which a vacancy can be produced at this jog. Diffusion of vacancies is known to occur so rapidly at temperatures above one-half of the melting temperature that $n^- \simeq n_o$, the equilibrium concentration of vacancies.

Therefore $n^-/n_s \simeq n_o/n_s$. Since the super jog of the screw dislocation moves forward one Burgers vector per p vacancies that are produced

$$\dot{\gamma} = \frac{{}^s\rho b^2}{p}(z-1)\,\nu e^{-g_d/kT}\left\{e^{\tau l_j b^2/pkT} - 1\right\} \tag{5.8}$$

where $g_d = g_f + g_m$ is the free energy for activation of diffusion. A similar expression is readily obtained for the forward motion of a vacancy forming super jog. No special consideration need be given the interstitial forming jogs, since they can move with about the same velocity as vacancy forming jogs. Very likely, however, some of the interstitial forming jogs will slide conservatively along the screw dislocation and thus be annihilated as suggested by Hirsch.[61]

Although the qualitative bases for the formulation if Eq. 5.8 for high temperature creep are rather sound, it is yet necessary to show that it is in good quantitative agreement with the experimental facts. The major issues concern whether it predicts reasonably accurately both the effect of temperature and the effect of stress on the creep rate. Unfortunately a simple direct comparison is not obtainable inasmuch as the substructural changes taking place over the primary stages of creep are dependent on the stress. Thus the substructural parameters ${}^s\rho/p$ and l_j/p appearing in Eq. 5.8 might depend implicitly on the stress as well as the substructure.

The apparent activation energy, obtained by the effect of an abrupt change in temperature on the creep rate is given by

$$g = \frac{\partial \ln \dot{\gamma}}{\partial(-1/kT)} = \frac{\partial \ln {}^s\rho}{\partial\left(-\frac{1}{kT}\right)} + h_d - \frac{e^{\frac{\tau l_j b^2}{pkT}}\,\tau l_j b^2/p}{\left\{e^{\frac{\tau l_j b^2}{pkT}} - 1\right\}} \tag{5.9}$$

where hd is the enthalph for diffusion, and is obtained from the well-known thermodynamic relationship

$$h_d = \frac{\partial \left(g_d / kT \right)}{\partial \left(1/kT \right)} \tag{5.10}$$

The presence of the term involving the change in the density of screw dislocations with temperature arises from the fact that the interaction stress fields of dislocations decrease as the temperature increases. Consequently some dislocations that are just at rest near a peak interaction stress will be released when the temperature is increased. It is expected, however, that this contributes only a small positive term to q. Since the observed activation energy for high temperature creep is known to be about equal to that for self diffusion, it necessarily follows also that $\tau l_j b^2 <$ pkT for the cases studied. Under these conditions, the apparent activation energy for creep is independent of the stress and differs only slightly from that for self diffusion.

A further justification of the smallness of l_j /p is obtained when we consider the known effects of abrupt decreases in stress on the creep rate. We suggest here that

$$\beta = \frac{\partial \ln \dot{\gamma}}{\partial \tau} = \frac{\partial \ln {}^{s}\rho}{\partial \tau} + \frac{\frac{l_j b^2}{pkT} e^{\frac{\tau l_j b^2}{pkT}}}{\left\{ e^{\tau l_j b^2 / pkT} - 1 \right\}} \tag{5.11}$$

The major difference, therefore, between previous formulations of the theory for the motion of jogged screw dislocations and the present one concerns retention of the first term following the second equality sign. It arises from the fact that dislocations within the subgrain interact with

each other. As shown schematically in Fig. 5.2, the interaction stresses τ^* vary over the slip plane. When a stress τ_2 is applied, all the dislocations excepting 'f will be moving through the crystal. But when the stress is changed to τ_1 dislocations c and d will no longer contribute to the total length of moving dislocations. Thus ${}^s\rho$ decreases for a given substructure as τ is decreased. It has been shown in Sec. 3 of this report that β is insensitive to the temperature, an experimental fact which requires that

$$l_j b^2/\rho kT < \frac{\partial \ln {}^s\rho}{\partial \tau}$$

This suggests that most of the effect of changes in stress on the creep rate must arise from the change in the density of moving dislocations with stress. According to this interpretation, the creep data for Al require that l_j cannot be much greater than about 40b. Therefore the distance between the jogs of moving dislocations is less than the equilibrium distance

$$l_j = b e^{+g_i/kT} \tag{5.12}$$

where g_i is the free energy of formation of a jog. But since we have confined out attention to high stacking fault metals in which cross-slip can occur easily, the small value suggested for l_j is quite reasonable.

Partial confirmation of the validity of Eq. 5.8 was obtained by the low stress tests on creep of Al which were reported some time ago by Harper and Dorn.[16] For low stresses Eq. 5.8 reduces to the linear relationship between strain rate and stress

$$\dot{\gamma} = \frac{{}^s\rho\, l_j (Z-1) \nu b^4}{\rho^2 kT} e^{+s_d/k} e^{-h_d/kT} \tau \tag{5.13}$$

The creep curves at the lower stress levels gave practically zero initial straining and gave the secondary creep rate almost immediately, indicative

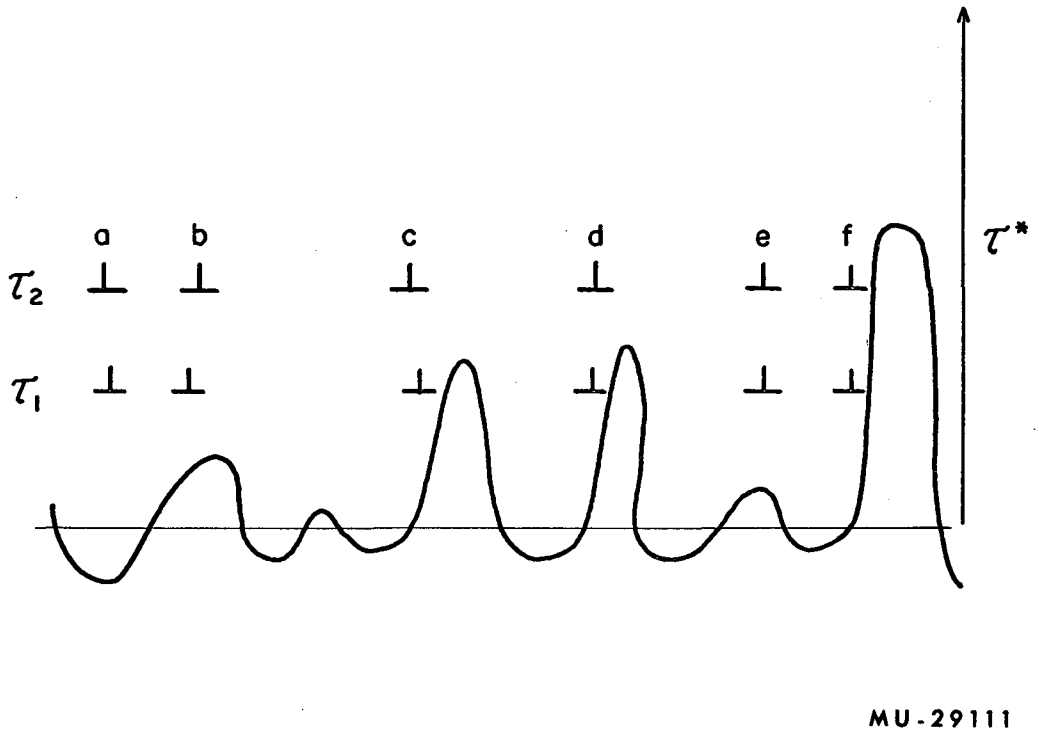

Fig. 5.2. Schematic of variation of interaction stresses τ^* over the slip plane.

of the concept that only negligible changes in substructure took place. The apparent activation energy for creep was found to be 35,500 cal./mole, and the steady state creep rate shown in Fig. 5.3 as a function of stress was obtained. Using the values of

$$D_o = \frac{b^2 \nu}{6} e^{\Delta_d/k} \simeq 5$$

$z = 12$

$b = 2.86 \times 10^{-8}$ cm

we deduce that $\frac{{}^s\rho\, l_j}{p^2}$ has the value of about 1.6×10^{-5} cm^{-1}. In view of the low stresses employed here, the density of moving dislocations as low as is suggested by the small value of $\frac{{}^s\rho\, l_j}{p^2}$ is quite possible.

When stresses above about 1.2×10^6 dynes/cm^2 are applied, the usual initial creep strain followed by primary creep is obtained, the creep rate no longer being linear with the stress. Under these circumstances Eq. 5.8 should apply. Since l_j is not expected to vary much with stress or temperature, we must assume that ${}^s\rho$ is the major pertinent structural variable. The initial straining upon loading increases the number of dislocations present. During the course of primary creep, however, ${}^s\rho$ must decrease as dislocations enter either the subgrain boundaries or entanglements and as more effective barriers to the motion of dislocations are established. The decreasing creep rate over the primary stage of creep is therefore directly related to the decreasing density of the mobile dislocations.

Inasmuch as no direct measure of l_j/p has yet been established, it is not possible to accurately determine the value of ${}^s\rho$. The trends, however, can be illustrated by arbitrarily selecting l_j/p to equal, for example, the not unreasonable value of 20b. The values of ${}^s\rho$ obtained for this rather arbitrary illustration are shown in Fig. 5.4.[62] These values

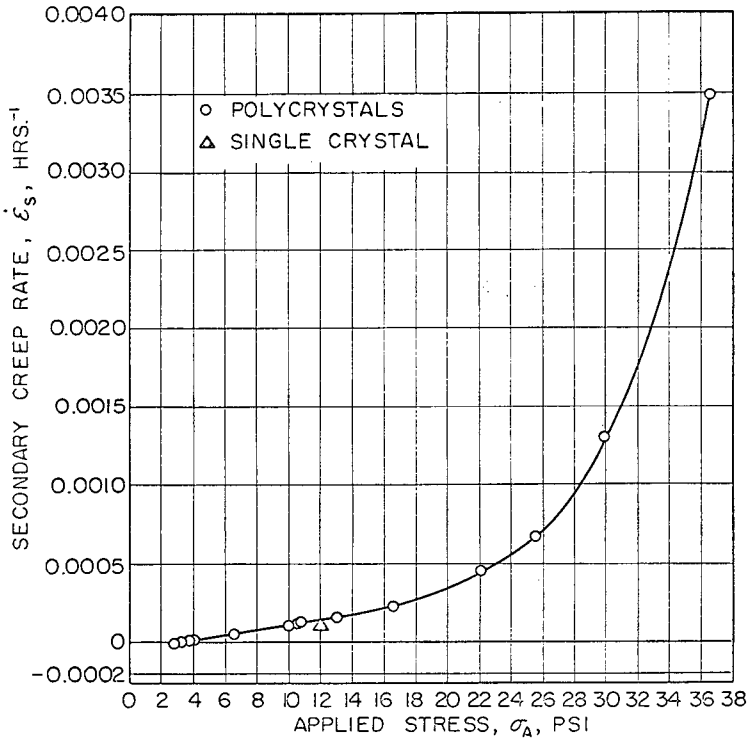

MU-29112

Fig. 5.3. Effect of low stresses on the secondary creep rate of high purity aluminum at 920°K. (After Harper and Dorn.)

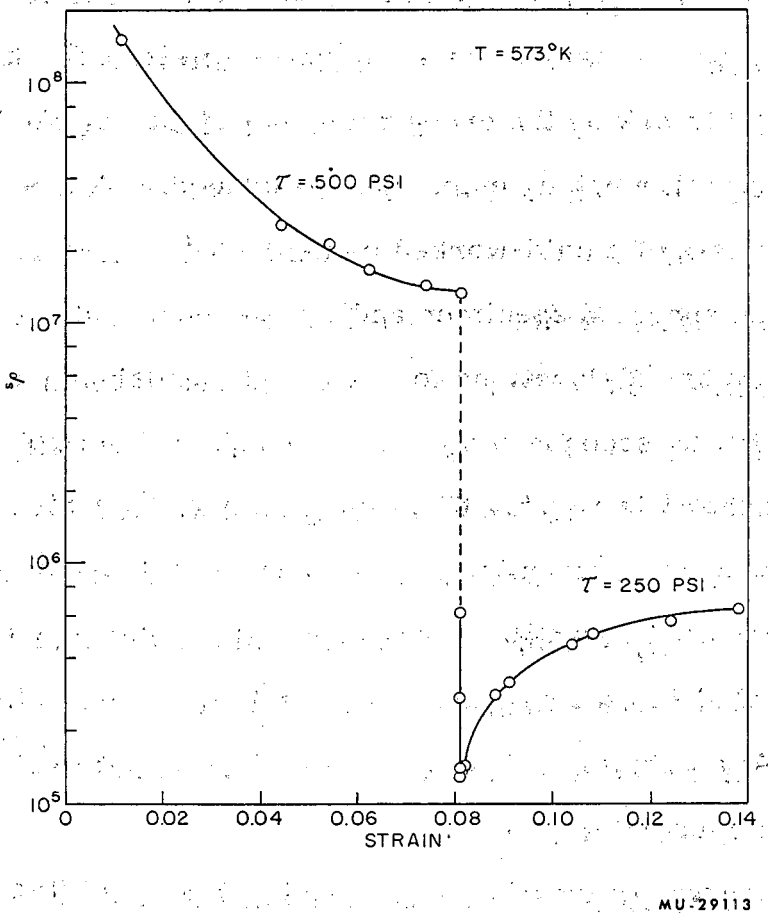

Fig. 5.4. Variation of the density of moving screw dislocations with strain in pure annealed aluminum. (Unpublished data of Raymond.)

of ${}^{s}\rho$ are not unreasonable, particularly in view of the fact that selection of somewhat higher values of l_j would result in lower estimates of ${}^{s}\rho$. It therefore appears that this theory is consistent with all of the experimental facts.

The concept that ${}^{s}\rho$ is the major substructural variable in the high-temperature creep of many metals is further confirmed by the study of the effect of cold work on the creep resistance. During cold work many dipoles and extensive entanglements are produced. We therefore expect that the creep rate of a cold-worked metal would therefore be much less than that for an annealed specimen and that recovery during creep, which would release extra dislocations for flow would result in an increasing creep rate until the secondary stage is reached. The validity of this suggestion is shown in Fig. 5.5 for severely cold-worked Al. The activation energy for creep was determined to be 36,000 cal/mole. Using the same assumed values of $l_j/p = 20b$, as in the example of the high temperature creep of annealed Al, the calculated value of ${}^{s}\rho$ increases with creep of cold-worked Al as shown in Fig. 5.6. Again lower values of ${}^{s}\rho$ are possible by selecting higher values of l_j.

The secondary stage of creep occurs when the rate of generation of substructure due to creep itself is balanced by the rate of disappearance of the substructure by recovery. Therefore additional information concerning creep can be obtained from recovery investigations. As we have seen, however, the substructure is quite complex, consisting of liberated dislocations, dipoles and entanglements in addition to subgrains. It is for this reason that no wholly satisfactory theory has yet been developed for the secondary creep rate.

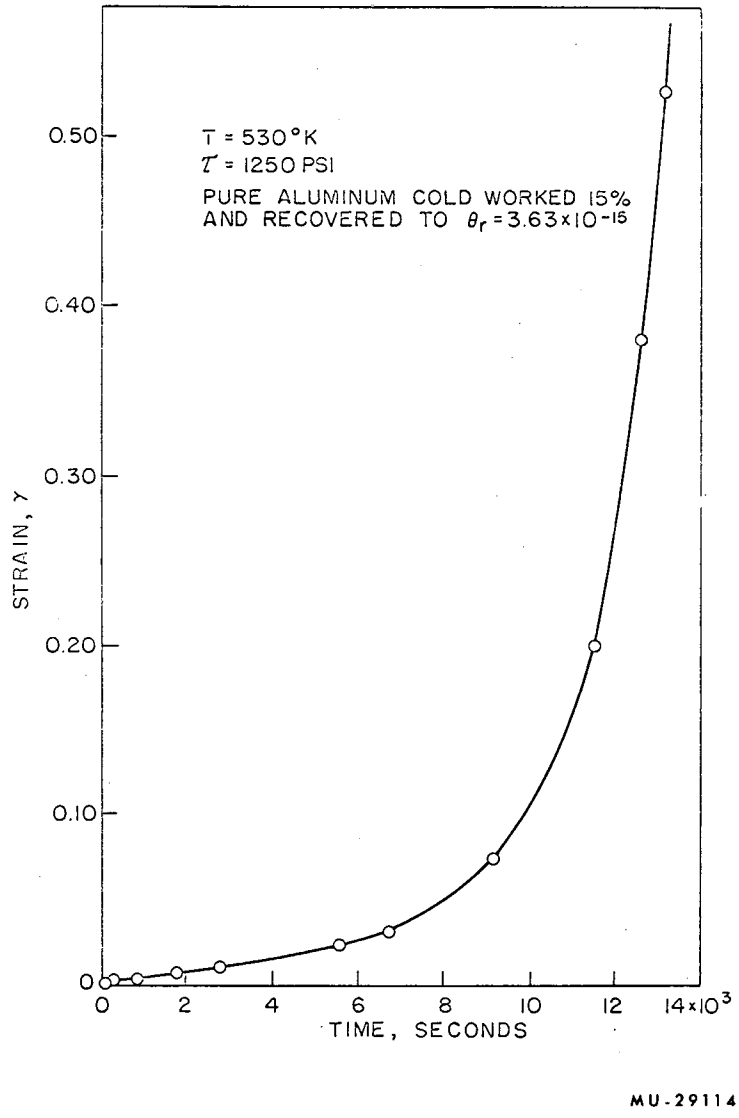

Fig. 5.5. Plot illustrating the increasing creep rate of pure aluminum.

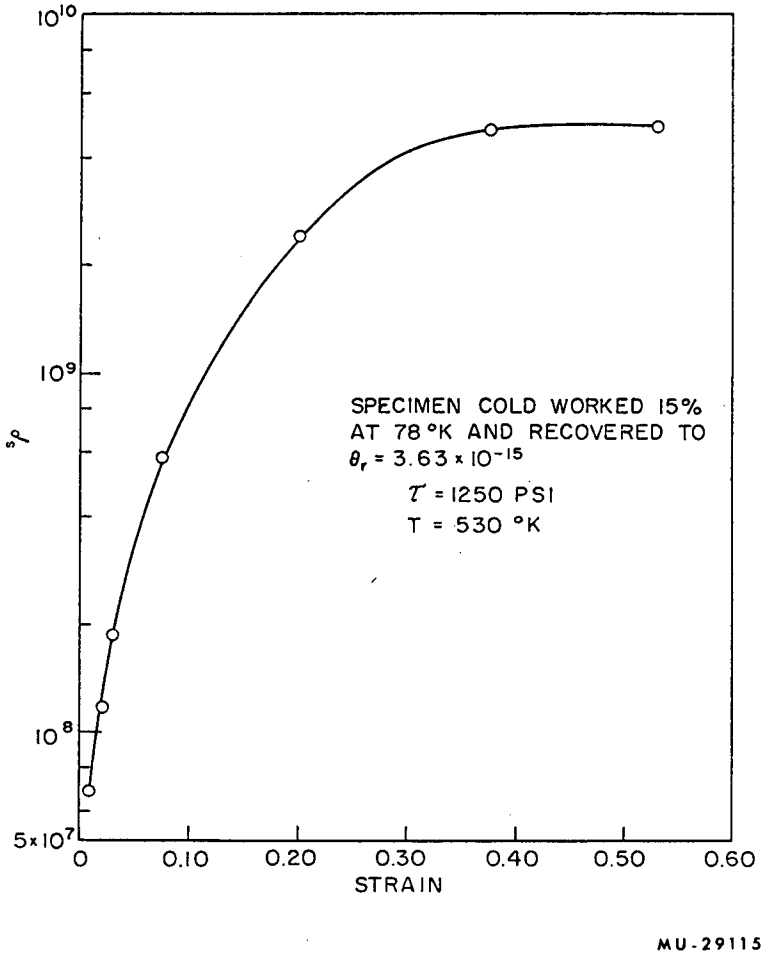

Fig. 5.6. Variation of $^s\rho$ with strain in cold worked pure aluminum.

The entanglements that are observed, appear to be the most significant substructural details seen in crept specimens of high stacking fault energy materials. And therefore a complete understanding of high temperature creep must depend on more detailed knowledge of how and why they form and how they might recover. Lacking sufficient information on this issue, we might nevertheless attempt some crude alternate analyses: For example, the existence of a steady state during the secondary stage of creep demands complete microscopic balance between the rate of formation and the rate of annihilation of any one of the numerous significant substructural details. Thus, although we cannot yet treat entanglements satisfactorily, we might first approach the easier problem of studying the formation and disappearance of dipoles. The analysis to be given here differs only slightly in content, but nevertheless significantly in concept from that suggested by Chang.[48]

We will let $n\{y\}$ be the number of dipoles per unit volume where the positive and negative edge dislocations are a distance y apart. We will assume that such dipoles are eliminated by climb induced by the stress σ_{xy} as shown in Fig. 5.7. Therefore the net rate of formation of dipoles of height y is given by

$$\frac{dn}{dt}\{y\} = (n\nu_c)_{y+a} - (n\nu_c)_y + k\{y\}^5 \rho \nu \tag{5.14}$$

where ν_c is the frequency for a unit climb. Therefore $(n\nu_c)_{y+a}$ is the number of dipoles that are gained as a result of climb from a separation $(y + a)$ to a separation y, $(n\nu_c)_y$ are those of height y that are lost due to climb, ν_c is the frequency of a unit climb and $k\{y\}$, the number of dipoles of height y that are formed as a result of slip of screw dislocations per unit area, can (to a good first approximation) be taken as a small constant. If L is the mean free path of cross-slip, elementary

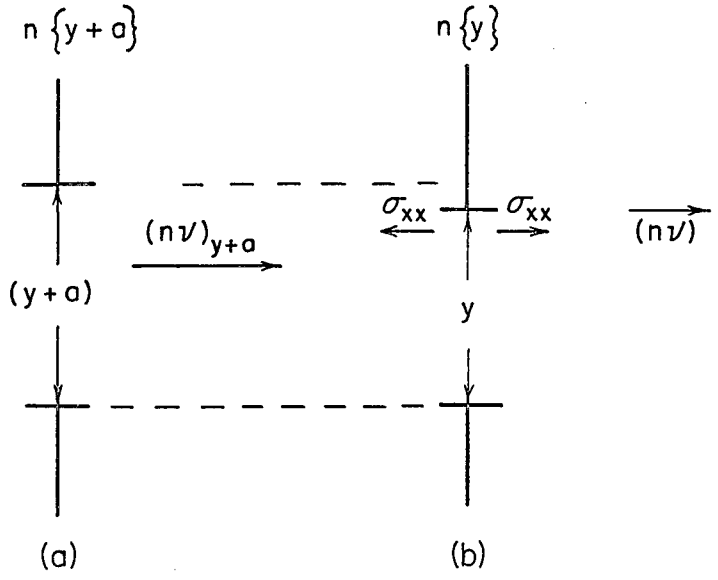

$$\sigma_{xx} = \frac{Gb}{8\pi(1-\mu)y}$$

MU-29116

Fig. 5.7. Elimination of dipoles by stress induced climb.

statistics demands that $k\{y\} = k_o e^{-y/L}$ and therefore at the secondary stage of creep, where $dn/dt = 0$, we have $\frac{\partial (n_s v_c) a}{\partial y} + k_o e^{-y_s/L} \times {}^s\rho_s v = 0$. This equation is readily integrated to give $n_s \equiv n_s(y)$.

The maximum value of y above which dipoles cannot form is $y_m = \frac{Gb}{8\pi(1-\nu)\tau}$.[63] For steady state conditions of n at y_m we have, from Eq. 5.14 that

$$(n_s v_c)_{y_m} = k_o e^{-y_m/L}\, {}^s\rho_s v$$

or

$$ {}^s\rho_s v = \frac{n_{s y_m} v_{c y_m}}{k_o e^{-y_m/L}} \tag{5.15}$$

Thus the secondary creep rate can be expressed either by

$$\dot{\gamma}_s = {}^s\rho_s b v = \frac{{}^s\rho_s b^2}{p}(Z-1) \nu e^{-g_d/kT}\left\{e^{\frac{\tau l_j b^2}{pkT}} - 1\right\} \tag{5.16}$$

in terms of the motion of jogged screw dislocations or by

$$\dot{\gamma}_s = \frac{n_{s at y_m} v_{c at y_m}}{k_o e^{-y_m/L}} \tag{5.17}$$

in terms of climb. Using Friedel's[56] expression, for climb we have

$$v_{c at y_m} = p_j \nu (Z-1) e^{-g_d/kT}\left\{e^{\frac{\sigma_{xx}\Omega}{kT}} - 1\right\} \tag{5.18}$$

where p_i is the probability of finding a jog on the climbing edge dislocations, Ω is about the atomic volume and

$$\sigma_{xx} = \frac{Gb}{8\pi(1-\mu) y_m}\tau$$

Consequently, expanding the term in the brackets of Eq. 5.16 into a Taylors series

$$\dot{\gamma}_s = n_{s at y_m} p_j \nu b (Z-1) e^{-g_d/kT} \frac{\tau\Omega}{k_o kT} e^{\frac{Gb}{8\pi L(1-\mu)\tau}} \tag{5.19}$$

Although this expression gives the experimentally observed activation energy for secondary creep, it is yet incomplete since n_s at y_m depends on the stress. The same criticism can be leveled at all previous theories purporting to determine the stress laws for the secondary creep rate. All previous theories for creep by climb developed the stress laws by introducing questionable assumptions. The eventual solution of the problem of steady state creep will depend on a more intimate understanding of the formation, nature, and recovery of the substructure, particularly entanglements, and the introduction of these concepts into a simple theoretical structure.

In order to obtain the empirical relationship that the secondary creep rate increases with the stress to the fifth power, Christy[64] and Weertman[65] had assumed that climb was induced by piled-up arrays of dislocations. But such arrays are not seen and therefore the details of their approach are highly suspect. On the other hand it is possible that the stress fields induced by entanglements lead to stress concentrations that are found necessary to give a creep rate that varies with about the fifth power of the stress.

From the viewpoint of understanding the variation of substructure during creep on the creep rate, the most important observation is contained in the empirical expression discussed in Sec. 3, that

$$\dot{\gamma} = f(\theta) \qquad \text{when } \tau = \text{constant} \tag{5.20}$$

where $\theta = te^{-\frac{q}{kT}}$. Therefore

$$\dot{\gamma} = \frac{\partial f}{\partial \theta}\frac{\partial \theta}{\partial t} = f'(\theta)\, e^{-q/kT} \tag{5.21}$$

Consequently, if the theory for creep based on the motion of jogged screw dislocations is to be acceptable, we must associate $f'\{\theta\}$ with ${}^{s}\rho$ such that

$$\frac{{}^{s}\rho b^2}{p}(z-1)\nu e^{+\Delta_d/kT}\left\{e^{\frac{\tau l_j b^2}{pkT}}-1\right\} \simeq f'\{\theta\} \tag{5.22}$$

for a given stress, assuming that q is to be associated with approximately U_d.

Although a completely satisfactory proof of the nominal validity of Eq. 5.22 is not yet available, it is possible to crudely set forth the fact that the theory for the motion of jogged screw dislocations, supplemented with recovery by climb, gives, at least very closely, the relationship demanded by experiment.

The rate of change of the density of screw dislocations depends on the rate at which they are born as a result of climb from entanglements, etc., minus the rate at which they enter the subgrain boundary or are otherwise arrested at entanglements or other points in the subgrain volume. We crudely let this be

$$\frac{d\rho}{dt} = \frac{N\rho^*}{\bar{t}_c} - k_1 \rho\nu \tag{5.23}$$

where N is the number of regions for climb per unit volume, ρ^* is the length of screw produced per released dislocation and $\bar{t}_c$ is the mean time of release of a dislocation due to climb. The first term beyond the equality therefore refers to the rate of formation of dislocations by climb whereas the second term states that their rate of disappearance depends on $\rho\nu$. When the previously discussed values for $\bar{t}_c$ and $\rho\nu$ are introduced, we immediately see that $\frac{d\rho}{dt}$ depends on the temperature principally through $e^{-\frac{U_d}{kT}}$. The major virtue of the proposed theory, therefore, resides in

the fact that, at least to a first approximation, it does account for the observed relationship of Eq. 5.20.

It is not proposed that all materials creep at high temperatures as a result of the motion of jogged screw dislocations. The Peierl's mechanism, cross slip, or some other process might be strain-rate controlling for prismatic slip in hexagonal metals and in some intermediate phases. Even when the motion of jogged screw dislocations determines the creep rate, some minor variants of the proposed theory might apply. For example, at temperatures near or slightly below one-half of the melting temperature, two variations of the proposed theory become possible, 1) Vacancies produced at jogs might not be able to diffuse away sufficiently rapidly and in this case h_d must be replaced by the smaller quantity h_f where h_f is the enthalpy for the formation of a vacancy in a supersaturation of vacancies. Here also the reverse reaction must be formulated to take such excess vacancies into account, 2) Alternately diffusion may take place along the cores of the dislocations. Here h_d in the theory must be replaced by the smaller value of h'_d which equals the sums of the enthalpies for formation and motion of vacancies along the dislocations.

Metals having low stacking fault energies might form piled-up dislocation arrays which would necessitate retaining the long-range back stress term, τ^*, in the formulation of the theory and perhaps modify the role of climb of dislocations in the recovery mechanism. Low stacking fault energy metals are expected to cross-slip less frequently and thus should exhibit higher values of l_j. From the practical viewpoint this suggests that the jogged screw dislocations in such metals will have higher velocities, but they will not climb as rapidly. The latter suggests that such metals should reach the secondary stage of creep earlier and that their secondary creep

rate should be lower than that for the higher stacking fault metals. From this basic viewpoint, lower stacking fault metals should give apparent activation energies, q, that decrease linearly with the applied stress. Furthermore, the strain rate sensitivity, β, should be slightly temperature sensitive. These two effects should also be noted in the higher stacking fault metals that are deformed at higher stress levels.

In the previous discussion it was assumed that p_j, the probability of finding a jog, was always high, there being an ample supply of jogs to permit rapid climb. If this is not the case, p_j might be given by the equilibrium number of jogs, $e^{-g_i/kT}$, where g_i is the free energy of formation of a jog. In this event the enthalpy term, h_d in the equation for climb must be replaced by $h_d + h_j$ where h_j is the enthalpy for the formation of a jog. It is also possible under forced climb that the jogs are being used up more rapidly than new ones are created. In this event the term hd in the climb equation must be replaced with $hd + h_j'$ where h_j' approaches the activation enthalpy for the formation of a jog and is therefore greater than h_j.

Although these variations in the theory need to be considered, the current evidence suggests that Eq. 5.22, is nevertheless, in good agreement with the known facts. The missing information concerns the theoretical determination of how ρ_i^s changes during the course of creep and how, in detail, it depends on stress, structure and time. This formulation, of course, must be based on more complete evidence from electron microscopy relative to the types of substructure that are significant to creep.

6. Polyphase Alloys

All highly creep resistant alloys contain at least two phases and at least one of these is hard and strong. Three separate types of creep resistant polyphase structures, shown schematically in Fig. 6.1, exist, And all three types of structures can coexist at one time in a single polyphase alloy. Each type of structure is significantly different from the others, and each provides its own unique mechanism of creep strengthening. Such structures can change during the course of creep by more precipitation, overaging, and spheroidization; furthermore, dislocations in the matrix can interact with the solute atoms that are present. We will postpone consideration of such complications for the present and also confine our attention to cases where the polyphase structure remains reasonably stable during the course of creep.

Each structure has its own unique effect on the creep resistance of a polyphase alloy. The alloy that has a continuous hard phase about the ductile matrix can only creep as the hard phase itself either creeps or fractures. When the continuous phase is tenacious, strong and stable, highly creep resistant alloys are obtained, but they will be brittle at low temperatures.

Creep in each soft matrix grain of the aggregated alloy must take place in a fashion analogous to that of an alpha solid-solution alloy. But, dislocations will pile-up at the boundary of the hard phase resulting in back stresses on other dislocations in the soft grains and thereby arresting their motion. Such back stresses can be relieved by recovery in the soft matrix grain, deformation of the hard phase as a result of high stress concentrations, and also fracturing of the hard brittle phase. The aggregated structure has lower creep resistance than the two remaining types.

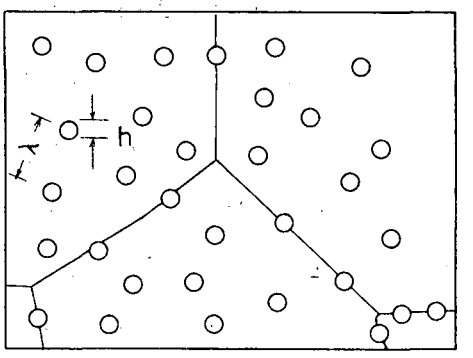

A. DISPERSION ALLOY.

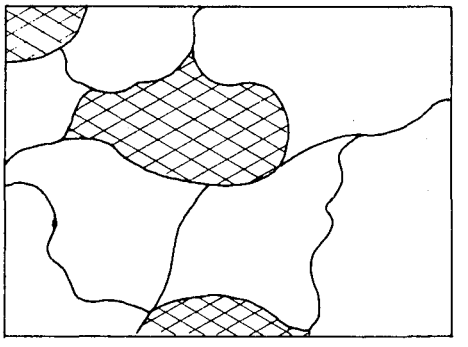

B. AGGREGATED ALLOY.

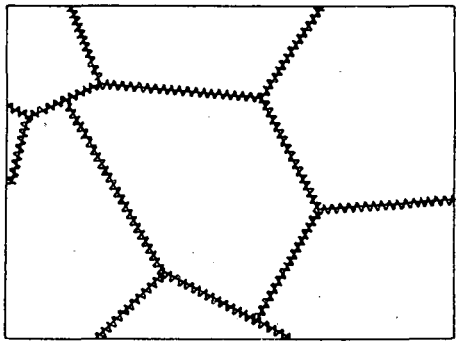

C. CONTINUOUS HARD PHASE ALLOY.

MUB-1579

Fig. 6.1. Schematic diagram of creep resistant polyphase structures.

The most commonly practiced method of improving the creep resistance consists in forming a rather stable dispersion strengthened alloy by precipitation hardening. Dispersed particles in the boundaries of the matrix grains serve to prevent grain boundary shearing. This not only reduces the creep rate by the amount of grain boundary shearing, but it also results in the presence of higher back stresses on dislocations by the amount the back stresses would have been relaxed by grain boundary shearing. Moving dislocations in the grain of a dispersion strengthened alloy can interact in various ways with the dispersed particles; they might cross-slip, climb, cause deformation in the particles, or fracture of the particles. It is not surprising that, in view of the complexity of this problem, very little quantitative experimental work or theoretical analyses have been made to foster a better understanding of the creep of polyphase alloys.

As discussed by Grant and Preston[66] in their 1956 review of the subject and as presented more recently by Guard[67] in the 1960 A.S.M. Symposium on Strengthening Mechanisms in Solids, current theories of dispersion strengthening are based on Fisher, Hart and Pry's[68] extension of Orowan's[69] original concept. Orowan suggested that as slip takes place, dislocation loops can extrude between adjacent particles on the slip plane, as shown in Fig. 6.2. Consequently the yield strength τ depends on the particle spacing λ according to the Frank-Read equation

$$\tau - \tau^* = \frac{\Gamma}{b\,\lambda/2} \tag{6.1}$$

where τ^* is the back stress acting on the moving dislocations. Fisher, Hart and Pry further suggest that the loops of dislocations left about the

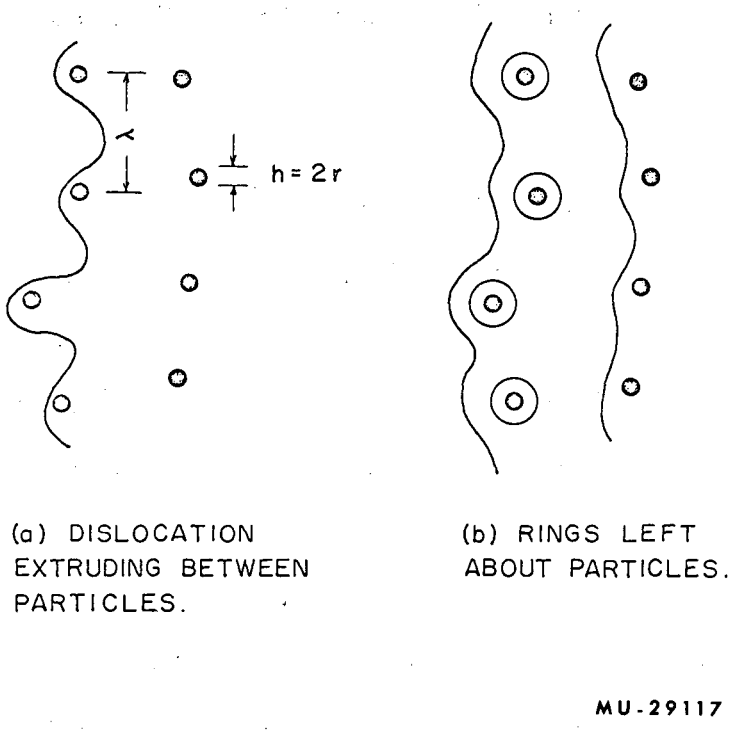

Fig. 6.2. Schematic of dislocations extruding between particles as suggest by Orowan.

particles result in a back stress

$$\tau^* = \frac{3NGbf^{3/2}}{r} \tag{6.2}$$

where

N = the average number of loops about the particle and depends on the strain

r = the mean particle radius and

f = the volume fraction of dispersed phases

which causes very rapid strain hardening. Therefore the flow stress for plastic deformation depends on the particle spacing λ and the mean particle radius, r . The finer the dipersion, the greater is the strengthening. At low temperatures they assumed that the hardening increased with strain as a result of the increasing number of loops about the particles. The maximum hardness that can be achieved is either that which causes plastic deformation or fracture of the particle under the stress concentrations due to piled-up dislocations. Under a constant stress, a fixed strain results when the back-stress fields due to arrested dislocations and loops equals the applied stress.

Weertman,[70] and Ansel and Weertman[71] have shown that deformation of a dispersion hardened alloy under constant stress can continue to take place at high temperatures as a result of climb of dislocations. They assumed that dislocations originated at fixed Frank-Read sources, of which there are M distributed at random per unit volume. Under the action of an applied stress, dislocations move out from these sources producing a series of concentric rings about the sources to a maximum radius L , until they interact with each other and thus stop the sources. When the dislocations in the outermost rings from the series of sources

climb and annihilate each other, an area πL^2 is swept out per source. Consequently, the steady state creep rate should be given by

$$\dot{\gamma}_s = M \pi L^2 b / \bar{t}_c \tag{6.3}$$

where $\bar{t}_c$ is the average time for complete climb of a dislocation. If however the near sources reside on slip planes about a distance h apart

$$M \pi L^2 h \simeq 1$$

and, therefore

$$\dot{\gamma}_s = \frac{b}{h \bar{t}} \tag{6.4}$$

where the height of climb, h , is now associated with the mean height of the particle.

Weertman[70] suggested that two types of creep laws were operative dependent on the stress. When $2\Gamma/bL < \tau < 2\Gamma/b\lambda$ dislocations cannot form loops about the particles, but Weertman suggests that they nevertheless climb. From the frequency of a unit climb given by Eq. 5.18, we obtain

$$\frac{1}{t} = \frac{a\nu(Z-1)}{h} p_j e^{-g_d/kT} \left\{ e^{\frac{\sigma_{xx}\Omega}{kT}} - 1 \right\} \tag{6.5}$$

suggesting that, since σ_{xx} is small here,

$$\dot{\gamma}_s = \frac{ba\nu(Z-1)}{h^2} p_j e^{-g_d/kT} \frac{\sigma_{xx}\Omega}{kT} \tag{6.6}$$

This coincides with Weertman's equation when σ_{xx} is taken to equal τ. It is, however, difficult to justify this equality since the major stress field that is acting in this instance arises from the image field of the blocked dislocation which gives $\sigma_{xx} = 0$ at the core of the dislocation.

At higher stress levels Weertman[70] suggests that piled-up dislocations give

$$\sigma_{xx} = \frac{2\tau^2 \lambda b^2}{G} \tag{6.7}$$

and, loops do form about the particles. The distance a loop must climb before another can form is

$$\Lambda = \frac{G^2 b^2}{2\tau^2 \lambda} \tag{6.8}$$

But it is difficult to visualize the details of climb if all loops start out on the same slip plane because here again $\sigma_{xx} = 0$. For the higher stresses Weertman gets, the equivalent of

$$\dot{\gamma}_s = \frac{2b\tau^2 \lambda a}{h G^2 b^2} \nu (z-1) p_j \cdot e^{-g_d/kT} \left\{ e^{\frac{2\tau^2 \lambda b}{Gkl}} - 1 \right\} \tag{6.9}$$

for the secondary creep rate.

Unfortunately there is practically no good data available to check Weertman's theory. The most pertinent appears to be that obtained by Giedt, Sherby and Dorn[72] a number of years ago on the creep of dispersions of $CuAl_2$ in an Al solid solution matrix. An activation energy for creep of 37,000 cal./mole was obtained, a value only 1,500 calories per mole above that estimated for self diffusion of Al and therefore in crude agreement with the theory in this respect. The secondary creep rate could be approximated in most cases by

$$\dot{\gamma}_s = A \tau^n e^{-\frac{37,000}{kT}} \tag{6.10}$$

where the average constants shown in Table 6.1 were obtained.

Table 6.1

Alloy %Cu	Temperature °K	λ cm	h cm	A	n
3.05	422	9.7×10^{-3}	1.57×10^{-4}		1.5
3.05	422	9.6×10^{-4}	$.15 \times 10^{-4}$	8.85×10^{10}	0.88
3.05	477	9.7×10^{-3}	1.57×10^{-4}	20×10^{10}	.81
3.05	477	9.6×10^{-4}	$.15 \times 10^{-4}$	64×10^{10}	.81
3.05	530	9.7×10^{-3}	1.57×10^{-4}	13×10^{11}	.63
3.05	530	9.6×10^{-4}	$.15 \times 10^{-4}$	9.64×10^{2}	1.56
3.05	578	9.7×10^{-3}	1.57×10^{-4}	20.2×10^{11}	.49
3.05	578	9.6×10^{-4}	$.15 \times 10^{-4}$	30.6×10	1.6

As noted in Table 6.1, the value of n was always greater than that suggested by theory (namely, 4 as expansion of Eq. 6.9 into a Taylor's series reveals). Furthermore A was not proportional to λ^2/h. Consequently, the theory does not agree well with the limited, somewhat scattered, data currently available.

In their creep studies on a SAP alloy, Ansel and Weertman obtained an activation energy of about 150,000 cal./mole. Since climb in a dispersion hardened Al alloy should give a value of about 35,500 cal./mole, that estimated for diffusion, the creep of SAP, as we will describe more fully later, must undertake some other mechanism than that postulated for the usual dispersion strengthened alloys.

Our understanding of high-creep resistance of dispersion strengthened alloys could be advanced appreciably by more critical experimental investigations, covering determination of the activation energy and the stress law as well as the nature of the primary stage of creep in terms of particle size and distribution. Additional work is required on the nature of the substructures

and dislocation patterns that are obtained during creep of dispersion strengthened alloys. And finally, perhaps, better theories for the high temperature creep of dispersion strengthened alloys can be developed in extending Weertman's critical and most significant concept that the secondary creep rate at high temperatures is controlled by the dislocation climb mechanism.

A more realistic approach to the problem of dispersion strengthening is based on the concept that the Orowan model gives a gross idealization of the true state of affairs. Recent electron microscopic investigations by Thomas[73] have shown that in the initial dislocation pattern, dislocations go from one to another particle. Frequently upon stressing, new dislocations are formed not at Frank-Read sources, but at the boundary of the dispersed particles and they loop out into the matrix. Thomas, Nutting and Hirsch[74] have observed that the presence of hard dispersed particles induces cross-slip. And Mitchell, Mitra and Dorn[75] have shown that most of the low temperature strain hardening of dispersion strengthened alloys does not arise from the Fisher-Hart-Pry mechanism of back stresses from concentric planar loops but rather, is due to the extremely dense dislocation population in the entanglements. Although these observations were based on the low temperature behavior of dispersion strengthened alloys, it is nevertheless reasonable to believe that most of these features with only minor modifications also apply to the creep behavior.

A tentative concept of the issues involved in the high-temperature creep of a dispersion strengthened alloy might now be suggested. In this discussion we will consider only the case of a stable dispersion embedded in a matrix wherein no interactions take place between the dislocations and solute atoms. Under these conditions, we believe that the primary stage of

creep can be described by Eq. 5.16 for the motion of jogged screw dislocations. This creep should differ from that in the dispersion free alpha solid solution due to the extensive cross-slip induced by the dispersed particles. Poly-slip and cross-slip in the neighborhood of the dispersed particles should result in a greater number of centers for entanglements and should therefore reduce the number of freely moving screw dislocations more rapidly than in a similar alpha solid solution. Due to the particles and their associated entanglements, the density of moving screw dislocations will be less at the same stress level and temperature than in an alpha solid solution. When the dislocations are highly jogged, the activation energy for creep at the lower stress levels should approximate that for self diffusion. But at higher stress levels and particularly for low stacking fault metals the activation energy for creep should decrease linearly with the applied stress. Because ρ^s, as well as the activation energy depends on the stress, it is not possible to make any reasonable predictions of the stress law for high-temperature creep of dispersion strengthened alloys at this time. The secondary creep rate should be given either by Eq. 5.16 for the motion of jogged screw dislocations or by the rate of release of arrested and entangled dislocations as a result of recovery by climb. In this model the value of σ_{xx} to be used in calculating the frequency for climb will be given by the steady state conditions of the nature and density of the dislocations in the entanglement. Such steady state conditions of course will depend on the applied shear stress. It is suggested therefore that the high creep resistance of dispersion strengthened alloys is due to the low rate at which dislocations issue by climb from the entanglements and particularly the short distances they move before they again become entrapped.

A qualitative discussion on the creep behavior of SAP in terms of dispersion strengthening was presented by Grant and Preston.[66] However, the data obtained by Ansel and Weertman[71] that the activation energy for creep of SAP is about 150,000 cal./mole, disqualifies the thought that its creep resistance follows the dispersion strengthened model. More recently, Meyers and Sherby[76] and Meyers, Shyne and Sherby[78] investigated the creep of SAP and obtained very high activation energies, much above those for the activation enthalpy for diffusion in Al and in much better agreement with that for volume diffusion of the anions in Al_2O_3. Specimens also remained rigid and were crept at temperatures above the melting temperature of pure Al. The creep behavior of SAP was therefore attributed to follow what is expected from the presence of a thin film of Al_2O_3 adhering more or less continuously to the fine grained Al.

7. Overaging and Spheroidization during High-Temperature Creep

It is well known that the creep resistance of two-phase alloy systems decreases during the course of high-temperature creep as a result of spheroidization and particle growth. The driving force for this reaction is the decrease in free surface energy; and the rate at which it takes place depends on diffusion. The continuous hard film type of two-phase alloy spheroidizes, as shown schematically in Fig. 6.1, and assumes the low creep resistant characteristics of a two-phase agglomeration. The dispersion strengthened alloy develops a more widely spaced configuration of larger dispersed particles. As a result of such coarsening there are fewer points per unit volume at which cross-slip is induced and therefore there is less jogging and fewer points where entanglements might be induced to form. This also results in a decrease in creep resistance.

Since the design of high temperature alloys for long-term high-temperature creep resistance depends on the stability of the structure, we will analyze the factors that are involved, following an earlier discussion by Schoeck.[78] The problem will be simplified by considering the coarsening rate of a spherical dispersion of an incoherent precipitate. We will not concern ourselves here with the nucleation of the precipitate, coherency stresses, precipitate shape and other auxiliary problems such as changes in composition of the precipitate.

The free energy of a system consisting of a spherical particle of n_B atoms embedded in a matrix solid solution of B atoms in A, assumed to be ideal, involves the free energies of the particle, the solution and the free surface energy. At equilibrium the change in free energy,

when one B atom is removed from the surface of the particle and deposited in solution, is zero. The free surface energy of the system is

$$^{\gamma}F = 4\pi r^2 \gamma \tag{7.1}$$

where γ is the free surface energy per unit area. And the number of B atoms in the particle is

$$^{p}n_B = 4/3 \frac{\pi r^3}{\Omega} \tag{7.2}$$

where Ω is the atomic volume. Therefore, the change in free surface energy upon adding one atom to the particle is

$$\frac{\partial\, ^{\gamma}F}{\partial\, ^{p}n_B} = \frac{\partial\, ^{\gamma}F}{\partial r}\frac{\partial r}{\partial\, ^{p}n_B} = (8\pi r\gamma)\frac{\Omega}{4\pi r^2} = \frac{2\gamma\Omega}{r} \tag{7.3}$$

The free energy per atom of the particle is

$$\frac{\partial\, ^{p}F}{\partial\, ^{p}n_B} = {}^{p}u_B + p\,^{p}\Omega_B - T\,^{p}s_B \tag{7.4}$$

where $^{p}u_B$ is the energy per atom in the particle phase, p is the pressure, $^{p}\Omega_B$ is the atomic volume, and $^{p}s_B$ is the entropy per B atom in the particle phase. Assuming an ideal solid solution with random mixing of n_A atoms and n_B atoms, the free energy of the solution is

$$^{s}F = {}^{s}n_A({}^{s}u_A + p\,^{s}\Omega_A - T\,^{s}s_A) + n_B({}^{s}u_B + p\,^{s}\Omega_B - T\,^{s}s_B) - kT\ln\frac{(n_A+n_B)!}{n_A!\,n_B!} \tag{7.5}$$

where the last term arises as a result of the configurational entropy. Therefore the chemical potential of each B atom in solution is

$$\frac{\partial\, ^{s}F_B}{\partial\, ^{s}n_B} = {}^{s}u_B + p\,^{s}\Omega_B - T\,^{s}s_B + kT\ln\frac{n_B}{n_B+n_A} \tag{7.6}$$

The total change in free energy upon transfer of one atom of B to the solution is, at equilibrium

$$-\frac{\partial {}^{p}F}{\partial {}^{p}n_B} - \frac{\partial {}^{r}F}{\partial {}^{p}n_B} + \frac{\partial {}^{s}F_B}{\partial {}^{s}n_B} = 0 \tag{7.7}$$

Letting $n_B/(n_B+n_A) = C$, the composition of the solution, and noting that at ${}^{s}\Omega_B \simeq {}^{p}\Omega_B$ and the thermal entropy at high temperature, ${}^{s}S_B \simeq {}^{p}S_B$, we obtain

$$C \simeq e^{-\frac{({}^{s}U_B - {}^{p}U_B)}{kT}} \; e^{\frac{2\gamma\Omega}{rkT}} \tag{7.8}$$

where ${}^{s}U_B - {}^{p}U_B$ is the heat of solution per B atom. Therefore, the concentration, C_0 of B atoms in equilibrium with a flat surface $(r = \infty)$ is

$$C_0 = e^{-\frac{{}^{s}U_B - {}^{p}U_B}{kT}} \tag{7.9}$$

and

$$C = C_0 e^{\frac{2\gamma\Omega}{rkT}} = C_0 e^{\rho/r} \tag{7.10}$$

where

$$\rho = 2\gamma\Omega/kT \tag{7.11}$$

Consequently, the equilibrium concentration of solute atoms about a small particle is somewhat greater than that around a large particle. Therefore, the smallest particles will dissolve and the solute will precipitate out on the largest particles until a uniform distribution of particle sizes is obtained. Final equilibrium will be achieved only when a single large spherical particle is formed in the matrix.

We now wish to estimate how long it will take for a small particle of radius r to dissolve. An exact solution to this problem is very difficult

because as the smallest particles dissolve, those of intermediate size first get larger. When all of the smallest sized particles have dissolved those that originally had intermediate sizes and therefore grew at first, now being the smallest, begin to dissolve. Fortunately an exact solution is not necessary to illustrate the principles and to identify the major factors involved.

For simplicity we consider the two particles shown in Fig. 7.1 having initial radii r_0 and r where $r_0 > r$. We assume that steady state diffusion is established and that the concentration gradient is linear between the two particles. Very little error is introduced if we assume ρ to be small relative to r. Therefore the concentration gradient between particles a distance λ apart is crudely estimated to be

$$\frac{\partial c}{\partial r} = \frac{C_0\left(e^{+\rho/r} - e^{+\rho/r_0}\right)}{\lambda} \simeq \frac{C_0 \rho}{\lambda}\left(\frac{1}{r} - \frac{1}{r_0}\right) \tag{7.12}$$

The diffusing flux is

$$\frac{d\left\{\frac{4\pi}{3}\frac{r^3}{\Omega}\right\}}{dt} = -\pi r_0^2 \frac{D C_0 \rho}{\lambda}\left\{\frac{1}{r} - \frac{1}{r_0}\right\} \tag{7.13}$$

where the term to the left of the equality gives the number of atoms leaving the smaller particle per second, D is the diffusivity, and πr_0^2 is the area of the larger particle through which the flux moves. When Eq. 7.13 is integrated for $r_0 > r$ we obtain

$$t = \frac{\lambda r^4 kT}{D C_0 \gamma \Omega r_0^2} \tag{7.14}$$

In spite of the gross approximations that were made, Eq. 7.14 suggests how the various variables enter the problem. Because $t \propto r^4$ small particles dissolve in a short time. As the particles become larger the time for their dissolution increases substantially, not only because r is increased, but also because λ is increased.

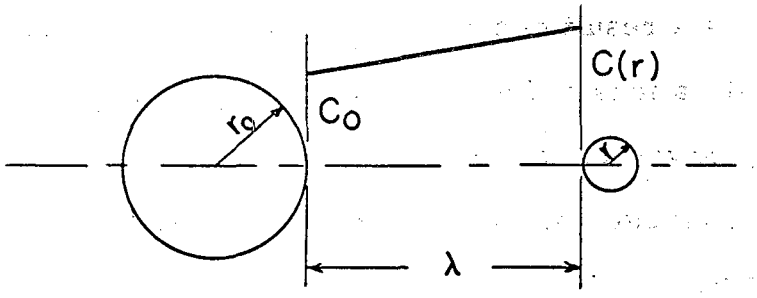

MU-29118

Fig. 7.1. Schematic of precipitate disolution.

Whereas γ and Ω usually change only mildly with the system in question, D plays a much more important role, since it can be quite different for different systems and temperatures. But the major factor in determining the time for dissolution of the smaller particles is c_o.

It is essential to point out, however, that the coarsening of a dispersion strengthened alloy during creep might proceed somewhat more rapidly than it would in the absence of creep. A small increase in the diffusivity is to be expected as a result of the excess vacancies generated at moving jogs on screw dislocations and as a result of climb of edge dislocation. More significant, however, is the fact that moving dislocations can considerably increase the average diffusivity because of rapid pipe diffusion along the dislocation core.

To illustrate the great importance of C_o, Schoeck[78] considered a Ni-Al alloy which might have either Ni_3Al or Al_2O_3 precipitates and calculated the time t for the case $r_o = 10^{-6}$cm, $r = 10^{-7}$cm, $\lambda = 1\mu$ and 700°C, as shown below

Precipitate	Diffusing Element	D	C_o	t sec.
Ni_3Al	Al	10^{-10}	$\sim 5\times10^{-2}$	$\sim 10^2$
Al_2O_3	O	10^{-7}	$\sim 10^{-14}$	$\sim 10^{11}$

whereas the small Ni_3Al particle would have dissolved in 100 seconds, the Al_2O_3 particle under similar conditions, and in spite of the higher diffusivity of O that was assumed, would take about 1000 years to dissolve.

This example illustrates clearly that the compounds having the greatest heats of formation should provide the greatest structural stability. From the viewpoint of stability, oxide dispersion strengthened alloys appear to be most

promising although some slightly less stable systems might have other advantages. Adherence between the matrix and the precipitate is also significant.

8. Effect of Solute Atoms on High Temperature Creep

Several excellent reviews[79-81] have been written on the influence of solute atoms on the mechanical behavior of alloys. Although most of what has been said pertains to the behavior of alpha solid solutions at low temperatures, some of the same principles also apply under conditions of high-temperature creep. On the other hand, the relative importance of the various strengthening mechanisms changes as the temperature is increased and new factors enter into the analyses at high temperatures. Therefore, the factors that provide great solid solution strengthening at low temperatures are not necessarily the best for developing creep resistance at high temperatures. For this reason it is appropriate to consider the special factors of solid solution effects that are particularly significant for high-temperature creep.

The high creep resistance of some complex ceramic materials is due to a high Peierls activation energy, solute atom pinning of dislocations, and high activation energies for diffusion. Among the more ductile materials, however, the highest creep resistance is achieved, as we have already discussed in Sec. 6, by the introduction of hard and stable phases in a ductile matrix of refractory body-centered cubic solid solutions. The creep resistance of such alloys is determined not only by the nature and distribution of the second phase but also on the creep resistance of the softer matrix in which the hard phase is embedded. Additional creep resistance can be achieved in a dispersion hardened alloy by further strengthening the ductile matrix. We will consider here, however, only single phase alpha solid solutions to illustrate what factors are involved.

There are a number of different effects of solid solution alloying on the creep resistance and these effects do not all vary linearly with the atomic percentage of the alloying element. Consequently the effects of two or more elements are not simply additive. Furthermore, the greatest benefits are achieved by using a series of solute elements (not just one) so selected as to provide optimum coverage of all factors involved. Although a quantitative approach to the design of alloys for creep resistance from this viewpoint has not yet been developed, qualitatively at least, these concepts are employed and the significance of this complexity effect has been recognized. Therefore, many of the highest strength high temperature alloys now in use have compositions that appear to represent a roll-call of almost all of the metallic and many of the non-metallic elements in the periodic table.

The following issues are significant in solid solution alloying for high temperature creep resistance:

A. Diffusion Effects

B. Stacking Fault Energy Modification

C. Peierls Stress Modification

D. Mott-Nabarro Hardening

E. Guinier-Preston Hardening

F. Suzuki Locking

G. Cottrell Locking

H. Fisher Short-Range Order Hardening.

We will discuss each in turn.

A. Diffusion Effects

Although we shall emphasize here the factors that lead to high temperature strengthening, it is necessary to point out that some alloying elements actually decrease the high temperature strength of alpha solid solutions.

A typical example is the alloy of C in γ- Fe. Whereas C in solution in α- Fe causes appreciable low temperature strengthening, when dissolved in sufficient quantity in γ- Fe it increases significantly the creep rate under a given stress. Sherby,[36] as noted in Sec. 3, has shown that this arises from the fact that C increases the rate of self-diffusion of Fe in γ- Fe. In general, therefore, an important effect of alloying elements on creep arises from their effect on the diffusivity. This factor, of course, has special significance to the high temperature plastic behavior of materials because diffusion is not involved in the low temperature plastic behavior, and because the high temperature plastic behavior is usually diffusion controlled. The same trend is noted in defect lattices of intermediate phases; those compositions that have a greater equilibrium number of either vacancies or interstitials exhibit lower strengths at high temperatures because of their higher diffusivities. Vacancy-solute atom binding will increase the activation energy for diffusion and improve the creep resistance.

B. Stacking Fault Energies

Dislocations lying in the (111) plane of FCC metals dissociate with a decrease in energy into pairs of Shockley partials forming between the particles two layers of atoms packed according to the HCP arrangement. A twin boundary consists of a single layer of atoms packed according to the HCP basis. Thus a stacking fault boundary has roughly about twice the twin boundary energy. The energy γ of a unit area of a stacking fault is almost equal to

$$\gamma = \frac{2h}{V}\left\{{}^{h}F - {}^{c}F\right\} \tag{8.1}$$

where h is the spacing in the [111] direction, V is the molar volume, and ${}^{h}F$ and ${}^{c}F$ are the molar free energies of the hexagonal and cubic phases.

The separation of the partial dislocations is determined by γ and is estimated to be about[82]

$$d \simeq \frac{G a^2}{32 \pi \gamma} \tag{8.2}$$

where a is the lattice constant. Since alloying elements influence γ, they change the spacing between the partials. For example, as Co is added to Ni the composition approaches that for the transition from the FCC to the HCP phase. Therefore $^{h}F - {}^{c}F$ decreases as the Co content is increased, causing γ to decrease and thereby increasing the separation of the partial d. At high temperatures the separation of the partials becomes yet greater because solute atoms distributed themselves between the two phases in such a way as to further decrease the free energy of the system. Theoretical deductions by Seeger[83] suggest that increasing electron/atom ratio as a result of adding solute elements to Cu, Ag, or Au, causes a decrease in the stacking fault energy. This is consistent with the increased ease of twinning in the higher electron/atom ratio solutions of these metals. Howie and Swann[84] have also measured the change in stacking fault energy upon alloying in a number of cases. In general the stacking fault energy may either increase or decrease upon alloying, dependent on the system. The stacking fault energy can also vary slightly with temperature.

Relative to FCC metals that creep by the motion of jogged screw dislocations and by the climb of edge dislocations, those alloying elements that lower the stacking fault energy should have greater values of l_j because of their higher constriction energies and the lowered probability for cross-slip. Equally the rate of climb should be lower because p_j is smaller.

C. Peierls Stress Modification

The Peierls stress for pure FCC metals is so small that it never plays a role in the plastic deformation of these metals even at low temperatures. Although the Peierls stress is greater for BCC metals, the Peierls mechanism is so easily activated that it is never significant above room temperature. Alloying may modify the Peierls stress in BCC metals, but it appears that such modification would not be large enough to play a role in high temperature creep. Recent data,[85] however, suggest that the Peierls stress for prismatic slip in Mg is reduced considerably by alloying with Li. The Peierls mechanism, however, may be important in the creep of intermediate phases and ceramic materials.

D. Mott-Nabarro Hardening

Periodic volumetric hydrostatic tension stresses are introduced in the lattice by substitutional solid solution alloying. The motion of the screw components of dislocations will not be resisted by such stress fields but such local stresses will restrain the motion of edge components. Although the dislocations are somewhat flexible their line tension tends to keep them more or less straight. Consequently, when the stress centers are close together, as they are in the usual case of solid solution alloying, the dislocations move more or less as rigid units, through the average stress of the periodically varying field. Consequently these stress fields have almost zero effect on the flow stress.

The stress fields of interstitial solute elements interact with both edge and screw dislocations. Generally the concentration of interstitial elements is comparatively low so that dislocations can bow out between the high stress centers. In this case the applied stress must force the dislocations over the peaks of stress. Consequently somewhat higher solid solution

strengthening is obtained from interstitial alloying. So long as the alloying remains random, however, neither of these mechanisms aid much in improving high temperature creep resistance because they are easily thermally activated.

E. Guinier-Preston Zone Hardening

During the early stages of precipitation in some systems, like atoms cluster to form Guinier-Preston zones and finally stable phase precipitates. Such clusters of atoms and Guinier-Preston zones also restrain the motion of dislocations but usually much less effectively than critical dispersions of stable phase incoherent precipitates. The presence of such clusters and Guinier-Preston zones have only very short lives at high temperatures and therefore are not usually significant to high temperature creep.

F. Suzuki Locking

Suzuki locking[86] constitutes a potential mechanism for improving the high temperature creep resistance of FCC alloys and therefore deserves more detailed attention. The stacking fault between the Shockley partials of the FCC system consists of two atomic layers of HCP packing of atoms. At high temperatures, where diffusion can occur, solute atoms will distribute themselves between the fault and the FCC crystal, in a manner analogous to the distribution of solute atoms between two phases. Although a complete and accurate analytical description of such a distribution is available,[87] it will be convenient here, in emphasizing the physical aspects of the problem, to treat the stacking fault as a separate phase rather than a surface.

The geometry of the problem is illustrated in Fig. 8.1. At equilibrium the stacking fault between the partials A and B, shown as the cross-hatched region, has a composition c_f whereas the composition of the crystal

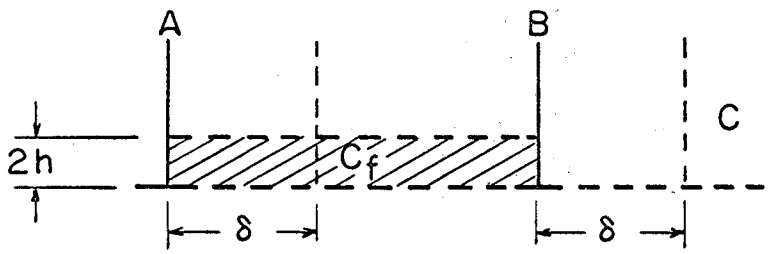

MU-29119

Fig. 8.1. Stacking fault in Suzuki locked alloy.

remains about the average value of the alloy, namely c. If then, a unit length of the dislocation is moved a distance δ, assumed to be identical for both partials in this approximation, the work done is $(\tau-\tau^*)b\delta$. This work must equal the increase in chemical free energy. In moving the partial dislocations an amount δ, the volumes of the phases changed $2h\delta$; for the first dislocation this volume of the matrix phase was produced at a composition c_f resulting in the disappearance of the same stacking fault volume of the same composition; and at the second dislocation this volume of the stacking fault was produced resulting in the disappearance of the same volume of the matrix phase at the composition c. Consequently

$$(\tau-\tau^*)b\delta = \frac{2h\delta}{V}\left\{(F-F^f)_{c_f} + (F^f-F)_c\right\} \qquad (8.3)$$

where V is the molar volume, assumed identical regardless of stacking, F is the free energy per mole of the matrix, F^f is the free energy per mole of the faulted region, and the subscripts c_f and c refer to the compositions at which the free energies must be evaluated. Therefore

$$(\tau-\tau^*) = \frac{2h}{bV}\left\{(F^f-F)_c - (F^f-F)_{c_f}\right\} \qquad (8.4)$$

In general both $(F^f - F)_c$ and $(F^f - F)_{c_f}$ are positive as, e.g., in the case of Ni-Cu alloys where the stable phase is always FCC, the faulted region having the higher free energy regardless of composition. But $(F^f - F)_{c_f} \leq (F^f - F)_c$ since the composition c_f was obtained as a result of equilibrium. Consequently the total term in the braces of Eq. 8.4 is always positive.

An additional relationship between the variables of Eq. 8.4 is obtained by invoking quasi-equilibrium conditions between the matrix phase and the faulted region. Complete equilibrium, of course, is never achieved inasmuch as this would demand the disappearance of the faulted regions. We consider, therefore, open matrix and faulted phases for which, at equilibrium, the virtual change in free energy $\delta F'_t$ for the total system is

$$\delta F_t' = \left(\frac{\partial F'}{\partial n_a}\right)\delta n_a + \left(\frac{\partial F'}{\partial n_a}\right)\delta n_b + \left(\frac{\partial F'^f}{\partial n_a^f}\right)\delta n_a^f + \left(\frac{\partial F'}{\partial n_b^f}\right)\delta n_b^f$$

where F' refers now to the free energy of the matrix containing n_a "a" atoms and n_b "b" atoms, etc. The partial derivatives are, therefore, the chemical potentials. At equilibrium, $\delta F_t'$ for the total system is zero. To arrive at the equilibrium condition we let $\delta n = \delta n_a = -\delta n_b = \delta n_b^f = \delta n_a^f$. This is merely the expression for conservation of mass which yet permits atom species transfer of δn atoms of type "a" from the fault to the matrix and δn atoms of type "b" from the matrix to the fault. For equilibrium, therefore,

$$\frac{\partial F'}{\partial n_a} - \frac{\partial F'}{\partial n_b} - \frac{\partial F'^f}{\partial n_a^f} + \frac{\partial F'^f}{\partial n_b^f} = 0 \qquad (8.5)$$

In general, the thermodynamic data that are needed to achieve a simultaneous solution of Eqs. 8.4 and 8.5 are not available. Furthermore, theories on the thermodynamics of solid solutions have not yet been well enough developed to provide reliable analyses of the thermodynamics of unstable solid solutions (e.g., hexagonal Cu-Ni alloys). But in order to obtain an initial concept of possible trends, the regular solution laws might be invoked. To simplify the analysis this will be done not only for the matrix but equally for the faulted volume, in spite of the fact that the stacking fault region should be treated as a surface.

The free energy of an open regular solution consisting of n_a "a" atoms and n_b "b" atoms can be written as

$$F' = \frac{n_a F_a}{N} + \frac{n_b F_b}{N} + \frac{n_a + n_b}{N}\Delta H_m - kT \ln \frac{(n_a + n_b)!}{n_a!\, n_b!} \qquad (8.6)$$

where N is Avogadro's number, F_a and F_b are the free energies per mole of pure "a" and "b" atoms and the last term refers to the contribution of the entropy for random mixing. A similar expression applies to the faulted region. When C is defined as

$$C = \frac{n_a}{n_a + n_b} \tag{8.7}$$

Equation 8.6 written for one mole of the alloy reduces to

$$F_c^f = (1-c)F_a^f + c\,F_b^f + \Delta H_m(c) + RT\{c \ln c + (1-c)\ln(1-c)\} \tag{8.8}$$

with similar expressions for the remaining free energies in Eq. 8.4. Then

$$(F^f - F)_c = (1-c)(F_a^f - F_a) + c(F_b^f - F_b) + (\Delta H_m^f - \Delta H_m)_c \tag{8.9}$$

where the entropy terms vanish. Also

$$(F^f - F)_{c_f} = (1-c_f)(F_a^f - F_a) + c_f(F_b^f - F_b) + (\Delta H_m^f - \Delta H_m)_{cf} \tag{8.10}$$

Introducing Eqs. 8.9 and 8.10 into 8.4 gives

$$\begin{aligned}(\tau - \tau^*) = \frac{2h}{bV}\Big\{&(c - c_f)\left[(F_b^f - F_b) - (F_a^f - F_a)\right] \\ &+ (\Delta H_m^f - \Delta H_m)_c - (\Delta H_m^f - \Delta H_m)_{cf}\end{aligned} \tag{8.11}$$

For equilibrium conditions, we apply Eqs 8.6, etc. to the condition given by Eq. 8.5. For example

$$\frac{\partial F'}{\partial n_a} = \frac{F_a}{N} + \frac{\Delta H_m}{N} + \frac{n_a + n_b}{N}\frac{\partial \Delta H_m}{\partial c}\frac{\partial c}{\partial n_a} + kT \ln \frac{n_a + n_b}{n_a} \tag{8.12a}$$

and

$$\frac{\partial F'}{\partial n_b} = \frac{F_b}{N} + \frac{\Delta H_m}{N} + \frac{n_a + n_b}{N}\frac{\partial \Delta H_m}{\partial c}\frac{\partial c}{\partial n_b} + kT \ln \frac{n_a + n_b}{n_b} \tag{8.12b}$$

recalling that

$$\frac{\partial c}{\partial n_a} = -\frac{n_b}{(n_a+n_b)^2} \quad \text{and} \quad \frac{\partial c}{\partial n_b} = \frac{1}{n_a+n_b} - \frac{n_b}{(n_a+n_b)^2} \tag{8.13}$$

and similarly for the faulted region

$$\frac{\partial F'^f}{\partial n_a^f} + \frac{\partial F'^f}{\partial n_b^f} = \frac{F_a^f - F_b^f}{N} - \frac{1}{N}\left(\frac{\partial \Delta H_m^f}{\partial C_f}\right) - kT\ln\frac{C_f}{1-C_f} \tag{8.14}$$

Consequently the equilibrium condition obtained by introducing Eqs. 8.12 and 8.13 into 8.5 is given by

$$\frac{C_f}{1-C_f} = \frac{c}{1-c}\exp\left\{-\frac{1}{kT}\left[(F_b^f - F_b) - (F_a^f - F_a) + \frac{\partial \Delta H_m^f}{\partial C_f} - \frac{\partial \Delta H_m}{\partial c}\right]\right\} \tag{8.15}$$

Eqs. 8.11 and 8.15 therefore constitute the solution to the problem. An explicit expression for c_f is not obtainable from Eq. 8.15 since $\frac{\partial}{\partial C^f}\Delta H_m^f$ also depends on c_f. But the quantities in the braces of the exponential term will be positive and therefore c_f will be somewhat smaller than c. This difference will be greatest at the absolute zero and as the temperature increases c_f will increase very slowly to approach c.

When the solution is ideal the ΔH_m's are zero and the Eqs. 8.11 and 8.15 reduce to the simple expressions, respectively, of

$$(\tau - \tau^*) = \frac{2h}{bV}(c - C_f)\,\Delta F \tag{8.16}$$

$$\frac{C_f}{1-C_f} = \frac{c}{1-c}\,e^{-\Delta F/kT} \tag{8.17}$$

where

$$\Delta F = (F_b^f - F_b) - (F_a^f - F_a) \tag{8.18}$$

and

$$\frac{2h}{V}\Delta F = \gamma_b^{\ell} - \gamma_a^{\ell} \tag{8.19}$$

γ_b^{ℓ} and γ_a^{ℓ} being the stacking fault energies in pure b and a. Therefore $(\tau - \tau^*)$ can vary mildly with temperature depending on the variation in stacking fault energies of pure a and pure b with temperature.

We now wish to illustrate that substantial high temperature strengthening can be achieved by the Suzuki mechanism. For this purpose we will consider reasonable values for the pertinent thermodynamic quantities. For example, let

$$\gamma_b^{\ell} - \gamma_a^{\ell} = \begin{cases} 50 \text{ ergs/cm}^2 \\ 100 \text{ ergs/cm}^2 \\ 150 \text{ ergs/cm}^2 \end{cases}$$

$$V = 10 \text{ cm}^3$$

$$h = 2.5 \times 10^{-8} \text{ cm}$$

Then $$\Delta F = \frac{V}{2h}(\gamma_b^{\ell} - \gamma_a^{\ell}) = \begin{cases} 1.66 \times 10^{-14} \\ 3.32 \times 10^{-14} \\ 4.98 \times 10^{-14} \end{cases} \text{ ergs/atom}$$

Introducing this into Eq. 8.17 we find that the results given for $c - c_f$ shown in Fig. 8.2 are obtained. Thus according to Eq. 8.16, we obtain the $\tau - \tau^*$ versus T data shown in Fig. 8.3.

These estimates reveal that substantial strengthening can be obtained as a result of Suzuki locking. In general the strength of Suzuki locked alloys decrease only slightly with an increase in temperature. This trend, however, might be slightly modified by the additional effect of temperature on $\gamma_b^{\ell} - \gamma_a^{\ell}$ which was neglected in this estimate.

When the stacking fault is only a few Burgers vectors wide, it may be possible to have thermal fluctuations aid in unlocking the dislocations.

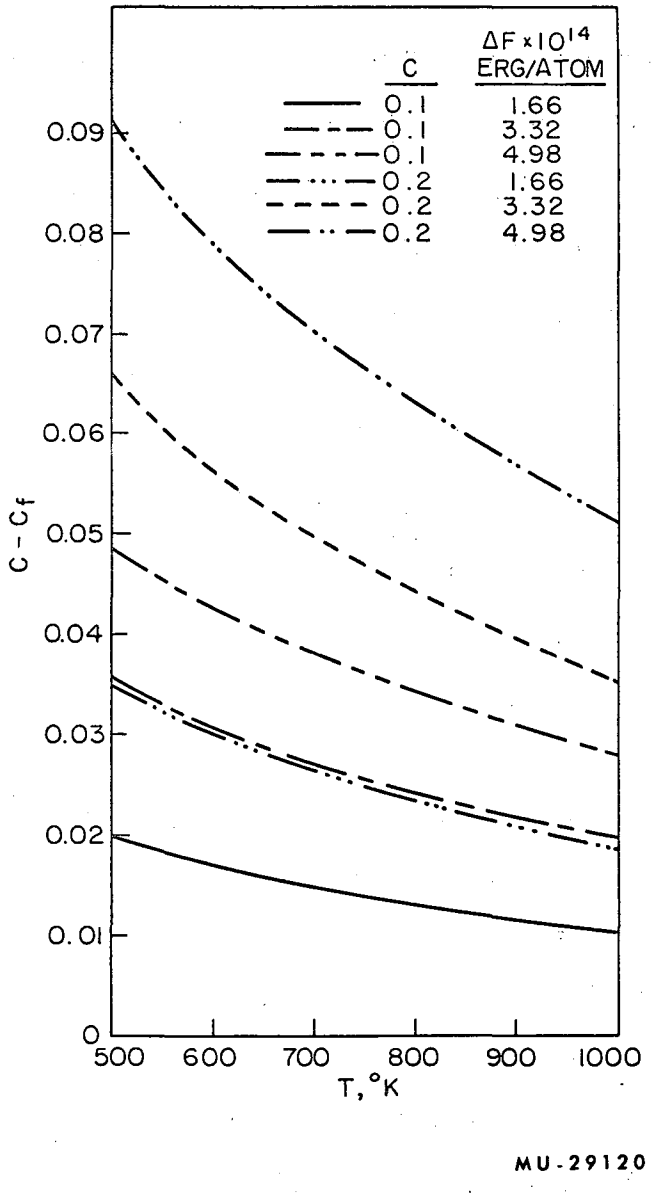

Fig. 8.2. Variation of C - C_f with temperature.

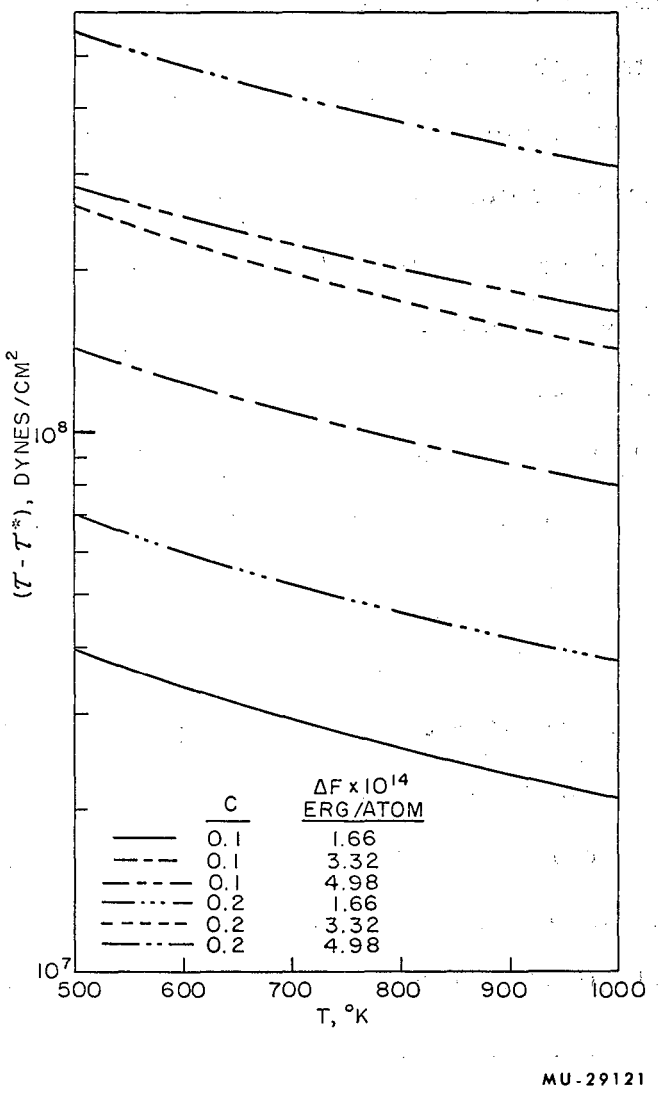

Fig. 8.3. Theoretical variation of $(\tau - \tau^*)$ with temperature for several stacking fault energy differences and two compositions.

At high temperatures, however, such released dislocations would relock very rapidly as a result of diffusion of solute atoms. This would result in relatively few moving dislocations and thus give low creep rates. Such locking would also take place with all freshly generated dislocations.

When the stacking fault is more than a few Burgers vectors wide, the activation energy for unlocking the dislocations should be so great that the frequency of unlocking becomes negligibly small. Consequently, practically no creep will take place unless the stress itself is large enough to unlock the dislocations.

In spite of the rather good theory for Suzuki locking, no unique examples of high temperature strengthening by this mechanism have yet been announced.

G. Cottrell Interaction Effects

Cottrell[88] interactions also play an important role in creep, particularly near the lower temperature limit of the high temperature creep range. Substitutional atoms that have atomic radii which differ from the solvent species introduce local strain centers in the lattice. Such strain centers can react elastically with the hydrostatic tension stress fields around edge dislocations. As shown by Cottrell,[88] and Cottrell and Bilby,[89] the interaction energy between an edge dislocation lying along the z axis of a cylindrical coordinate system and a solute atom at r and α is given by

$$V = \frac{A}{r} \sin\alpha \tag{8.20}$$

where $A = 4 R^3 \varepsilon Gb$, R being the atomic radius of the solvent and $R(1 + \varepsilon)$ being the atomic radius of the solute atom.

Interstitial atoms interact with both edge and screw components of dislocations as described by Cochardt, Schoeck, and Wiedersich.[90] The

interaction energy in this case differs in detail from that given for substitutional solid solutions but nevertheless, is reasonably well approximated in its essential features by Eq. 8.20. We will therefore develop our analysis exclusively in terms of substitutional solutions since analogous descriptions apply to interstitial solid solutions.

In Fig. 8.4 are shown the circles of constant interaction energy. Taking $\mathcal{E}$ to be positive, an atom at r and α will be acted upon by a force equal to the potential energy gradient and directed along the conjugate circle shown broken in the graph. Consequently at sufficiently high temperatures where diffusion can take place the solute atoms will migrate along the orthogonal set of conjugate circles to concentrate just below the core of the dislocation. Simultaneously the region just above the core of the dislocation will become depleted in solute atoms.

We will now attempt to ascertain the situation that will prevail at equilbirium. For this purpose we will assume that we are always dealing with a solid solution. Such complications as arise from precipitation will be described later. As shown by Lücke[91] and also Thomson,[92] the interaction energy between a dislocation and a solute atom is independent of other sources of strain energy. This arises from the fact that the stresses in the elementary theory of elasticity are linear functions of the strains. Consequently the principle of superposition applies. Therefore regardless of the presence of other sources of strain the interaction energy between a dislocation and solute atom is always given by Eq. 8.20. This statement is correct even when a precipitate forms at the dislocation core. Therefore a dislocation does not saturate, as was suggested in some of the earlier literature on this subject, as a result of satisfying the strain at the dislocation core. Due to their strain fields solute atoms, of course, interact with

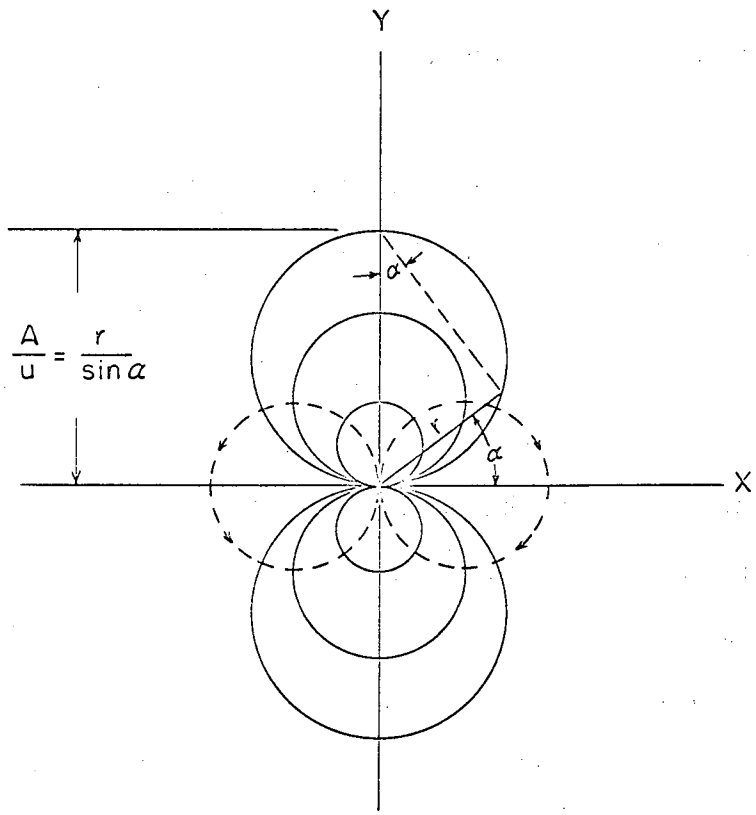

MU-29122

Fig. 8.4. Circles of constant interaction energy.

each other. As shown by Crussard,[93] however, this interaction decreases with the sixth power of the distance between the atoms and therefore involves only local, almost only nearest neighbor, interactions. Solute atom migration occurs as a result of the gradient in the strain energy until the reversed diffusion due to the composition gradient balances the forward diffusion. Solute atom interactions can be incorporated into the analyses by assuming the regular solution laws. In large measure this procedure accounts for the interaction stress fields between solute atoms.

We will first estimate the equilibrium distribution of substitutional solute atoms about an edge dislocation. For this purpose we consider solute atoms distributed between two potential energy levels, V and V_o as follows:

Energies	No. Sites	No. Solute Atoms	No. Solvent Atoms
V	n	p	n - p
V_o	n_o	p_o	$n_o - p_o$

We will assume that the alloy forms a regular solution, so that the bond energy for random mixing of the atoms at a potential energy V is

$$E = \frac{zp}{2}\frac{p}{n}\mathcal{E}_{AA} + \frac{z}{2}\frac{(n-p)}{n}\mathcal{E}_{BB} + zp\frac{(n-p)}{n}\mathcal{E}_{AB} \tag{8.21}$$

where z is the coordination number, and $\mathcal{E}_{AA}$, $\mathcal{E}_{BB}$, and $\mathcal{E}_{AB}$ are the energies of an A-A, B-B, and A-B bond, respectively. A similar result applies for the atoms at the potential energy V_o. Therefore, the free energy of the system at the potential energy V is

$$F = pV + \frac{zp^2}{2n}\mathcal{E}_{AA} + \frac{z(n-p)^2}{2n}\mathcal{E}_{BB} + \frac{zp(n-p)}{n}\mathcal{E}_{AB} - kT\ln\frac{n!}{p!(n-p)!} \tag{8.22}$$

and the chemical potential of the solute atoms is

$$\left(\frac{\partial F}{\partial p}\right) = V + \frac{2p}{n}\mathcal{E}_{AA} - \frac{2}{n}(n-p)\mathcal{E}_{BB} + \frac{2}{n}(n-2p)\mathcal{E}_{AB} - kT\ln\left(\frac{n-p}{p}\right) \quad (8.23)$$

A similar chemical potential applies to the system at V_o. At equilibirum the chemical potentials for each system are identical and

$$V - V_o - Z\left\{\frac{p}{n} - \frac{p_o}{n_o}\right\}2\bar{\mathcal{E}} - kT\ln\left(\frac{n-p}{p}\right)\left(\frac{p_o}{n_o-p_o}\right) = 0 \quad (8.24)$$

where $\bar{\mathcal{E}} = \mathcal{E}_{AB} - \frac{\mathcal{E}_{AA}}{2} - \frac{\mathcal{E}_{BB}}{2}$ is the increase in energy upon breaking an A-B bond and making one half an A-A and B-B bond. We now let the composition be $c_o = \frac{p_o}{n_o}$ where V_o is zero. Consequently

$$c = \frac{c_o e^{+2Z/kT(c-c_o)\bar{\mathcal{E}}} e^{-V/kT}}{1 - c_o + c_o e^{+2Z/kT(c-c_o)\bar{\mathcal{E}}} e^{-V/kT}} \quad (8.25)$$

This constitutes a slightly more accurate and detailed description of the equilibrium concentration of solute atoms around an edge dislocation than that previously suggested by Louat.[94]

The concentration of atoms c in the regions around a dislocation where V is negative is greater than average composition c_o of the alloy. The concentration of atoms, however, also depends on $\bar{\mathcal{E}}$, and since the interaction energy, $\bar{\mathcal{E}}$, can be positive or negative, the concentration of atoms about the dislocation can be smaller or greater than that which would be obtained if the solution were ideal. Since the product $(c - c_o)\bar{\mathcal{E}}$ is usually small, however, the effect of non-ideality of the solution is small particularly at high temperatures.

To illustrate the effect of dislocations on the distribution of solute atoms, we will consider the special case of Mg in Al, assuming that $\bar{\mathcal{E}}$ is negligibly small. We will calculate the concentration of Mg atoms at a point

2.5b below the core of the dislocation. There

$$V = -\frac{4\pi R^3 \varepsilon G b}{2.5b} \tag{8.26}$$

for which we take the following reasonable values

$$R = 2.86 \times 10^{-8}$$

$$\varepsilon = 0.12$$

$$G = 2.5 \times 10^{11} \text{ dynes/cm}^2$$

The results are recorded in Fig. 8.5 on which the solubility limit of Mg in Al is also shown.

Neglecting the effect of local stress fields on the usual phase diagram as well as the problems involved in nucleation of new phases, a precipitate should form on the dislocation for all concentrations above the solubility limit. As seen in Fig. 8.5, precipitates might form near the cores of dislocations even in extremely pure metals. The rate at which such precipitates form will depend on the diffusion rate of the impurity atom and the kinetics of nucleation and growth. The feed-in potential of the dislocation, however, will remain substantially unmodified in spite of the formation of a precipitate. Nevertheless, the local strains resulting from the formation of the precipitate will interact with the solute atoms. In general, however, this effect is small. During this process the precipitate, originally strung out along the edge dislocations, will begin to spheroidize. Experience reveals that dislocations decorated in this way are strongly locked and will not ordinarily participate in slip. Such locking, since it takes place in a region where localized stressing has caused dislocation to move, is very effective in restraining the motion of other dislocations. Furthermore, the presence of the precipitate does not materially alter the stress field of the dislocation and therefore such locked dislocations yet react to restrain the motion of newly generated free dislocations. As shown in Fig. 8.5, at high temperatures

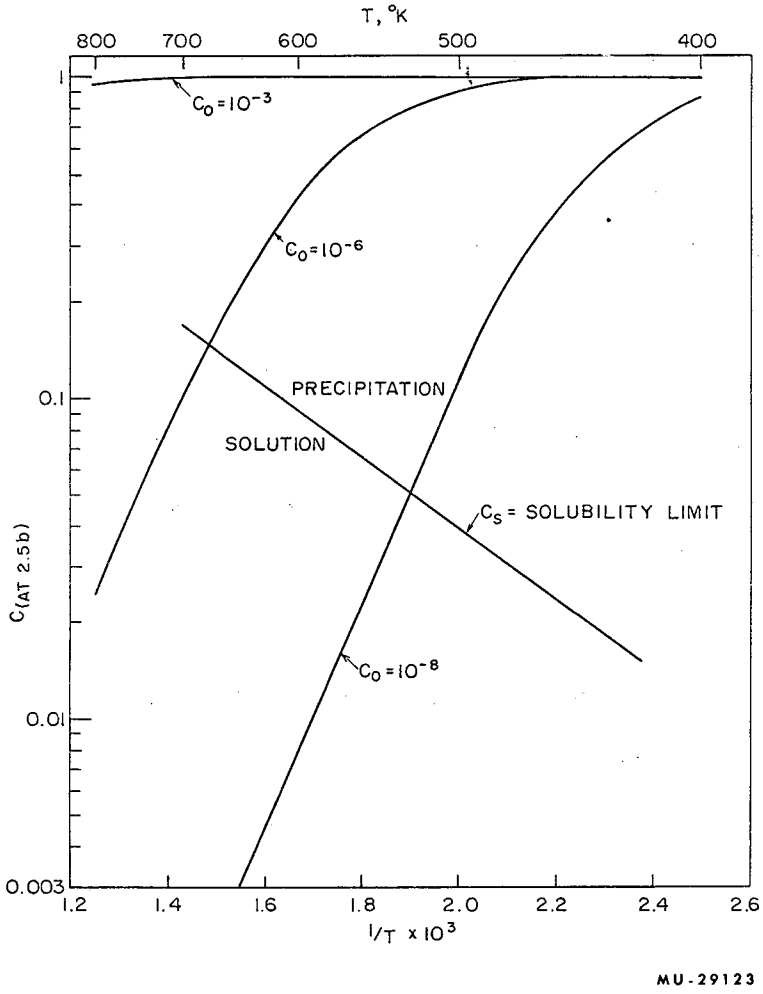

Fig. 8.5. Concentration of Mg 2.5b below an edge dislocation in aluminum vs 1/T.

at the left of the solubility curve, precipitation will not take place and an atmosphere of solute atoms will form about the dislocation. As the temperature is increased the atmosphere becomes less dense. The most dense atmospheres are obtained where the concentration of the solute atom approximately equals its solubility limit at the temperature in question.

A similar analysis applies for interstitial solid solutions. In this case, however, the free energy of the solution in the region where the potential energy is V is better approximated by

$$F = pV + p\mathcal{E}\left\{\frac{p}{n}\right\} - kT\ln\frac{n!}{p!(n-p)!} \tag{8.27}$$

where $\mathcal{E}\{p/n\}$ is the increase in energy of the solution per interstitial atom, a quantity, of course, that is some function of the occupancy of the sites, $\left\{\frac{p}{n}\right\}$, and is also dependent on the temperature. Consequently the chemical potential of the solute atom in an interstitial solid solution is

$$\frac{\partial F}{\partial p} = V - \mathcal{E}\left\{\frac{p}{n}\right\} + \frac{p}{n}\frac{\partial \mathcal{E}}{\partial\left(\frac{p}{n}\right)} - kT\ln\left(\frac{n-p}{p}\right) \tag{8.28}$$

A similar expression is obtained for the region where the potential energy is V_o. Consequently, equating the chemical potentials of the two regions for equilibrium, we obtain

$$V - V_o + \mathcal{E}\left\{\frac{p}{n}\right\} - \mathcal{E}\left\{\frac{p_o}{n_o}\right\} + \frac{p}{n}\frac{\partial \mathcal{E}}{\partial(p/n)} - \frac{p_o}{n_o}\frac{\partial \mathcal{E}}{\partial p_o/n_o}$$
$$- kT\ln\left(\frac{n-p}{p}\right)\left(\frac{p_o}{n_o - p_o}\right) = 0 \tag{8.29}$$

We let the lattice be one which has q equivalent interstitial sites per solvent atom. Then

$$c = \frac{p}{p + n/q} \quad \text{or} \quad \frac{n}{p} = q\,\frac{1-c}{c} \tag{8.30}$$

and letting $c = c_o$ at $V_o = 0$, we obtain

$$\frac{c}{q(1-c)-c} = \frac{c_0 e^{-A/kT} e^{-V/kT}}{q(1-c_0)-c_0} \tag{8.31}$$

where

$$A = \mathcal{E}\left\{\frac{p}{n}\right\} - \mathcal{E}\left\{\frac{p_0}{n_0}\right\} + \frac{p}{n}\left[\frac{\partial \mathcal{E}}{\partial (p/n)}\right]_{p/n} - \frac{p_0}{n_0}\left[\frac{\partial \mathcal{E}}{\partial p/n}\right]_{p_0/n_0} \tag{8.32}$$

The locking trends of interstitial solid solutions are quite similar to those already described for substitutional solid solutions. Screw as well as edge dislocations, however, will attract interstitial atoms.

Dislocations surrounded by atmospheres are also pinned into position, but the pinning is much weaker than that which is obtained when the dislocations become decorated with a precipitate. Such solute-atom atmosphere pinning, however, loses its significance at elevated temperatures, since the unpinning can be thermally activated, as described by Cottrell. In contrast the binding of a dislocation that is completely decorated with a precipitate is very strong, and current evidence indicates that in general the release of such decorated dislocations cannot be thermally activated.

In their classical paper on interactions between solute atoms and dislocations, Cottrell and Bilby[89] presented a beautiful analysis of the viscous drag of atmospheres on moving dislocations. At high temperatures, the atmosphere of solute atoms moves along with a very slowly moving dislocation by diffusion. Since the center of the atmosphere is located at the core of the dislocation in this case, it does not perturb the slow motion of the dislocation. Furthermore, an atmosphere cannot form about a very rapidly moving dislocation because the dislocation does not remain sufficiently long in any one place to permit diffusion of the solute atoms. When a dislocation is moving at some intermediate velocity, however, a partial atmosphere

lags slightly behind the core of the moving dislocation. The back force due to the atmosphere, in this case, decreases the velocity of the dislocation. As shown by Cottrell and Bilby, the greatest drag on the dislocation will take place at the critical velocity, v_c, as determined from Einstein's mobility relationship, when

$$v_c \simeq \frac{4 D_s kT}{A} \tag{8.33}$$

where D_s is the diffusivity of the solute atom.

High temperature creep appears to be controlled by the motion of jogged screw dislocations. Such dislocations, which only interact strongly with interstitial alloying elements, have been shown to have an average velocity

$$\bar{v} = \frac{b\nu}{p} e^{-\bar{g}_d/kT} \left\{ e^{\frac{\tau l_j b^2}{pkT}} - 1 \right\} \tag{8.34}$$

where g_d now refers to the average free energy of activation for diffusion of all substitutional elements in the solid solution. Consequently the most effective alloying element for providing additional drag on the moving dislocation due to Cottrell interactions are interstitial solute elements for which

$$\frac{D_s}{A} \simeq \frac{b\nu}{4pkT} e^{-\bar{g}_d/kT} \left\{ e^{\tau l_j b^2/pkT} - 1 \right\} \tag{8.35}$$

Consequently, that interstitial alloying element which is most effective for increasing the creep resistance of an alloy at one temperature and one stress, will not be effective at either higher or lower temperatures or stresses. It therefore follows that the highest creep resistant alloys, from the viewpoint of solute atom drag on moving dislocations, should contain a series of judiciously selected interstitial alloying elements in order to

provide solute atom atmosphere drag over the significant ranges of temperatures and stresses to be used. Since the moving dislocations are never in pure screw orientation, some effects due to viscous drag of substitutional alloying elements can also occur.

Solute atoms not only can affect the high temperature creep rate as a result of viscous drag on the moving dislocations but also as a result of their effect on the rate of climb of arrested edge dislocations. Those elements that reduce the rate of recovery by decreasing the rate of climb will result in a more rapid decrease in the creep rate over the primary stage and a lower secondary creep rate. The effect of alloying on recovery has been reviewed by Perryman.[95] Whereas alloying elements frequently increase significantly the temperature for recrystallization, their effect on recovery is usually much less. Furthermore, as shown by Perryman, the recovery rate can either be increased or decreased as a function of alloying. For example, Mg in solid solution increases the rate of recovery of Al. Perryman has shown that this is principally due to the fact that Mg increases the vacancy concentration in Al.

When the solute atom concentration is high enough to decorate the edge dislocations with a precipitate, climb is restrained. But it appears unlikely that a solute atom atmosphere per se can materially influence climb. Consequently the frequency of climb in an alloy might be approximated by Eq. 5.18, namely

$$\nu_c = \nu(z-1)\, p_j \cdot e^{-\bar{g}_d/kT}\left\{e^{\sigma_{xx}\Omega/kT} - 1\right\}$$

where the two significant variables are the probability of finding a jog, p_j, and $\bar{g}_d$, which here refers to the average activation energy for diffusion of the substitutional alloying elements. Therefore those alloying elements that

decrease p_j and increase $\bar{g}_d$ should be most effective in decreasing the creep rate. The probability of finding a jog can be decreased in FCC metals by decreasing the stacking fault energy. Other factors such as the rate of nucleation of additional jogs and the possible effect of solute atoms on the climb has not yet been explored deeply enough to provide additional judgment of this subject.

Short-Range Order Strengthening

Several years ago Fisher[96] demonstrated that appreciable solid-solution strengthening is obtained as a result of short-range ordering. Our analysis will follow somewhat the more recent discussions by Flinn[97] on the details of this mechanism. Whereas each atom in a crystal is bound to all other atoms, the bond interaction is rather local and exists principally as interactions between nearest neighbors, the second nearest neighbor reactions being small, and third nearest neighbor reaction being almost zero. In our discussion we will consider only nearest neighbor interactions.

It has proven convenient to classify solid solution alloys into one of three idealized categories, namely ideal solid solutions, regular, solid solutions, and short-range ordered solutions. This classification is easily described in terms of the bond energies of nearest neighbors. Consider, for example, the bond equation

$$\tfrac{1}{2}\,A\text{-}A + \tfrac{1}{2}\,B\text{-}B \longrightarrow A\text{-}B \tag{8.36}$$

for which the energy change is

$$\bar{\mathcal{E}} = \mathcal{E}_{A\text{-}B} - \tfrac{1}{2}\mathcal{E}_{AA} - \tfrac{1}{2}\mathcal{E}_{BB} \tag{8.37}$$

per 1/2 A-A and 1/2 B-B bond that is broken to form an A-B bond. When $\bar{\mathcal{E}}$ is zero the alloy is ideal and the atoms are distributed among the lattice

sites in a purely random manner. Although some solid solutions of metals begin to approach ideality no truly ideal solutions have yet been found. Generally, the energy $\bar{\varepsilon}$ differs from zero. When $\bar{\varepsilon}$ does not differ too much from zero, the atoms may yet be distributed over the lattice in almost a random way and the thermodynamic behavior can be approximated by the regular solution laws. In most alloys, however, $\bar{\varepsilon}$ is rather large, due either to electronic or strain energy effects, and short-range ordering is significant.

When $\bar{\varepsilon}$ is negative, the energy of the system is lowered by making as many A-B bonds as possible. Consequently, under equilibrium conditions alloys for which $\bar{\varepsilon}$ is negative will have a greater number of A-B bonds and fewer A-A and B-B bonds than a random solid solution. A atoms will prefer B atoms as neighbors, thus leading to local or short-range ordering. When $\bar{\varepsilon}$ is positive, the opposite takes place and A atoms prefer A atoms as neighbors, and B atoms prefer B atoms as neighbors. This results in clustering. This clustering, however, is merely the negative of ordering and is quite distinct from the agglomeration of similar atoms over a wide region during the early stages of formation of Guinier-Preston zones; essentially only nearest neighbors participate in true clustering.

Since the grand partition function for a short-range ordered alloy has not yet been formulated approximations to the exact statistical mechanical formulation of the problem must be employed. We will use Cowley's[98] approach to short-range order here, and we will limit our discussion only to nearest neighbor interactions. Let α be the degree of order, and p_{AB} the probability that an A atom is next to a B atom. By definition of α

$$p_{AB} = m_A(1-\alpha) \tag{8.38a}$$

where m_A is the mole fraction of A atoms. When the solution is random, p_{AB} must be equal to m_A. When α is positive there are fewer than the average number of A atoms about a B and the alloy exhibits clustering; when α is negative there are more than the average number of A atoms about a B atom and the alloy exhibits short-range ordering. Thus for an ordered alloy both $\bar{\varepsilon}$ and α are negative whereas for a clustered alloy both are positive. The product $\bar{\varepsilon}\alpha$ is always positive or, in a random solid solution, zero. The range of α is limited. When $p_{AB} = 0$, α has its maximum value of 1, and when p_{AB} is 1; α has its minimum value of $\alpha = 1 - \frac{1}{m_A} = \frac{m_A - 1}{m_A} = -\frac{m_B}{m_A}$. The probabilities for the remaining arrangements, shown below, follow directly from the definition given in Eq. 8.38a, namely,

$$p_{BB} = 1 - p_{AB} = 1 - m_A + m_A\alpha = m_B + m_A\alpha \tag{8.38b}$$

$$p_{BA} = m_B(1 - \alpha) \tag{8.38c}$$

$$p_{AA} = (1 - p_{BA}) = m_A + m_B\alpha \tag{8.38d}$$

We now consider an alloy containing N atoms in a structure that has a coordination number Z. In this alloy there are a total of $\frac{NZ}{2}$ bonds and we plan to express the total energy of the alloy in terms of the degree of order α as

$$E\{\alpha\} = \frac{NZ}{2}\,\varepsilon\{\alpha\} \tag{8.39}$$

where $\varepsilon\{\alpha\}$ is the average energy per bond in an alloy that has order . The total energy of the alloy is the sums of the energies of the A-A, the B-B, and the A-B bonds; which is

$$E\{\alpha\} = \left(m_A \frac{ZN}{2}\right) p_{AA} \varepsilon_{AA} + \left(m_B \frac{ZN}{2}\right) p_{BB} \varepsilon_{BB} + \left(m_A \frac{ZN}{2}\right) p_{BA} \varepsilon_{BA} + \left(m_B \frac{ZN}{2}\right) p_{AB} \varepsilon_{AB} \tag{8.40}$$

When Eqs 8.38 are introduced and Eq. 8.39 is solved,

$$\varepsilon\{\alpha\} = m_A^2 \varepsilon_{AA} + m_B^2 \varepsilon_{BB} + 2 m_A m_B \varepsilon_{AB} - 2 m_A m_B \alpha \varepsilon \tag{8.41}$$

where $\bar{\varepsilon}$ is given by Eq. 8.37. Since α and $\bar{\varepsilon}$ always have the same sign, $\varepsilon\{\alpha\}$ is always less than the average energy of a bond in the randomly arranged alloy where $\alpha = 0$.

When a dislocation moves through the lattice it displaces its nearest neighbors across the slip plane and replaces them by next nearest neighbors. But next nearest neighbors are almost random. Consequently if two or more dislocations pass, the alloy becomes almost completely disordered across the slip plane. The average increase in energy per bond that is broken is

$$\bar{\varepsilon} = \varepsilon\{0\} - \varepsilon\{\alpha\} = 2 m_A m_B \alpha \varepsilon \tag{8.42}$$

In order to illustrate the determination of the flow stress, we will consider as shown in Fig. 8.6 slip on the (110) plane in the [111] of a BCC crystal. The dislocation line of length CD moves one $\bar{b}$ breaking the former bonds of A with B and C and making new bonds with B' and C'. Therefore, the work done

$$(\tau - \tau^*) \frac{\sqrt{3}}{2} a \frac{\sqrt{2}}{2} a^2 = 2 \bar{\varepsilon} \tag{8.43}$$

Therefore,

$$\tau - \tau^* = \frac{8 m_A m_B \alpha \bar{\varepsilon}}{\sqrt{6}\, a^3} \tag{8.44}$$

This can indeed be quite a large quantity.

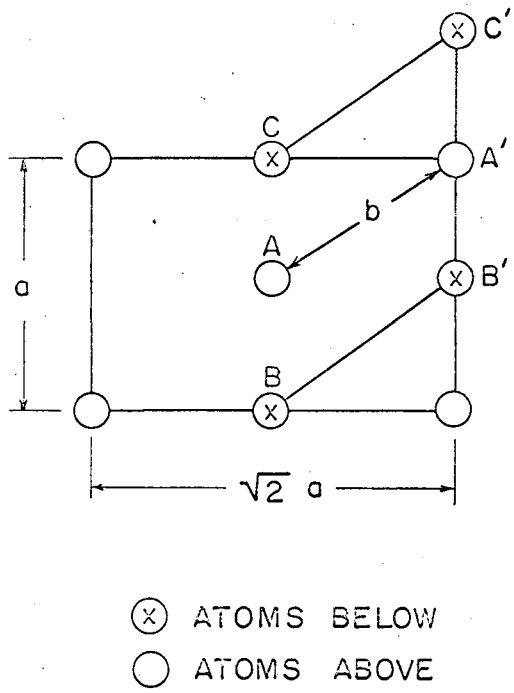

WHEN ATOM A ABOVE SLIP PLANE MOVES TO A′, IT IS NO LONGER CO-ORDINATED WITH ATOMS C AND B BELOW THE SLIP PLANE, BUT WITH ITS FORMER NEXT NEAREST NEIGHBORS B′ AND C′.

MU-29124

Fig. 8.6. Change in neighbor arrangement during deformation of a short range ordered alloy.

It has been shown that the equilibrium degree of order α_0 is given by[99]

$$\frac{(m_A + m_B\alpha_0)(m_B + m_A\alpha_0)}{m_A m_B (1-\alpha_0)^2} = e^{2\bar{\varepsilon}/kT} \tag{8.45}$$

Therefore, at sufficiently high temperatures, where diffusion is possible, the absolute value of the degree of order α_0 decreases slowly with increasing temperature. Below somewhat less that 1/2 the melting temperature, however, the flow stress ($\tau - \tau^*$) is dependent on the "frozen-in" degree of order α and therefore is insensitive to the temperature.

When a long segment of a dislocation moves forward in a short-range ordered alloy, the activation energy needed to overcome the short-range ordered bonding energy is extremely high. For this reason it has been suggested that the motion of a dislocation through a short-range ordered alloy cannot be thermally activated. Therefore at low temperatures where the degree of order α is frozen-in, the flow stress, as shown by Eq. 8.44, should be independent of the temperature. And correspondingly above about 1/2 the melting temperature where diffusion takes place to maintain the equilibrium degree of order, the flow stress should decrease only mildly with an increase in temperature in accord with the rather mild decrease of the degree of order with increasing temperature. As we shall see, however, there now appears to be examples of high temperature creep of short-range ordered alloys which demand that dislocation motion in short-range ordered alloys becomes thermally activated and diffusion controlled at high temperatures. We therefore suggest that the high temperature creep of short-range ordered alloys is not yet fully understood. Perhaps the motion of small dislocation segments must become possible in ordered alloys at high temperatures.

The flow stress at a strain rate of $\dot{\gamma} \simeq 10^{-2}\ \mathrm{min}^{-1}$ for prismatic slip of Ag (67 at%) Al (33 at%) is shown in Fig. 8.7 [100] as a function of temperature. Current evidence suggests that the thermally activated Peierls mechanism is operative over Region I. Flow in Region II, over which the yield strength is insensitive to the temperature, must arise from some athermal mechanism. Since the dislocations on the prismatic plane are not dissociated, the athermal mechanism cannot be due to Suzuki locking. The only known mechanism that can account simultaneously for the athermal behavior and the high flow strength is the Fisher mechanism of short-range order strengthening. The equivalent of Eq. 8.44 for slip on the prismatic plane of the hexagonal system is

$$\tau_p = \frac{8 m_A m_B \bar{\varepsilon}_p \alpha_p}{1.61\, a^3} \tag{8.46}$$

We might assume that diffusion is so slow below about 475°K, which is about one-half of the melting temperature, that the existing short-range order is that which is frozen-in at 475°K, for which $\tau = 15 \times 10^8$ dynes/cm^2. Solving Eq. 8.45 and 8.46 simultaneously at 475°K suggests that $\bar{\varepsilon} = -760$ cal/mole and $\alpha = 0.30$, a reasonable value for short-range order. Using these values in Eqs. 8.45 and 8.46, we determine that flow stress should be given by the broken curve of Fig. 8.8 in the absence of thermally aided flow mechanisms. Above 475°K, the experimentally determined flow stress decreases precipitously with an increase in temperature and lies below the curve predicted in terms of short-range order flow stress. Obviously some thermally activated dislocation mechanism is operative above 475°K.

Thorough investigations on the creep behavior of this alloy above 475°K have shown that a thermally activated slip mechanism is operative. [101]

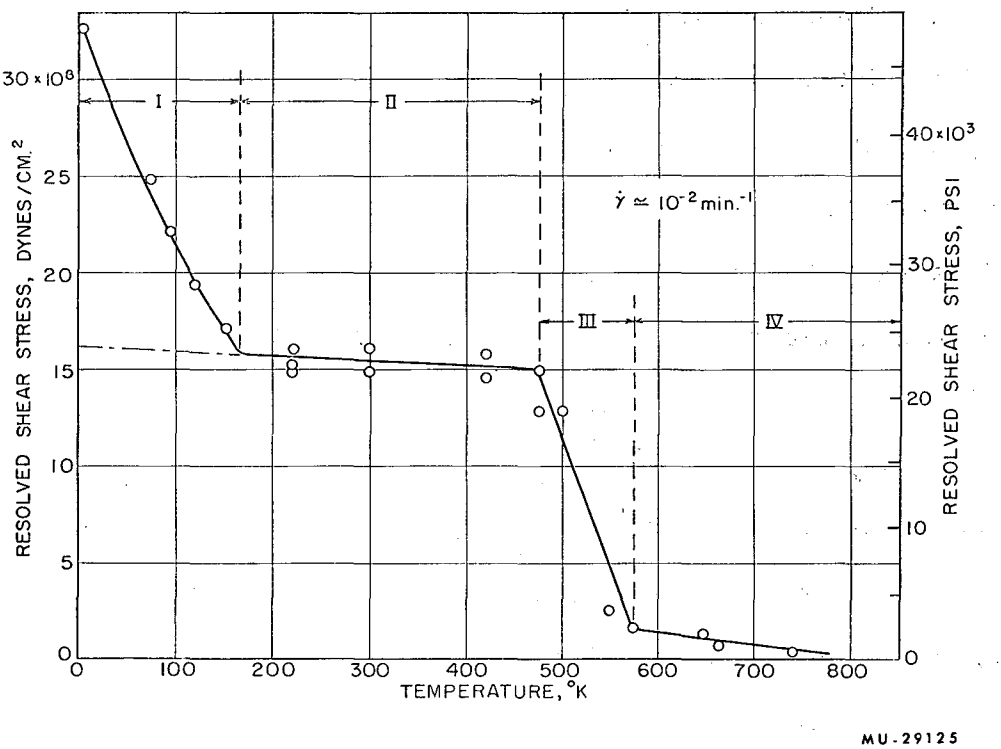

Fig. 8.7. Effect of temperature on the critical resolved shear stress for prismatic slip.

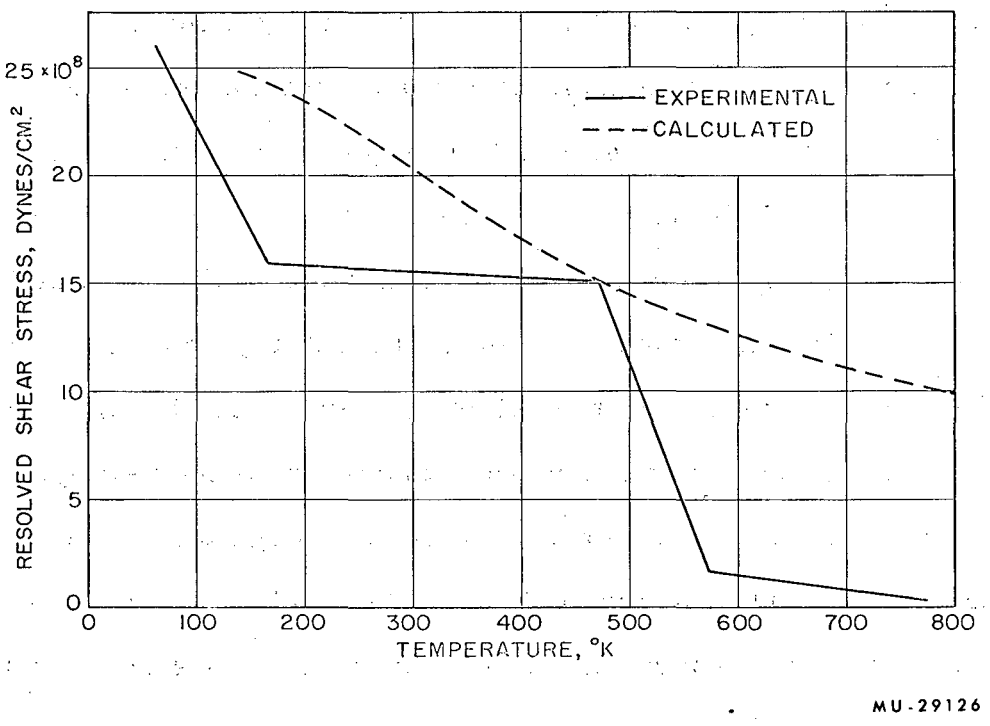

Fig. 8.8. Comparison of the critical resolved shear stress for slip with the value calculated in terms of the equilibrium degree of order.

Following a brief inverted primary stage of creep, over which the creep rate increases slightly, a steady state creep rate is obtained which obeys the relationship

$$\dot{\gamma} = (1.4 \pm 0.3)\tau^{3.6 \pm 0.1} e^{-Q/RT} \text{ per sec} \tag{8.47}$$

The activation energy, $Q = 3.3 \times 10^4 \pm 0.1 \times 10^4$ cal/mole, is insensitive to the stress and is in reasonable agreement with the estimated activation energy for diffusion. Although Eq. 8.47 suggests that this creep might be controlled by the climb mechanism, the creep curve, which does not exhibit the usual decreasing creep rate with strain, reveals that edge dislocations are not being piled-up against barriers. Therefore, some other diffusion controlled mechanism of creep must apply. Since the stress is much below the value that was calculated necessary to overcome short-range order as long lengths of dislocations move athermally through the lattice, it appears necessary to conclude that the applied stress can be aided by thermal fluctutation in moving short segments of the dislocations in short-range ordered alloys.

Lowley, Coll, and Cahn[102] observed similar creep behavior in Fe alloys containing 22.0 to 25.5 at% Al over a range of temperatures where short-range order is known to prevail. These authors attributed the acceleration of creep over the initial stages to a Shoeck[103] reordering effect under stress. Such an explanation, however, cannot apply to the Ag (67 at%) Al (33 at%) alloy since Al and Ag have almost identical atomic radii. They observed that the creep rate for their Fe-Al alloys was given by

$$\dot{\gamma} = A e^{-Q/RT} \tau^{n} \tag{8.48}$$

where $4.6 \leq n \leq 6.0$ and where the activation energy closely approximates that for diffusion of Al in Fe. Although the power of the stress term in Eq. 8.48 was extremely high, these authors nevertheless correlated their results with Weertman's[104] theory for viscous drag of a solute atmosphere on the dislocations. But again, such a viscous drag cannot be operative in the Ag-Al alloys just described because the dislocation to solute atom interaction is practically zero.

The data on the creep of the two above-mentioned short-range ordered alloys clearly reveal that the high strengthening that can be achieved by short-range ordering at low temperatures is not maintained at temperatures where diffusion is facile, an experimental fact that contradicts previous concepts on short-range order strengthening. Although the high temperature creep of short-range ordered alloys appears to be diffusion controlled, the dislocation mechanism for this process is not yet completely understood.

9. Summary

Substantial strides have been made over the past 15 years in uncovering the role of many of the important factors that determine the physical mechanisms of high temperature creep. In certain special materials, high temperature creep might occasionally occur as a result of thermal activation of special non-diffusional dislocation processes. More frequently, however, creep at high temperatures is determined by diffusional processes, principally the stress directed diffusion of vacancies, motion of jogged screw dislocations and the climb of edge dislocations.

Whereas some of the proposed atomistic mechanisms for high temperature creep, such as the stress-directed diffusion of vacancies, are based on sound, well-understood, detailed theories, others, such as the motion of jogged screw dislocations and, especially, recovery as a result of climb of edge dislocations, yet require additional attention. The major problems in these areas concern not so much the formalities of the theories, which are now well-conceived, but rather the effect of the details of dislocation patterns and arrangements on these mechanisms. In view of the current interest in this subject, it can be expected that considerable light will be shed on these issues as a result of observation of dislocation patterns in crept metals by means of electron-transmission microscopy. On the other hand the principle judgement of the validity of any theory will remain the actual experimentally determined creep behavior of materials. This is necessarily so because most of the significant details of creep mechanisms are on atomic scale so as to remain below the resolution of the electron-microscope. Consequently the electron microscope will provide the essential preliminary data needed to cull the unrealistic theories from those that have some basis in fact. Theory must yet be extended to provide more detailed information

on subgrain formation, all of the details on dipoles, entanglements, and all other significant structural features that might be revealed by the electron microscope. Additional theoretical advances coupled with experimental verification are required on the problems of diffusion in multicomponent systems including investigations on grain boundary diffusion and pipe diffusion along dislocations.

Up to the present, most of the effort to understand the physical basis for high temperature creep has been based on the results of carefully controlled experiments on rather pure metals. Furthermore, some progress has already been made in uncovering some of the basic issues related to the effects of dispersions and alpha solid solution alloying on the creep behavior of metals. Many of these issues, however, require more detailed study before a comprehensive coherent theory for high temperature creep can be formulated.

Today many of the concepts outlined above are being employed, at least qualitatively, in the design of creep resistant alloys; and some fundamental research has already been undertaken to unravel the basic processes that contribute to the creep resistance of complex high temperature engineering alloys. It was not the purpose of this review to cover this most important and interesting area. A voluminous literature now exists on various aspects of this subject. At the risk of serious omission of other important investigations we should like, at least, to mention the outstanding contributions that are being made by Glen[105] on this difficult subject.

REFERENCES

1. J. L. Lytton, L. A. Shepard, and J. E. Dorn, "The Activation Energies for Creep of Single Aluminum Crystals Favorably Oriented for (111) [101] Slip," Trans. AIME 212, 220-225 (1958).
2. T. A. Trozera, J. Mote, and J. E. Dorn, "Activation Energies for Basal Slip in Magnesium Single Crystals," Trans. ASM (1960).
3. J. J. Gilman, "Plastic Anisotropy of Zinc Monocrystals," Trans. AIME 206, 1326 (1956).
4. "Creep and Fracture of Metals at Elevated Temperatures," Proceedings of Symposium, National Physical Laboratory, 1954, H. M. Stationery Office (1956).
5. A. H. Sully, "Recent Advances in Knowledge Concerning the Process of Creep in Metals," Prog. in Met. Phys. 6, 135-180 (1956).
6. "Creep and Recovery," Seminar of Am. Soc. Metals, Cleveland (1957).
7. D. McLean, "Point Defects and the Mechanical Properties of Metals and Alloys at High Temperature," Symposium on Vacancies and Other Point Defects in Metals and Alloys, The Institute of Metals, London (1958), pp. 159-198.
8. Mechanical Behavior of Materials at Elevated Temperature, J. E. Dorn, Ed. (McGraw-Hill Book Co., New York, 1961).
9. "Structural Processes in Creep," Report of a Symposium, Iron and Steel Institute and Institute of Metals, London (1961).
10. J. E. Dorn, "Progress in Understanding High-Temperature Creep," Gillett Memorial Lecture, ASTM (1962), to be published.
11. F. R. N. Nabarro, "Deformation of Crystals by the Motion of Single Ions," Report of a Conference on the Strength of Solids, Phys. Soc. London (1948), pp. 75-90.
12. C. Herring, "Diffusional Viscosity of a Polycrystalline Solid," J. Appl. Phys. 21, 437-445 (1950).
13. A. L. Prantis and G. M. Pound, "Viscous Flow of Copper at High Temperatures," Trans. AIME 203, 664-668 (1955).
14. A. P. Greenough, "The Deformation of Silver at High Temperature," Phil. Mag. 43, 1075-1082 (1952).
15. F. H. Buttner, E. R. Funk, and H. Udin, "Viscous Creep of Gold Wires Near the Melting Point," Trans. AIME 194, 401-407 (1952).

16. J. Harper and J. E. Dorn, "Viscous Creep of Aluminum Near Its Melting Temperature," Acta Met. 5, 654-655 (1957).

17. R. Chang, "Creep of Al_2O_3 Single Crystals," J. Appl. Phys. 31, 484 (1960).

18. R. C. Folweiler, "Creep Behavior of Pore-Free Polycrystalline Aluminum Oxide," J. Appl. Phys. 32, 5, 773-778 (1961).

19. R. L. Coble and J. E. Burke, "Sintering in Crystalline Solids," in Reactivity of Solids, Proc. 4th International Symposium on the Reactivity of Solids, J. H. DeBoer et al., Eds. (Elsevier Publishing Company, Amsterdam, 1961) pp. 38-51.

20. S. I. Warshaw and F. H. Norton, "Deformation Behavior of Polycrystalline Aluminum Oxide," J. Am. Ceram. Soc. 45 [10], 479-486 (1962).

21. R. Chang, "High Temperature Creep and Anelastic Phenomena in Polycrystalline Refractory Oxides," J. Nuclear Materials 2, 174-181 (1959).

22. S. B. Austerman, Discussion in Kinetics of High-Temperature Processes, Endicott House Conference (The Technology Press, MIT, and John Wiley and Sons, Inc., New York, Chapman and Hall, Ltd., London, 1959), pp. 67-68.

23. R. R. Vandervoort and W. L. Barmore, "Compressive Creep of Polycrystalline Beryllium Oxide," UCRL-6748 (1962).

24. R. Scott, A. R. Hall, and J. Williams, "The Plastic Deformation of Uranium Oxides Above 800°C," J. Nuclear Materials 1, 39-48 (1959).

25. A. B. Auskern and J. Belle, "Diffusion of Oxygen in Uranium Dioxide," J. Chem. Phys. 28, 171 (1958).

26. W. D. Kingery, Introduction to Ceramics (John Wiley and Sons, Inc., New York, 1960).

27. J. E. Dorn, "Some Fundamental Experiments on High Temperature Creep," J. Mech. Phys. Solids 3, 81-116 (1954).

28. O. D. Sherby and J. E. Dorn, "The Creep Properties of Cold Rolled Aluminum Alloy Sheet Metals," Trans. ASM 43, 611 (1951).

29. D. McLean, "Grain Boundary Slip During Creep of Aluminum, J. Inst. Metals 81, 293-300 (1952-53).

30. L. A. Shepard and J. E. Dorn, "Role of Subgrains in High Temperature Creep," 1st Tech. Rept., Ser. No. 108, Issue 1, Contract AF33(616)-3860, Materials Res. Lab., Inst. of Engr. Res., Univ. of Calif., Berkeley.

31. I. S. Servi, J. T. Norton, and N. J. Grant, "Some Observations of Subgrain Formation During Creep in High Purity Aluminum," Trans. AIME 194, 965 (1952).

32. D. McLean, "Creep Processes in Coarse-Grained Aluminum," J. Inst. Metals 80, 507 (1951-52).

33. D. McLean and M. H. Farmer, "The Relation During Creep Between Grain Boundary Sliding, Subcrystal Size and Extension," J. Inst. Metals 85, 41 (1956-57).

34. F. Garofalo, L. Zwell, A. S. Keh, and S. Weissman, "Substructure Formation in Iron During Creep at 600°C," Acta Met. 9, 721-729 (1961).

35. O. D. Sherby, T. A. Trozera, and J. E. Dorn, "The Effect of Creep Stress History at High Temperatures on the Creep of Aluminum Alloys," Proc. Am. Soc. Testing Materials 56, 789 (1956).

36. O. D. Sherby, "Factors Affecting the High Temperature Strength of Polycrystalline Solids," Acta Met. 10, 135-147 (1962).

37. P. L. Gruzin, U. V. Kornev, and G. V. Kurdimov, Doklady Akad. Nauk S.S.S.R. 80, 49 (1951).

38. H. W. Mead and C. E. Birchenall, "Self-Diffusion of Iron in Austenite," Trans. AIME 206, 1336 (1956).

39. P. Feltham, "The Plastic Flow of Iron and Plain Carbon Steels Above the A_3-Point," Proc. Phys. Soc. (London) B66, 865 (1953).

40. J. E. Dorn, "Progress in Understanding High Temperature Creep," The 1962 Horace W. Gillett Memorial Lecture, American Society for Testing and Materials, to be published.

41. H. Laks, "Effect of Low Stresses on the Creep Rates of a Polycrystalline Aluminum Alloy under Constant Structure," M. S. Thesis, University of California, Berkeley, 1953.

42. D. McLean and K. F. Hale, "The Stress Sensitivity of Creep," Structural Processes in Creep," Report of a Symposium organized by the Iron and Steel Institute and the Institute of Metals, London, Special Report No. 70 (1961).

43. D. McLean, "Crystal Slip in Aluminum During Creep," J. Inst. Metals 81, 133-144 (1952-53).

44. I. S. Servi and N. J. Grant, "Creep and Stress Rupture Behavior of Aluminum as a Function of Purity," Trans. AIME 191, 909 (1951).

45. P. Feltham and G. J. Copley, "Creep in Face-Centered Metals and Solid Solutions with Special Reference to α-Brasses," Phil. Mag. 5 649 (1960).

46. R. E. Frenkel, O. D. Sherby, and J. E. Dorn, "Activation Energies for Creep of Cadmium, Indium, and Lead," Acta Met. 3, 472 (1955).

47. P. Feltham and J. D. Meakin, "Creep in Face-Centered Cubic Metals with Special Reference to Copper," Acta Met. 7, 614 (1959).

48. P. Feltham, "The Plastic Flow of Iron and Plain Carbon Steels Above the A_3-Point," Proc. Phys. Soc. (London) B66, 865 (1953).

49. J. Weertman and P. Shaninian, "Creep of Polycrystalline Nickel," Trans. AIME 206, 1223 (1956).

50. P. Feltham, "On the Mechanism of High-Temperature Creep in Metals with Special Reference to Polycrystalline Lead," Proc. Phys. Soc. (London) 69B, 1173 (1956).

51. O. D. Sherby, "Creep of Polycrystalline Alpha and Beta Thallium," Trans. AIME 212, 708 (1958).

52. O. D. Sherby, R. Frenkel, J. Nadeau, and J. E. Dorn, "Effect of Stress on the Creep Rates of Polycrystalline Aluminum Alloys Under Constant Structure," J. Metals, AIME, 275-279 (Feb. 1954).

53. A. E. Bayce, W. D. Ludemann, L. Shepard, and J. E. Dorn, "Effect of Stress on the Creep of Aluminum in the Dislocation Climb Range," Trans. ASM 52 (1960).

54. Butcher, Thesis, Cornell University, Ithaca, New York, 1962.

55. J.C.M. Li, "Theory of Strengthening by Dislocation Groupings," in Electron Microscopy and Strengthening in Crystals, J. Washburn and G. Thomas, Eds. (John Wiley and Sons, Inc., New York, 1963), p. 713.

56. J. Friedel, "Les Dislocations," Gauthier-Villars, Paris (1956).

57. N. F. Mott, "A Theory of Work-Hardening of Metal Crystals," Phil. Mag. 43, 1151 (1952).

58. A. Seeger, "The Generation of Lattice Defects by Moving Dislocations and Its Application to the Temperature Dependence of the Flow Stress of FCC Crystals," Phil. Mag. 46, 1194-1217 (1955).

59. J. Friedel, "On the Linear Work-Hardening Rate of Face-Centered Cubic Single Crystals," Phil. Mag. 46, 1169-1193 (1956).

60. P. B. Hirsch and D. H. Warrington, "The Flow Stress of Aluminum and Copper at High Temperature," Phil. Mag. 6, 735-768 (1961).

61. P. B. Hirsch, See N. F. Mott, "The Work-Hardening of Metals," 1960 Institute of Metals Lecture, Trans. AIME 218, 962-968 (1960).

62. L. Raymond, unpublished data.

63. A. H. Cottrell, Dislocations and Plastic Flow in Crystals (Oxford University Press, London, 1953), p. 48.

64. R. W. Christy, "Theory of Creep Limited by Self-Diffusion," J. Appl. Phys. 30, 60 (1959).

65. J. Weertman, "Theory of Steady State Creep Based on Dislocation Climb," J. Appl. Phys. 26, 1213 (1955); "Steady State Creep Through Dislocation Climb," J. Appl. Phys. 28, 362 (1957).

66. N. J. Grant and O. Preston, "Dispersed Hard Particle Strengthening of Metals," Trans. AIME 209, 349 (1957).

67. R. Guard, "Mechanism of Fine-Particle Strengthening," Strengthening Mechanisms in Solids, Seminar of the ASM, (1960), pp. 253-278.

68. J. C. Fisher, E. W. Hart, and R. H. Pry, "The Hardening of Metal Crystals by Precipitate Particles," Acta Met. 1, 336-339 (1953).

69. E. Orowan, "Theory of Dispersion Strengthening," Symposium on Internal Stresses in Metals and Alloys (1948), p. 451.

70. J. Weertman, "Theory of Creep of Dispersion-Hardened Alloys," Naval Research Laboratory Report No. 5123 (1958).

71. G. S. Ansell and J. Weertman, "Creep of a Dispersion-Hardened Al Alloy," Trans. AIME 215, 838-843 (1959).

72. W. H. Giedt, O. D. Sherby, and J. E. Dorn, "The Effect of Dispersions on Creep Properties of Aluminum-Copper Alloys," Trans. Am. Soc. Mech. Engrs. (1955), pp. 57-63.

73. G. Thomas, private communication.

74. G. Thomas, J. Nutting, and P. B. Hirsch, J. Inst. Metals 86, 7 (1957).

75. J. B. Mitchell, S. K. Mitra, and J. E. Dorn, "Dispersed Particle Strengthening at Low Temperatures," to be published Trans. AIME.

76. C. L. Meyers, Jr., and O. D. Sherby, J. Inst. Metals 90, 380 (1961-62).

77. C. L. Meyers, Jr., J. C. Shyne, and O. D. Sherby, "Relation of Properties to Structure in Sintered Aluminum Powder," Dept. of Materials Science Report No. 62-10, Stanford University, Stanford, Calif.

78. G. Schoeck, "Thermodynamic Principles in High-Temperature Materials," in Mechanical Behavior of Materials at Elevated Temperatures, J. E. Dorn, Ed. (McGraw-Hill Book Co., New York, 1961), pp. 70-74.

79. R. W. K. Honeycombe, "The Effect of Temperature and Alloying Additions on Deformation of Metal Crystals," Progr. in Materials Sci. 19, 95-130 (1961).

80. P. A. Flinn, "Solid Solution Strengthening," Strengthening Mechanisms in Solids, ASM (1960), pp. 17-50.

81. E. R. Parker and T. H. Hazlett, "Principles of Solution Hardening," Relation of Properties to Microstructure Seminar, ASM (1953), p. 30.

82. J. E. Dorn, "Energetics in Dislocation Mechanics," UCRL-10455.

83. A. Seeger, "Mechanism of Glide and Work-Hardening in Face-Centered Cubic and Hexagonal Closed Packed Metals," in Dislocations and Mechanical Properties of Crystals (John Wiley and Sons, Inc., New York, 1957), p. 243.

84. A. Howie and P. R. Swann, "Direct Measurement of Stacking-Fault Energies from Observations of Dislocation Nodes," Phil. Mag. 6, 1215 (1961).

85. A. Ahmadieh, Lawrence Radiation Laboratory, Berkeley, unpublished data.

86. H. Suzuki, "The Yield Strength of Binary Alloys," in Dislocations and Mechanical Properties of Crystals (John Wiley and Sons, Inc., New York, 1957), pp. 361-390.

87. J. E. Dorn, "Thermodynamics of Stacking Faults in Binary Alloys," to be published, Letter to Editor, Acta Met.

88. A. H. Cottrell, "Effect of Solute Atoms on the Behavior of Dislocations," Report of a Conference on Strength of Solids, The Physical Society (1948), p. 30.

89. A. H. Cottrell and B. A. Bilby, "Dislocation Theory of Yielding and Strain Ageing of Iron," Proc. Phys. Soc. (London) A62, 49 (1949).

90. A. Cochardt, G. Schoeck, and H. Wiedersich, "Interaction Between Dislocations and Interstitial Atoms in Body-Centered Cubic Metals," Acta Met. 3, 533 (1955).

91. K. Lücke, See A. H. Cottrell, "Interactions of Dislocations," Relation of Properties to Microstructure Seminar, ASM (1953), Ref. 31, p. 144.

92. R. Thomson, "The Non-Saturability of the Strain Field of a Dislocation by Point Imperfections," Acta Met. 6, 23 (1958).

93. C. Crussard, Metaux et Corrosion 25, Ur. 301, 203.

94. N. Louat, "The Effect of Temperature on Cottrell Atmospheres," Proc. Phys. Soc. (London) B69, 459 (1956).

95. E. C. W. Perryman, "Recovery of Mechanical Properties," Creep and Recovery Seminar, ASM (1956), p. 111.

96. J. C. Fisher, "On the Strength of Solid Solution Alloys," Acta Met. 2, 9 (1954).

97. P. A. Flinn, "Solute Hardening of Close-Packed Solid Solutions," Acta Met. 6, 631-635 (1958).

98. J. M. Cowley, "An Approximate Theory of Order in Alloys," Phys. Rev. 77, 350 (1950).

99. P. A. Flinn, "Electronic Theory of Local Order," Phys. Rev. 104, 350 (1956).

100. J. Mote, K. Tanaka, and J. E. Dorn, "Effect of Temperature on Yielding in Single Crystals of the Hexagonal Ag-Al Intermetallic Phase."

101. E. M. Howard, W. L. Barmore, J. D. Mote, and J. E. Dorn, "On the Thermally Activated Mechanism of Prismatic Slip in the Ag-Al Hexagonal Intermediate Phase, UCRL-10588.

102. A. Lawley, J. A. Coll, and R. W. Cohn, "Influence of Crystallographic Order on Creep of Iron-Aluminum Solid Solutions," Trans. AIME 218, 166 (1960).

103. J. L. Snoek, "Effect of Small Quantities of Carbon and Nitrogen on the Elastic and Plastic Properties of Iron," Physica 8, 711 (1941).

104. J. Weertman, "Steady State Creep of Crystals," J. Appl. Phys. 28, 1185-1189 (1957).

105. See for example J. Glenn, "A New Approach to the Problems of Creep," J. Iron and Steel Inst. 189, 333 (1958); "The Shape of Creep Curves," Trans. ASME, J. Basic Eng. Paper No. 62 WA-133, presented at Winter Annual Meeting, 1962.

This report was prepared as an account of Government sponsored work. Neither the United States, nor the Commission, nor any person acting on behalf of the Commission:

A. Makes any warranty or representation, expressed or implied, with respect to the accuracy, completeness, or usefulness of the information contained in this report, or that the use of any information, apparatus, method, or process disclosed in this report may not infringe privately owned rights; or

B. Assumes any liabilities with respect to the use of, or for damages resulting from the use of any information, apparatus, method, or process disclosed in this report.

As used in the above, "person acting on behalf of the Commission" includes any employee or contractor of the Commission, or employee of such contractor, to the extent that such employee or contractor of the Commission, or employee of such contractor prepares, disseminates, or provides access to, any information pursuant to his employment or contract with the Commission, or his employment with such contractor.